

**REMOVAL OF MICROPOLLUTANTS IN BIOFILTERS:
HYDRODYNAMIC EFFECTS ON
BIOTRANSFORMATION RATES**

A Thesis

Presented to the Faculty of the Graduate School

of Cornell University

in Partial Fulfillment of the Requirements for the Degree of

Master of Science

by

Corey Michael George Carpenter

January 2017

© 2017 Corey Michael George Carpenter

ABSTRACT

Global water resources contain a variety of organic chemicals, including pharmaceuticals, personal care products, and pesticides at trace concentrations. This study investigated the application of biofiltration for the removal of these so-called micropollutants from drinking water resources. The objective of this work was to examine how hydrodynamics influence biotransformation rates in biofiltration processes. Measurements included biomass concentration, depths of the biological zone, and removal rates of 29 micropollutants at environmentally-relevant concentrations in bench-scale biofiltration columns operated under three distinct hydrodynamic regimes. Higher superficial velocities led to less concentrated surface biomass but a deeper biological zone and more total biomass. Eleven micropollutants underwent biotic removal and second-order rate constants were not significantly different between hydrodynamic regimes for each micropollutant. Of these micropollutants, five had significantly greater second-order rate constants at deeper biofilter depths. This work is an important step in improving our understanding of how hydrodynamics influence drinking water biofiltration performance.

BIOGRAPHICAL SKETCH

Corey Carpenter was born in Boston, Massachusetts in 1992. He obtained a Bachelor's of Science degree in Environmental Engineering from Syracuse University in 2014. While studying at Syracuse University, he worked with Dr. Charles Driscoll for two years at the Center for Environmental Systems Engineering investigating how stormwater management practices can improve local water quality. During the summer of 2013, he completed an internship with Raymond International, where he traveled across the Middle East studying the means and ways of transporting potable water in arid regions. In June 2014, he joined Dr. Damian Helbling's research group at Cornell University and started his study towards a Master's of Science degree in Civil and Environmental Engineering.

ACKNOWLEDGMENTS

First, and foremost, I would like to thank my major advisor, Dr. Damian Helbling, for his continued support throughout this project. His guidance and instructions were instrumental to the successful completion of this thesis. I came out of every weekly meeting feeling invigorated and ready to take on the next steps towards our research goals. I would also like to thank Dr. Ruth Richardson and Dr. Monroe Weber-Shirk for serving as minor advisors on my committee.

I am thankful for the rest of the Helbling research group for their friendship and support, especially Amy Pochodylo and Yuhang Ling for watching over my columns while I was out of town. I am also grateful for the support that came from my friends and family. I would like to specifically thank my fiancée, Sarah Wilkinson, for her moral support throughout this project—your encouragement and love helped me more than I can possibly describe.

TABLE OF CONTENTS

BIOGRAPHICAL SKETCH	iii
ACKNOWLEDGMENTS	iv
TABLE OF CONTENTS	v
LIST OF FIGURES	vi
LIST OF TABLES	viii
LIST OF EQUATIONS	ix
LIST OF ABBREVIATIONS	x
LIST OF SYMBOLS	xi
CHAPTER 1: Background.....	1
1.1 Micropollutants	1
1.2 Removal of micropollutants during drinking water treatment processes	3
1.3 Biofiltration	5
1.4 Previous studies on biofiltration for the removal of micropollutants.....	9
1.5 Research objectives	11
CHAPTER 2: Removal of micropollutants in biofilters: hydrodynamic effects on biotransformation rates	13
Abstract	13
2.1 Introduction.....	15
2.2 Materials and methods	19
2.2.1 Biofiltration columns	19
2.2.2 Feedwater and column setup.....	21
2.2.3 Tracer experiments.....	23
2.2.4 Biomass determination.....	24
2.2.5 Micropollutant selection	25
2.2.6 Micropollutant sampling and analysis	33
2.2.7 Statistical analysis	34
2.3 Results and Discussion	34
2.3.1 Spatial arrangement and concentration of biofilms	34
2.3.1.1 Longitudinal dispersivity	34
2.3.1.2 Surface biomass concentration	37
2.3.1.3 Total biomass	40
2.3.2 Micropollutant removal.....	42
2.3.2.1 Recalcitrance.....	47
2.3.2.2 Abiotic removal	48
2.3.2.3 Biotic removal.....	49
2.3.2.4 Biotransformation extents and rates.....	50
2.3.2.5 Oligotrophic environments	53
2.3.2.6 Transformation product formation.....	55
2.4 Conclusions.....	57
CHAPTER 3: Future work.....	59
APPENDICES	63
REFERENCES	132

LIST OF FIGURES

Main text:

Figure 1: Schematic of a biologically active filter in a drinking water treatment plant.	8
Figure 2: Biofilter design by group.....	20
Figure 3: Experimental setup.....	22
Figure 4: Total counts of unique biotransformation reactions predicted for 149 reference compounds.	26
Figure 5: Average longitudinal dispersivity in each filter group for the duration of the experiment.....	36
Figure 6: Average surface biomass concentration in each filter group for the duration of the experiment.....	38
Figure 7: Biomass concentration profiles on day 301	41
Figure 8: Dendrogram of micropollutant removal behavior for the duration of the experiment.	44
Figure 9: Average removal efficiencies of micropollutants that underwent biotic removal.	51
Figure 10: Average pseudo-first-order rate constants of micropollutants that underwent biotic removal.	52
Figure 11: Average second-order rate constants of micropollutants that underwent biotic removal.	53
Figure 12: Relative distributions of transformation products formed in each biofilter.	56

Appendices:

Figure C.1: Full spectrum scan of carbamazepine at 10 mg L ⁻¹	68
Figure D.1: Cumulative fractional tracer breakthrough curves for filter group 1.	74
Figure D.2: Cumulative fractional tracer breakthrough curves for filter group 2.	75
Figure D.3: Cumulative fractional tracer breakthrough curves for filter group 3a.....	76
Figure D.4: Cumulative fractional tracer breakthrough curves for filter group 3ab.....	77
Figure F.1: Removal efficiency of acetaminophen for the duration of the experiment.	86
Figure F.2: Removal efficiency of atenolol for the duration of the experiment.....	87
Figure F.3: Removal efficiency of atrazine for the duration of the experiment.	88
Figure F.4: Removal efficiency of azoxystrobin for the duration of the experiment.....	89
Figure F.5: Removal efficiency of caffeine for the duration of the experiment.....	90
Figure F.6: Removal efficiency of carbamazepine for the duration of the experiment.....	91
Figure F.7: Removal efficiency of carbaryl for the duration of the experiment.	92
Figure F.8: Removal efficiency of cimetidine for the duration of the experiment.....	93
Figure F.9: Removal efficiency of diazinon for the duration of the experiment.....	94
Figure F.10: Removal efficiency of diphenhydramine for the duration of the experiment.....	95
Figure F.11: Removal efficiency of estrone for the duration of the experiment.	96
Figure F.12: Removal efficiency of ethofumesate for the duration of the experiment.	97
Figure F.13: Removal efficiency of ibuprofen for the duration of the experiment.	98
Figure F.14: Removal efficiency of isoproturon for the duration of the experiment.	99
Figure F.15: Removal efficiency of metoprolol for the duration of the experiment.	100
Figure F.16: Removal efficiency of naproxen for the duration of the experiment.....	101
Figure F.17: Removal efficiency of phenytoin for the duration of the experiment.....	102
Figure F.18: Removal efficiency of progesterone for the duration of the experiment.....	103

Figure F.19: Removal efficiency of propachlor for the duration of the experiment.	104
Figure F.20: Removal efficiency of ranitidine for the duration of the experiment.	105
Figure F.21: Removal efficiency of simazine for the duration of the experiment.	106
Figure F.22: Removal efficiency of sucralose for the duration of the experiment.	107
Figure F.23: Removal efficiency of sulfamethoxazole for the duration of the experiment.	108
Figure F.24: Removal efficiency of triclosan for the duration of the experiment.	109
Figure F.25: Removal efficiency of trimethoprim for the duration of the experiment.	110
Figure F.26: Removal efficiency of trinexapc-ethyl for the duration of the experiment.	111
Figure F.27: Removal efficiency of valsartan for the duration of the experiment.	112
Figure F.28: Removal efficiency of venlafaxine for the duration of the experiment.	113
Figure F.29: Removal efficiency of warfarin for the duration of the experiment.	114
Figure G.1: Identification of 4-aminophenol.	117
Figure G.2: Identification of atenolol-acid.	118
Figure G.3: Identification of hydroxy-estrone.	119
Figure G.4: Identification of hydroxy-ibuprofen.	120
Figure G.5: Identification of O-desmethyl-metoprolol.	121
Figure G.6: Identification of propachlor-OXA.	122
Figure G.7: Identification of propachlor-ESA.	123
Figure G.8: Identification of 4-desmethyl-trimethoprim.	124
Figure G.9: Identification of hydroxy-trimethoprim.	125
Figure G.10: Identification of TRI-324.	126
Figure G.11: Identification of TRI-290.	127
Figure G.12: Identification of DAPC.	128
Figure G.13: Identification of VAL-335.	129
Figure G.14: Identification of VAL-251.	130
Figure G.15: Identification of valsartan-acid.	131

LIST OF TABLES

Main text:

Table 1: Micropollutants supplied to the biofilters and their classifications, uses, structures, predicted biotransformation reaction IDs, and physiochemical properties.	27
Table 2: Depth of the biological zone and total biomass found in each biofilter group.	42
Table 3: Average removal efficiencies of micropollutants in biofiltration studies.....	45

Appendices:

Table A.1: Target and actual filter flow rates, empty bed contact times, and superficial velocities for each column for the duration of the experiment.	64
Table B.1: Results of the micropollutant control experiments.	66
Table C.1: Loading pump gradient for micropollutant analyses.	70
Table C.2: Elution pump gradient for micropollutant analyses.	70
Table C.3: Elution pump gradient for transformation product analyses.....	71
Table D.1: Breakthrough curve results for days 44 and 241.	73
Table E.1: Reference standard information	79
Table E.2: Isotopically labeled internal reference standard structures	81
Table E.3: Isotopically labeled internal reference standard information.....	83
Table F.1: Average micropollutant influent concentrations and maximum recordable removal efficiencies based on individual limits of quantification.	84

LIST OF EQUATIONS

Equation 1: Empty bed contact time	17
Equation 2: Superficial velocity	17
Equation 3: Analytical solution to the 1-dimensional advection dispersion equation	23
Equation 4: Removal efficiency	33
Equation 5: Pseudo-first-order rate constant	33
Equation 6: Second-order rate constant.....	34

LIST OF ABBREVIATIONS

ANOVA	Analysis of variance
AOPs	Advanced oxidation processes
Biofilter	Biologically active filter
CCL	Chemical Candidate List
DWTP	Drinking water treatment plant
EBCT	Empty bed contact time
EIC	Extracted ion chromatogram
EPA	Environmental Protection Agency
FDA	Food & Drug Administration
GAC	Granular activated carbon
HPLC	High performance liquid chromatography
LOQ	Limit of quantification
m/z	Mass to charge ratio
MP	Micropollutant
PAC	Powdered activated carbon
RO	Reverse osmosis
RT	Retention time
SMILES	Simplified molecular-input line-entry system
SV	Superficial velocity
SWDA	Safe Water Drinking Act
TP	Transformation product
Tukey-HSD	Tukey's honest significance difference test
USA	United States of America
UV	Ultraviolet
WRF	Water Research Foundation
WWTP	Wastewater treatment plant

LIST OF SYMBOLS

α_L	Longitudinal dispersivity
$C(t)$	Concentration at time, t
$C(x,t)$	Concentration at depth, x , and time, t
C_0	Concentration of the tracer injected
C_e	Effluent concentration
C_i	Influent concentration
D	Dispersion coefficient
D^*	Diffusion coefficient
$F(t)$	Cumulative fractional tracer breakthrough
k'	Pseudo-first-order rate constant
k_a	First-order abiotic rate constant, feedwater
k_{bio}	Second-order rate constant
k_{stock}	First-order abiotic rate constant, stock
L	Length of the filter bed
D	Distribution coefficient
M	Mass of tracer injected
Q	Flow rate
t	Time
u	Average pore water velocity
x	Depth
X_{tot}	Total biomass
Δt_i	Time difference between i and $i-1$

CHAPTER 1: Background

1.1 Micropollutants

It is widely known that global drinking water resources contain a variety of trace organic compounds that include various types of anthropogenic and natural compounds (Benner et al., 2013; Evgenidou et al., 2015; Focazio et al., 2008; Luo et al., 2014; Richardson and Ternes, 2014). These compounds include (among others) pharmaceuticals, hormones, personal care products, antimicrobial agents, and pesticides. Once in the aquatic environment, organic compounds undergo a variety of abiotic and biotic transformations, yielding many transformation products (TPs) and metabolites (Evgenidou et al., 2015; Richardson and Ternes, 2014). These trace organic compounds, their TPs and metabolites are collectively known as micropollutants (MPs).

MPs can enter drinking water resources through point and non-point sources. Point sources of MPs include wastewater treatment or industrial effluent (Richardson and Ternes, 2014). For example, wastewater treatment plants (WWTPs) receive MPs through human urine and excrement, improper disposal of pharmaceuticals, and grey waters (shower, laundry, *etc.*). Pharmaceuticals that are only partly absorbed or metabolized by humans and animals are expelled unchanged and/or as metabolites. Many parent MPs and their metabolites are not fully removed during wastewater treatment (Evgenidou et al., 2015) and are consequently discharged into receiving surface waters. MPs have been detected throughout the urban water cycle, from WWTP influent and effluent to surface waters to drinking water treatment plant (DWTP) influent and effluent (Benner et al., 2013; Evgenidou et al., 2015; Luo et al., 2014). Non-point sources of MPs include surface runoff from agriculture (Gros et al., 2012; Veatch and Bernot, 2011), dispersion of groundwater polluted with landfill leachate (Oturan et al., 2015) or septic effluents (Erickson et al., 2014; Phillips et al., 2015).

For example, pesticides are applied to the ground for pest and weed control at agricultural, commercial, and residential sites. During precipitation events, pesticides can be transported by runoff into nearby water resources or infiltrate through the vadose zone into underlying aquifers. Natural transformation processes can alter the chemical structure of pesticides to create increasingly more mobile TPs that more readily enter the aquatic environment (Benner et al., 2013). Pharmaceuticals can be transported to water resources from non-point sources as well; veterinary drugs used for farm animals have been measured in surface waters (Gros et al., 2012).

The effects of long-term exposure to low-levels of MPs are still largely unknown, but there is growing evidence of harmful effects to aquatic ecosystems and to human health. For example, the presence of the hormone ethinylestradiol (EE2) at low ng L^{-1} concentrations has been shown to have estrogenic effects in fish, which include shift of sex ratios and decreased egg fertilization (Richardson and Ternes, 2014). Additionally, propachlor (a herbicide) is a likely human carcinogen; studies have shown that it causes thyroid, ovarian, and liver tumors in mice (McCarroll et al., 2002). Additionally, combined effects of complex mixtures of MPs complicate the assessment of the toxicological impacts (Altenburger et al., 2013).

The lack of toxicological data on MPs limits current drinking water quality regulations in the United States of America (USA). Under the Safe Water Drinking Act (SWDA), the Environmental Protection Agency (EPA) regulates a number of MPs (including various insecticides and herbicides) with the National Primary Drinking Water Regulations. Additionally, the EPA manages a contaminant candidate list (CCL) that contains a number of contaminants that are known or anticipated to occur in public water systems and may require regulation in the future, but are not currently regulated under the SDWA. There are a growing number of MPs appearing on the EPA's CCL, including pharmaceuticals, hormones, and pesticides (U.S. EPA, 2015).

However, there are only 20 pesticides and 1 pesticide TP regulated by the National Primary Drinking Water Regulations (U.S. EPA, 2014) even though there are about 85,000 industrial chemicals in the EPA's Toxic Substances Control Act Inventory (U.S. EPA, 2016a), about 43,000 pesticides regulated under the EPA's Federal Insecticide, Fungicide, and Rodenticide Act (U.S. EPA, 2016b), and over 2,600 active pharmaceutical ingredients approved by the U.S. Food & Drug Administration (FDA) (FDA, 2016).

1.2 Removal of micropollutants during drinking water treatment processes

Existing drinking water treatment technologies such as coagulation and adsorption, activated carbon adsorption, membrane filtration, and advanced oxidation processes (AOPs) are capable of partially or fully removing some MPs. The development and application of novel advanced drinking water treatment processes is partially driven by the increased awareness of the occurrence of emerging contaminants and more stringent water quality standards. An ideal treatment technology would be economical, energy efficient, simple to operate, and capable of simultaneously removing complex mixtures of pollutants with a wide range of physicochemical properties. Henceforth, the term “removal” refers only to the loss of the parent compound and not necessarily complete mineralization. It is important to distinguish mineralization and transformation because the disappearance of MPs may not coincide with decreases in toxicity due to the formation of toxic TPs.

Most conventional DWTPs use coagulation and flocculation to destabilize particulate matter to enable the aggregation of the destabilized particles into larger flocs prior to sedimentation and filtration. These processes can effectively remove organic and inorganic solids. During these processes, MPs can adsorb onto the surfaces of the precipitates which are removed during sedimentation and filtration. However, only very hydrophobic compounds ($\log K_{ow} > 6$) are

expected to be removed during coagulation as they would be more likely to adsorb onto precipitates (Snyder et al., 2007). Because most MPs found in water resources are polar (low log K_{ow} values) coagulation is not considered to be a suitable primary treatment technology for MP removal; any observed MP removal during coagulation is ancillary.

Adsorption is a treatment technology that is more specifically utilized for MP removal. Organic compounds adsorb onto the surface of a highly porous adsorbent and are removed from water. The most commonly used adsorbent for drinking water treatment is activated carbon, which can be used as either granular activated carbon (GAC) or powdered activated carbon (PAC). The applications of GAC and PAC have been proven to be effective at removing some MPs, including typically recalcitrant MPs like the pharmaceuticals carbamazepine and sulfamethoxazole (Altmann et al., 2014; Reungoat et al., 2012). However, like coagulation but to a lesser extent, activated carbon adsorption is not effective for many of the more hydrophilic MPs (Kovalova et al., 2013). Additionally, activated carbon needs to be regenerated when its adsorption capacity is reached. Regeneration is an energy intensive process and cannot completely restore the performance of the adsorbent (Margot et al., 2013). Furthermore, adsorption capacity is reduced by the presence of competing organic matter (Nam et al., 2014), which increases the number of regenerations needed and decreases the lifespan of the adsorbent.

Another water treatment process that has been explored for the removal of MPs from drinking water is membrane filtration. Membrane filtration utilizes semipermeable membranes to filter contaminants while allowing water to flow through. Reverse osmosis (RO) membranes have the highest selectivity, only allowing the smallest dissolved constituents through its pores (<0.1 nm). Membrane filtration removes organic compounds primarily through size exclusion and is not dependent on hydrophobicity like coagulation and adsorption. Removal efficiencies for a

wide range of MPs through RO processes are reported to be 95-100% (Drewes et al., 2007; Lee et al., 2012). However, membrane filtration is a pressure driven process which requires a large amount of energy to operate the necessary pumps. Additionally, the membranes are prone to fouling because they are designed for one-way flow and cannot be backwashed to remove solids. Membrane filtration is very expensive to operate due to the high operating costs associated with maintenance and energy requirements (Lee et al., 2012).

Advanced oxidation processes (AOPs) are used to remove organic compounds during wastewater and drinking water treatment, and are less costly alternatives to membrane filtration and activated carbon adsorption (Lee et al., 2012; Margot et al., 2013). AOPs frequently employ a combination of ozone and ultraviolet (UV) light or hydrogen peroxide to form highly reactive hydroxyl radicals that oxidize organic compounds. The application of AOPs can significantly reduce MP loads in water but does not always mineralize contaminants (Altmann et al., 2014; Lee et al., 2012; Reungoat et al., 2012). AOPs may result in the formation of oxidation products that retain toxic activity, as evidenced by residual toxicity measured in ozonated wastewaters (Prasse et al., 2012; Zimmermann et al., 2011). Although less expensive than membrane filtration processes, AOPs still have relatively high operating costs due to the energy demands for the UV lamps and are complex to operate due to changing chemical requirements and maintenance (Hollender et al., 2009; Lee et al., 2012; Zimmermann et al., 2011).

1.3 Biofiltration

Biofiltration is an alternative drinking water treatment technology that is underexplored and could contribute to the removal of MPs from water. Biofiltration is a natural biological process which utilizes native microbial communities attached to granular media to remove pollutants from water. Microorganisms stick to each other and to the granular media by excreting an extracellular

polymeric substance in groups called biofilms. Biofiltration is both a physical and biological process; it uses depth collection of solids to reduce turbidity and microorganisms, and biological activity to transform or mineralize inorganic and organic compounds (Bouwer and Crowe, 1988; Gimball et al., 2006). Biofiltration has been used for centuries for drinking water treatment through exploitation of the natural environment. For example, river bank filtration is a biofiltration processes in which a drinking water source is obtained from extraction wells some distance away from a river; this process allows water to be filtered through the river bank before it is used thereby removing particulates and microorganisms through depth filtration, and dissolved constituents by means of microbial metabolism.

Biofiltration has now been implemented as an engineered processes in wastewater treatment, water reuse, and drinking water treatment applications. For example, constructed wetlands are used as a tertiary treatment process in WWTPs to further degrade organic contaminants that were not removed during conventional wastewater treatment (Y. Li et al., 2014); they are designed to naturally remove contaminants from WWTP effluent without any additional energy costs before discharging into nearby surface waters. Managed aquifer recharge allows for the direct injection of WWTP effluent into dry aquifers in an attempt to treat and store water for later reuse (Rauch-Williams et al., 2010). In some DWTP applications, biologically active filters (biofilters) are used and consist of a granular media filter with living biofilms attached to the filter grains (Zhu et al., 2010). Biofiltration is widely accepted and implemented in Europe; about 16% of the drinking water produced in Germany is from river bank filtration while only 1% is from direct use of river water (Schmidt et al., 2003). There are no known biofiltration usage statistics in the USA, although a survey conducted by the Water Research Foundation (WRF) showed that

only about 10% of utility and regulator professionals believed that biofiltration is widely-to-moderately used for drinking water treatment in the USA (Evans et al., 2010).

Biofilters have been used for decades in DWTPs, but have only recently gained more attention for their advantages over other water treatment technologies (Evans et al., 2010; Zhu et al., 2010). A schematic of an engineered biofilter is given in **Figure 1** which shows a typical layout for a sand filtration unit. Granular media filters can be easily converted into biofilters by simply not pre-chlorinating the water prior to the granular media filter and by using unchlorinated water for backwashing (Hozalski and Bouwer, 1998). This allows native microbial communities to attach to the sand grains near the surface of the filter bed and grow into a concentrated biologically active layer (Rittmann et al., 1989; Wang et al., 1995). Advantages of using biofilters over abiotic granular media filtration to facilitate drinking water treatment include the reduction of dissolved organic carbon concentrations, which can reduce disinfection by-product formation and minimize microbial regrowth in distribution systems (Rittmann et al., 1989; Wang et al., 1995). Microbial communities are capable of transforming organic compounds, altering their chemical structures, for carbon and/or energy purposes or through cometabolism which does not support microbial growth (Alexander, 1981). Advantages of biofiltration processes over other advanced water treatment processes are that they are low cost, low maintenance, and simple to operate. The operation of biofilters is simple and economical because it does not require specific energy inputs for mechanical components, or added chemical reagents. The only routine maintenance required is the same as granular media filters—backwashing or scraping the top layer of sand to remove built-up solids (Rittmann et al., 1989). Additionally, the biofilms develop naturally on the granular media as the feedwater is filtered through (Rittmann et al., 1989; Wang et al., 1995). However, disadvantages of biofiltration include the possibility of biofilm detachment (known as sloughing)

that could release microorganisms into the finished water (Bouwer and Crowe, 1988), and a lack of process understanding and optimized operational parameters (Evans et al., 2010). However, the types of microorganisms found in biofilter effluents are dictated by the preceding biofilter microbial communities (Lautenschlager et al., 2014), which are not expected to be pathogenic and of no health concern at low concentrations (Rittmann et al., 1989). The WRF survey revealed that most of the treatment plants surveyed have not optimized their biofiltration processes and that one of the main issues with biofiltration acceptance is the general lack of process understanding (Evans et al., 2010). The survey also revealed that research will increase biofiltration acceptance by demonstrating contaminant removal attributes and MP removal was the most popular research priority among survey responses (Evans et al., 2010). Biofiltration is a low-cost and sustainable treatment process which can protect human health and the environment from a variety of contaminants but further research is need to better understand the underlying processes.

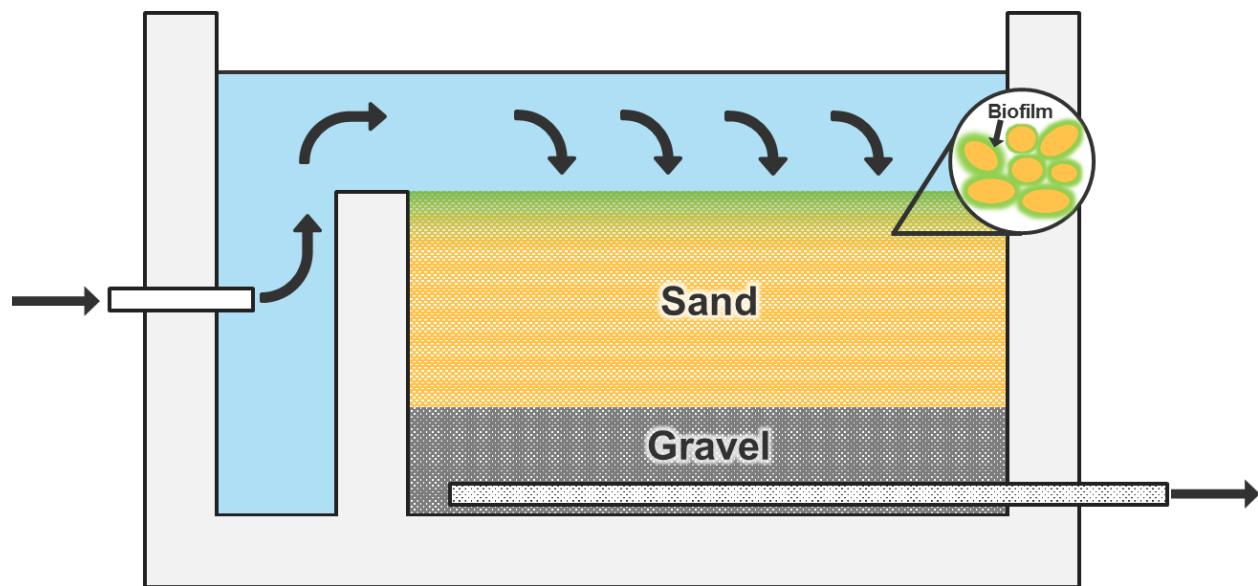


Figure 1: Schematic of a biologically active filter in a drinking water treatment plant.

The potential to exploit the microbial communities in biofiltration processes is exciting, though our current understanding of the operational parameters that influence biofiltration process performance is limited. Past studies have shown that several factors may influence biofiltration

performance including influent concentration and type of substrates, temperature, media type, chlorine in the backwash water, air scouring during backwashing, frequency of backwashing, and hydrodynamics (Urfer et al., 1997). The studies reported in the critical review by Urfer et al. revealed that the relationship between biomass formation and biofilter performance was critical to the understanding of biofiltration processes. Water utility managers cannot control certain operational parameters that are expected to influence biomass formation such as influent substrate concentration and type, or temperature. However, one operational parameter that is expected to influence biomass formation and can be directly controlled (within a certain range) is the hydrodynamics. The hydrodynamics of a biofiltration process can affect the biomass formation on the filter media in different ways. It is well known that biomass concentrations decrease with filter bed depth independently of hydrodynamics (Bertelkamp et al., 2014; Carlson and Amy, 1998; Collins et al., 1992; Rauch-Williams et al., 2010; Urfer and Huck, 2001; Wang et al., 1995); however, the role that hydrodynamics plays in shaping the spatial arrangement of the biomass is not well understood. One key hydraulic operating parameter is superficial velocity (SV) which is a measure of how quickly water passes through a cross section of the filter bed. Higher SVs increase the flux of substrates into the biofilms and allow substrates to penetrate deeper into the filter bed to facilitate more microbial growth which can improve biofiltration performance (Carlson and Amy, 1998), but can also lead to more sloughing which can inhibit biofiltration performance (Zhu et al., 2010). On the other hand, higher SVs also provide microbial communities less time to biotransform substrates which decreases biofilter performance.

1.4 Previous studies on biofiltration for the removal of micropollutants

Biofiltration can be an effective process for removing some MPs from drinking water (Bertelkamp et al., 2016a, 2016b, 2015, 2014; Summers et al., 2015) and wastewater (Alidina et

al., 2014; Escolà Casas and Bester, 2015; D. Li et al., 2014; Onesios and Bouwer, 2012; Onesios-Barry et al., 2014; Rauch-Williams et al., 2010; Teerlink et al., 2012). However, due to our lack of fundamental knowledge of biofiltration processes, their control and operation functions like a black box (Meckenstock et al., 2015; Zhu et al., 2010) and we cannot rationally modify their design or operation to enhance their performance.

MP removal through biofiltration processes is investigated in the laboratory using bench-scale granular media biofiltration columns and previous studies have focused on operational parameters that may enhance the biotransformation of MPs. These studies have investigated the associations between MP removal and feedwater composition (Onesios-Barry et al., 2014), primary substrate concentrations (Onesios and Bouwer, 2012), primary substrate types (Bertelkamp et al., 2016a; D. Li et al., 2014; Rauch-Williams et al., 2010), microbial community structure such as the role of nitrifiers (Rattier et al., 2014), and microbial community adaptation resulting from MP pre-exposure (Alidina et al., 2014). These studies have all provided important insights into links between water chemistry and microbial community structure and function. However, few studies have systematically explored operational parameters that can actually be controlled by water utility managers, like hydraulic operating parameters such as contact time (Escolà Casas and Bester, 2015; Zearley and Summers, 2012) and SV (Sharif et al., 2014; Teerlink et al., 2012).

The removal of several MPs were shown to be positively associated with contact time (ranging from 5 to over 50 hours) in sand columns simulating wastewater slow sand filtration, though these experiments were carried out by simply changing the flow rates to alter the contact times of an already developed biofilter (Escolà Casas and Bester, 2015). Similarly, a study also showed that the removal of MPs were dependent on contact time in bench-scale sand columns

simulating drinking water biofiltration (Zearley and Summers, 2012). In this study, contact time was controlled by varying the depth of the biofiltration columns and the biomass concentration was considered uniform throughout. Another study found a significant positive association between MP removal rates with SV and carbon loading rates in bench-scale microcosms simulating constructed wetlands (Sharif et al., 2014). As a final example, the long-term effects of different SVs (1 to 30 cm day⁻¹) manifested as an inverse relationship with MP removal efficiency for a subset of MPs examined in sand columns simulating soil treatment units for onsite wastewater treatment (Teerlink et al., 2012). Authors attributed the additional removal to longer contact time; however, many of the MPs examined showed no dependence on SV which somewhat contradicts that conclusion. This review of the literature reveals that past research has heavily focused on the association of contact time with MP removal, and the effects of spatial arrangement of biomass and the biomass concentrations are rarely considered. Further, there is little data available under environmentally-relevant conditions in which the impacts of different hydrodynamic regimes on MP removal are systematically explored.

1.5 Research objectives

The hypothesis of this work is that hydrodynamics influence the spatial arrangement and concentration of biofilms formed in biofiltration processes and consequently affect the biotransformation rates of MPs in different ways. As discussed in the preceding sections, hydrodynamic parameters of filtration processes are controlled by the SV which can lead to opposing and competing effects. Higher SVs will decrease the contact times between the biofilms and the MPs leading to less MP removal. However, higher SVs can also increase the formation of biomass on the filter media leading to more MP removal.

The experiments outlined in this thesis were designed to systematically explore SV within a practical range to investigate the spatial arrangement and concentration of biofilms and how the consequent biofilm spatial arrangements of the biofilms affect MP biotransformation. The primary objectives of this work are to:

- (i) Examine the temporal and spatial arrangements of biofilms formed on biofiltration columns operated under three distinct hydrodynamic regimes.
- (ii) Describe the performance of the biofiltration columns for the removal of 29 micropollutants from water at environmentally-relevant concentrations.
- (iii) Analyze the resulting data to characterize the effects of different spatial arrangements of biofilms on the biotransformation rates of MPs.

CHAPTER 2: Removal of micropollutants in biofilters:

hydrodynamic effects on biotransformation rates¹

Abstract

Global water resources contain a variety of micropollutants, including pharmaceuticals, personal care products, and pesticides. This study investigated the removal of micropollutants from drinking water using the process of biofiltration. The objective of this work was to examine how hydrodynamics influence MP biotransformation rates in biofiltration processes. We measured the removal rates of 29 micropollutants at environmentally-relevant concentrations ($1 \mu\text{g L}^{-1}$) in three groups of duplicate biofiltration columns operated continuously for 381 days under three distinct hydrodynamic regimes (superficial velocity: 0.1, 0.2, 0.4 m hr^{-1}). Total protein concentrations were used as a surrogate measurement for attached biomass and periodic tracer experiments were conducted to assess the depth of the biological zone in each filter bed. The biomass results revealed significant differences in biomass concentrations among the biofilters; higher superficial velocities led to less concentrated surface biomass but a deeper biological zone and more total biomass. Eleven of the 29 micropollutants underwent biotic removal; however, two micropollutants had to be excluded from further analysis because they were removed below our instruments detection limits throughout the experiment. Removal efficiencies for five of the micropollutants that underwent biotic removal did not significantly differ between hydrodynamic regimes, which indicates that any potential effects resulting from changes in hydrodynamics were negated. However, the removal efficiencies of the remaining four micropollutants showed a significant negative association with superficial velocity, suggesting that the reduction in contact time was

¹This chapter will be submitted to a peer-reviewed journal for publication with co-author D.E. Helbling.

more important than the increase in total biomass afforded by higher superficial velocities for the biotransformation of these micropollutants. Further, the estimated second-order rate constants for all nine micropollutants that underwent biotic removal were not significantly different between hydrodynamic regimes. However, five micropollutants had significantly greater second-order rate constants at deeper biofilter depths, suggesting that sparse microbial communities found in deeper and more oligotrophic biofilters had a greater activity for the biotransformation of these micropollutants. The identification of several transformation products at similar relative distributions in the biofilter effluents suggests that the oligotrophic environment non-selectively increased the activity of the microbial communities. These results suggest that biofiltration could be implemented in drinking water production for the removal of micropollutants and that the hydrodynamics of the system can influence the removal of some MPs.

2.1 Introduction

Drinking water resources around the world are increasingly impaired by anthropogenic activities that have negative effects on water quality (Schwarzenbach et al., 2006). Wastewater treatment plants are widely known sources of pharmaceuticals, personal care products, and other down-the-drain chemicals in surface water (Kolpin et al., 2002; Richardson and Kimura, 2016) and agricultural activities may result in the accumulation of pesticides and veterinary medicines in surface and groundwater (Boxall et al., 2003; Gilliom, 2007). The occurrence of these so-called micropollutants (MPs) in drinking water resources poses a significant challenge for drinking water utilities, as conventional drinking water treatment processes do not effectively remove many of these anthropogenic organic chemicals (Benner et al., 2013; Evgenidou et al., 2015; Focazio et al., 2008; Luo et al., 2014; Richardson and Ternes, 2014). Further, as a consequence of water scarcity, many drinking water providers are turning to direct or indirect potable reuse of wastewater (Harris-Lovett et al., 2015; Hering et al., 2013) which further exacerbates the need for efficient technologies to remove MPs during drinking water production.

A variety of advanced treatment processes have been explored as a means to remove MPs during drinking water production. Activated carbon adsorption has been used to remove pesticides from drinking water (Ormad et al., 2008; Stackelberg et al., 2007) and has recently been explored as a means to remove a variety of other types of MPs (Bonvin et al., 2016; Margot et al., 2013). However, activated carbon adsorption performs poorly for more polar MPs (Kovalova et al., 2013), can be fouled by natural organic matter (Nam et al., 2014), and adsorbent recovery and regeneration is expensive and energy-intensive (Margot et al., 2013). Advanced oxidation processes rely on ozone to produce hydroxyl radicals for the non-selective oxidation of MPs and other organic molecules in water. This approach has been demonstrated to significantly reduce MP

loads in wastewater effluents, though the process is energy intensive and relies on chemical reagents (Hollender et al., 2009; Zimmermann et al., 2011). Furthermore, advanced oxidation may result in the formation of oxidation products that retain toxic activity, as evidenced by residual toxicity measured in ozonated wastewaters (Prasse et al., 2012; Zimmermann et al., 2011). Membrane filtration utilizes semipermeable membranes to filter contaminants while allowing water to flow through, and reported removal efficiencies for a wide range of MPs are over 95% (Drewes et al., 2007; Lee et al., 2012). However, membrane filtration has high operating costs and lower water recovery (Lee et al., 2012).

Biofiltration is an alternative drinking water treatment process that has the potential for broad MP removal without the need for significant inputs of energy or chemical reagents. Biofiltration has been used for decades in drinking water treatment plants (DWTPs) as biologically active filters (biofilters) in rapid- and slow-sand filtration processes, but has only recently garnered attention as a sustainable and versatile treatment technology (Evans et al., 2010; Zhu et al., 2010). Biofiltration relies on the attachment of autochthonous microbial communities to the granular media in depth filtration processes to catalyze the biotransformation of organic chemicals, nitrogen and phosphorus nutrients, and dissolved metal constituents (Bouwer and Crowe, 1988). The potential to exploit the microbial communities in biofiltration processes to catalyze the removal of different types of pollutants is exciting, though our current understanding of the operational parameters that influence biofiltration process performance is limited and precludes rational design. A biofiltration process survey revealed that most of the treatment plants surveyed have not optimized their biofiltration processes and that one of the main issues with biofiltration acceptance is the general lack of process understanding (Evans et al., 2010).

Several recent studies have specifically explored the environmental or operational parameters that determine MP removal in bench-scale column experiments simulating different types of biofiltration processes. These studies have investigated the associations between MP removal and feedwater composition (Onesios-Barry et al., 2014), primary substrate concentrations (Onesios and Bouwer, 2012), primary substrate types (Bertelkamp et al., 2016a; D. Li et al., 2014; Rauch-Williams et al., 2010), microbial community structure such as the role of nitrifiers (Rattier et al., 2014) and microbial community adaptation resulting from MP pre-exposure (Alidina et al., 2014). These studies have all provided important insights into links between water chemistry and microbial community structure and function. However, few studies have systematically explored operational parameters that can actually be controlled by water utility managers, like hydraulic operating parameters such as empty bed contact time (EBCT) and superficial velocity (SV). The time that a parcel of water spends in a biofiltration process is commonly estimated using the EBCT and is calculated by **Equation 1**. Typical EBCTs for full-scale rapid sand filtration processes range from 5–30 min (Urfer et al., 1997; Zhu et al., 2010).

$$EBCT = \frac{Volume}{Flow Rate} \quad \textbf{Equation 1}$$

SV is a measure of how quickly water passes through a cross section of the filter bed and is calculated by **Equation 2**. Typical SVs for full-scale slow sand filtration processes range from 0.04–0.40 m hr⁻¹ (LeChevallier and Au, 2004).

$$SV = \frac{Flow Rate}{Cross sectional area} \quad \textbf{Equation 2}$$

The removal of several MPs were shown to be positively associated with contact time (ranging from 5 to over 50 hours) in sand columns simulating wastewater slow sand filtration, though these experiments were carried out by simply changing the flow rates to alter the EBCTs of an already

developed biofilter (Escolà Casas and Bester, 2015). Similarly, a study also showed that the removal of MPs were dependent on EBCT (7.9 and 15.8 min) in two sand columns simulating drinking water biofiltration, though the EBCTs were established by varying biofilter depth with assumed uniform biomass concentration (Zearley and Summers, 2012). Another study found a significant positive association between MP removal rates with SV and carbon loading rates in bench-scale microcosms simulating constructed wetlands (Sharif et al., 2014). As a final example, the long-term effects of different SVs (1 to 30 cm day⁻¹) manifested as an inverse relationship with MP removal efficiency for a subset of MPs examined in sand columns simulating soil treatment units for onsite wastewater treatment (Teerlink et al., 2012). Authors attributed the additional removal to longer contact time; however, many of the MPs examined showed no dependence on SV which somewhat contradicts that conclusion. This review of the literature reveals that past research has heavily focused on the association of contact time with MP removal and the effects of spatial arrangement of biomass and the biomass concentrations are rarely considered. Further, there is little data available under environmentally-relevant conditions in which the impacts of different hydrodynamic regimes on MP removal are systematically explored.

We hypothesize that hydrodynamics influence the spatial arrangement and concentration of biofilms formed in biofiltration processes and consequently affect the biotransformation rates of MPs in different ways. Higher SVs increase the flux of substrates into the biofilms and allow substrates to penetrate deeper into the filter bed to facilitate more microbial growth which can improve biofiltration performance (Carlson and Amy, 1998), but can also lead to more sloughing which can inhibit biofiltration performance (Zhu et al., 2010). On the other hand, higher SVs also reduce EBCTs which provide microbial communities less time to biotransform substrates which

decreases biofilter performance. The consequences of these competing effects on MP removal has never been systematically explored.

The primary objective of this work was to systematically explore SV within a practical range to investigate the spatial arrangement and concentration of biofilms and how the consequent biofilm spatial arrangements of the biofilms affect MP biotransformation. To meet this objective we measured the removal rates of 29 MPs at environmentally-relevant concentrations in three groups of duplicate biofiltration columns continuously operated under distinct hydrodynamic regimes for 381 days. Total protein concentrations were used as a surrogate measurement for biomass and periodic tracer experiments were conducted to assess the depth of the biological zone in each filter bed. The resulting data was used to describe the role of hydrodynamics in biofiltration processes for MP removal.

2.2 Materials and methods

2.2.1 Biofiltration columns

The bench-scale biofiltration columns were designed to have physical and hydraulic similitude with full-scale biofiltration processes. Biologically active sand was sampled from the slow-sand filter of the City of Auburn Water Filtration Plant in September 2014. The sand was sieved to a grain size of 0.707–0.841 mm (20–25 mesh) and packed into 2.5 cm inner diameter glass columns (borosilicate glass, 10 cm length, polypropylene end fittings, Kimble-Chase, Vineland, NJ) at a depth of 5 cm. Most of the biomass in full-scale biofiltration processes is in the top 5 cm of the filter bed (Collins et al., 1992; Urfer et al., 1997; Wang et al., 1995). Additionally, the inner diameter should be at least 25 times the grain size to minimize wall effects such as greater permeability near the column walls than the center of the filter bed, and the filter bed depth should be at least twice the diameter of the column for uniform dispersion of flow (Klotz and Moser,

1974). At least 1 cm of free surface water head was kept above the filter bed to avoid potential flow channeling (Tatari et al., 2013). The columns were kept at room temperature ($22 \pm 1^\circ\text{C}$) and were covered in aluminum foil to avoid photolysis of MPs and to prevent the growth of algae.

The columns were divided into three groups of filters with distinct hydrodynamic regimes. Each group consisted of a control filter (abiotic: C1, C2, C3a, C3b) and duplicate biofilters (biotic: B1-1, B1-2, B2-1, B2-2, B3-1a, B3-2a, B3-1b, B3-2b). Group 1 was designed to have an EBCT of 30 minutes and a SV of 0.1 m hr^{-1} . Group 2 was designed to have an EBCT of 16 minutes and a SV of 0.2 m hr^{-1} . Group 3 consisted of two columns in series, each with an EBCT of 8 minutes and a SV of 0.4 m hr^{-1} . Group 3ab refers to the combined columns in series and has a total EBCT of 16 minutes and a SV of 0.4 m hr^{-1} . An outline of the column groups is provided in **Figure 2** and the average flow rates, EBCTs, and SVs over the course of the experiment are provided in **Table A.1** of **Appendix A**. The duplicate biofilters will hereby be referred to as B1, B2, B3a, B3b, and B3ab to distinguish between the different groups of biofilters.

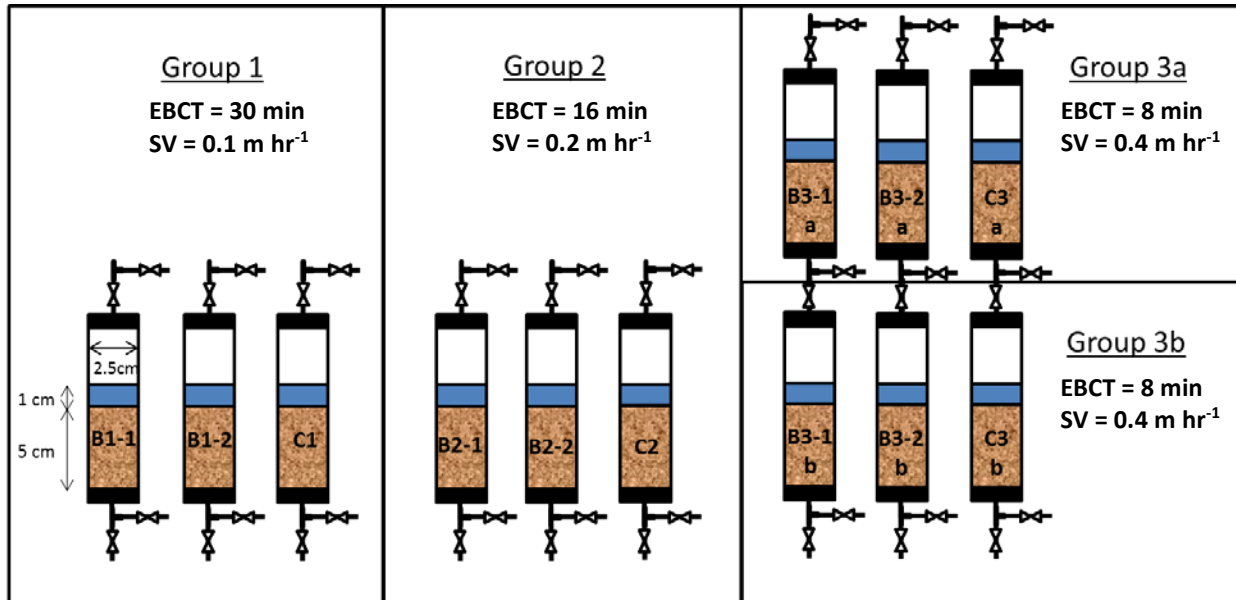


Figure 2: Biofilter design by group.

2.2.2 Feedwater and column setup

The columns received continuous flow for 381 days. The feedwater consisted of dechlorinated tap water, supplemented with acetate and MPs. The tap water was first dechlorinated with sodium bisulfite (NaHSO_3) supplied as sodium metabisulfite at 2 mg L^{-1} ($\text{Na}_2\text{S}_2\text{O}_5$, Sigma-Aldrich, Saint Louis, MO). The dechlorinated tap water was then supplemented with $1000 \text{ } \mu\text{g L}^{-1}$ of acetate supplied as sodium acetate ($\text{C}_2\text{H}_3\text{O}_2\text{Na}$, Sigma-Aldrich). Sodium acetate is an easily biodegradable primary substrate that has been previously used to promote biological growth in bench-scale biofiltration columns (Bertelkamp et al., 2014; Onesios and Bouwer, 2012; Onesios-Barry et al., 2014). Additionally, 29 micropollutants (Sigma-Aldrich) were added to the feedwater to generate a mixture where each MP was present at a target concentration of $1 \text{ } \mu\text{g L}^{-1}$. Finally, the abiotic control columns also received sodium azide (NaN_3 , Sigma-Aldrich) at 600 mg L^{-1} as a biocide to inhibit microbial growth from the start of the experiment as previously described (Bertelkamp et al., 2014; Rattier et al., 2014; Rauch-Williams et al., 2010).

A constant head 20 L water reservoir was continuously fed with cold tap water and heated to 21°C with an immersion heater (Cole Parmer, Vernon Hills, IL). Water then flowed by gravity into a 1 L open aeration vessel to saturate the water with dissolved oxygen at atmospheric conditions and to avoid the formation of air bubbles in the tubing or columns. The sodium metabisulfite reservoir was continuously pumped into the aeration vessel to dechlorinate the tap water before the addition of the MPs to avoid potential oxidation and chlorination reactions (Deborde and von Gunten, 2008). The aeration vessel then lead to a mixing vessel, where water from the sodium acetate and MP reservoir was continuously pumped, to completely mix the feedwater before distributing it to the columns. Both reservoirs were replenished weekly. Data from control experiments demonstrated that there were negligible MP transformations in the MP

stock solution over 1 week and in the feedwater over 2 hours; details of these experiments are presented in **Appendix B**. The sodium azide was kept in a separate reservoir. The sodium azide solution was pumped separately into each of the abiotic filters by a multichannel peristaltic pump (Cole Parmer) and was replenished monthly. An outline of the column setup is provided in **Figure 3**.

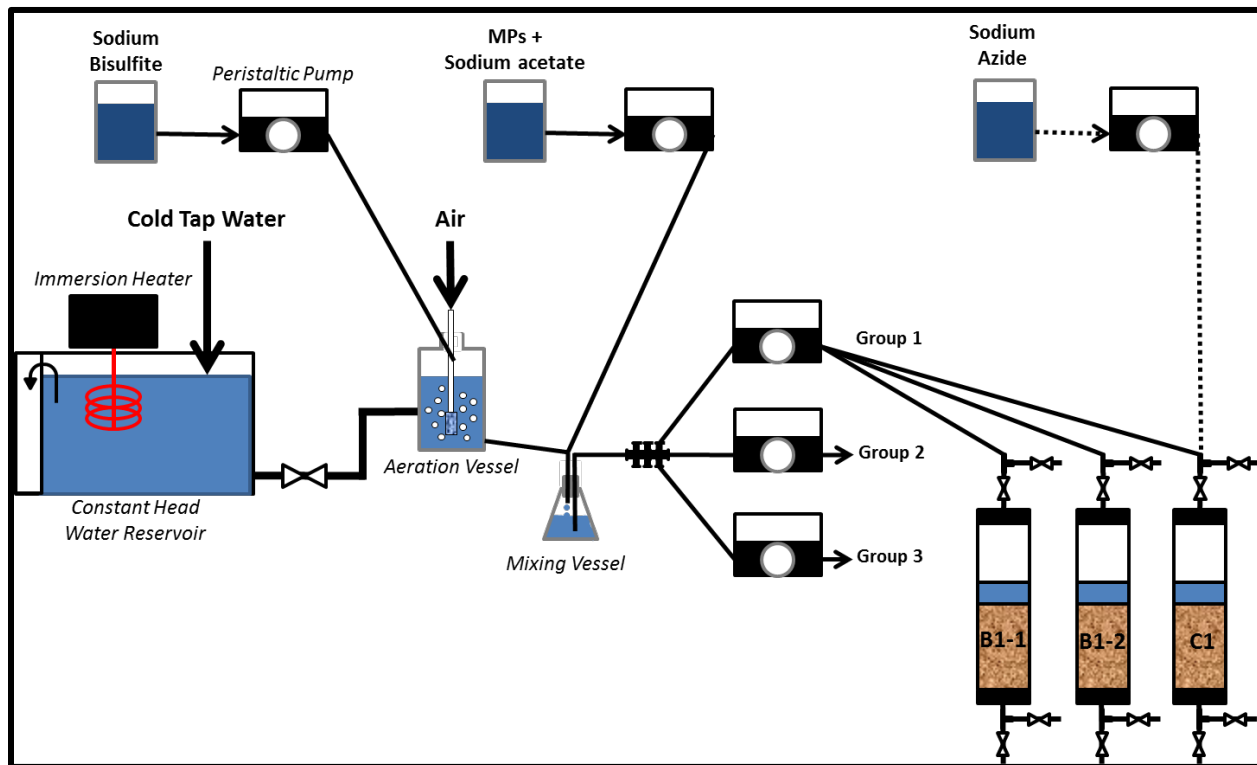


Figure 3: Experimental setup.

Because the columns were run in parallel from the same feedwater reservoir, the comparisons of biofilter performance is a function of hydrodynamic regime, not feedwater composition. However, the column groups received varying organic loading rates due to the varying SVs. Column sampling ports were located at the inlet and outlet of each column to accurately reflect the performance of the filters. The columns were operated as down-flow columns and fed by peristaltic pumps (Cole Parmer). Flowrates were monitored by measuring the time required for each column to discharge 10 mL of water into a graduated cylinder. Flowrates were

adjusted as needed to maintain the desired EBCT and SV in each column due to tubing fatigue and pressure buildup on the columns. Adjustments were made 24 hours prior to sampling.

2.2.3 Tracer experiments

Pulse input tracer experiments were conducted to determine the longitudinal dispersivity of each column. Carbamazepine was used as a conservative tracer; it is not readily biodegraded or retarded in sand filters (Bertelkamp et al., 2014; D'Alessio et al., 2015). The free surface water head in the columns was reduced to the top of filter bed and 2 mL of a 10 mg L⁻¹ solution of carbamazepine was injected directly above the sand. Samples were taken in 1.5 mL centrifuge vials (Eppendorf, Hamburg, Germany) directly from the column outlet, and centrifuged (5424 R Centrifuge, Eppendorf) for 5 min at 12000 rpm to remove particles before being transferred into 1 mL sample vials (Thermo Fisher Scientific). Concentrations of carbamazepine were measured using an HPLC system coupled to an UltiMate 3000 RS Variable Wavelength Detector (Thermo Fisher Scientific) and the analytical method is described in **Appendix C**. After the samples were processed, the longitudinal dispersivity (α_L) was calculated by minimizing the sum of squared errors between the discrete sample data and the analytical solution to the 1-dimensional advection dispersion equation for transport through porous media with asymmetrical boundary conditions (**Equation 3**, Ogata and Banks, 1961):

$$F(t) = \frac{1}{2} \left\{ \operatorname{erfc} \left(\frac{L - ut}{\sqrt{4 \alpha_L ut}} \right) + \exp \left(\frac{L}{\alpha_L} \right) \operatorname{erfc} \left(\frac{L + ut}{\sqrt{4 \alpha_L ut}} \right) \right\}$$

Equation 3

$$\text{Boundary conditions: } \begin{cases} C(L, 0) = 0 \\ C(\infty, t) = 0; t \geq 0 \end{cases}$$

where $F(t)$ is the cumulative fractional tracer breakthrough at time t , L is the length of the filter bed, and u is the average pore water velocity. See **Appendix D** for additional details.

2.2.4 Biomass determination

Total protein concentration was used as a surrogate measurement for biomass; the method was adapted from a previously reported study (Onesios and Bouwer, 2012). For surface biomass concentration measurements, approximately 0.5 mL of wet sand was sampled, in duplicate, from 1 cm below the sand-water interface of each filter. New sand was placed back into the columns to maintain constant filter bed volumes. For total biomass measurements, approximately 0.5 mL of wet sand was sampled in duplicate from 1 cm segments through the depth of each column. The sampled sand was placed into 2 mL centrifuge vials (Eppendorf) and 1.5 mL of nanopure water was added. The vials were vortexed (Mini Vortex, Thermo Fisher Scientific) for 10 seconds to disrupt the biofilms and sonicated (Ultrasonic Bath 2.8L, Thermo Fisher Scientific) for 5 min to lyse cells. Then, samples were centrifuged for 5 min at 4000 rpm to remove particles. The supernatant was then used as samples for a total protein assay.

A Micro BCA Protein Assay Kit (Thermo Fisher Scientific) was used to quantify the total protein concentrations in the samples by following the manufacturer's directions. Briefly, an albumin protein standard curve was created between 0.5 and 100 $\mu\text{g mL}^{-1}$. A working reagent was created by mixing the included proprietary reagents: 25 parts MA (alkaline tartrate-carbonate buffer), 24 parts MB (bicinchonic acid solution), and 1 part MC (copper sulfate solution). Cu^{+2} is reduced by proteins in an alkaline solution, forming Cu^{+1} , which reacts with the bicinchonic acid to form a purple chelation complex. Then, 1 mL of calibration standard or sample was mixed with 1 mL of the working reagent in a spectrophotometer cuvette (Thermo Fisher Scientific) and incubated in a 60°C water bath for 1 hour. Finally, the absorbance of the standards and samples was measured at 562 nm on a Genesys 10S UV-Vis Spectrophotometer (Thermo Fisher Scientific).

Samples were taken as duplicate, normalized by dry sand weight, and reported as μg protein per g dry sand. The dry sand weight was measured by washing the sampled sand with nanopure water and drying on pre-massed aluminum trays in a drying oven (Gravity Convection oven, VWR) at 105°C for 24 hours.

2.2.5 Micropollutant selection

Twenty nine environmentally-relevant MPs were selected for this study, including 18 pharmaceuticals, 9 pesticides, 1 biocide, and 1 food additive. All of the selected MPs have been previously detected or are likely to occur in surface water resources (Benner et al., 2013; Focazio et al., 2008; Richardson and Ternes, 2014). The MPs were selected to cover a broad range of predicted or known biotransformation reaction types based on the following analysis. First, a list of 149 compounds with available authentic reference standards was imported into the online biotransformation pathway prediction system, EnviPath (Wicker et al., 2015). EnviPath is a database and prediction system for microbial biotransformations of MPs; it predicts likely biotransformation pathways and products based on a set of biotransformation rules (identified by unique reaction IDs in the form of *br0000*) pertaining to the structure of the compound and known reaction pathways. Only aerobic and first level MP biotransformation reactions were predicted. MPs were then selected to represent a diverse group of biotransformation reactions that are predicted to occur in microbial systems. Of the 149 compounds imported into EnviPath, 60 unique biotransformation reactions were predicted. A histogram showing the total count of unique predicted reactions and the coverage of the selected MPs is provided in **Figure 4**. MPs were also selected to have a broad range of biodegradability based on previous bench-scale biofiltration studies (Alidina et al., 2014; Bertelkamp et al., 2014; Krkošek et al., 2014; Onesios and Bouwer, 2012; Onesios-Barry et al., 2014; Rattier et al., 2014; Reungoat et al., 2011; Teerlink et al., 2012;

Zearley and Summers, 2012). The selected MPs and their respective classification, use, structure, predicted biotransformation reaction IDs, and physiochemical properties are provided in **Table 1**.

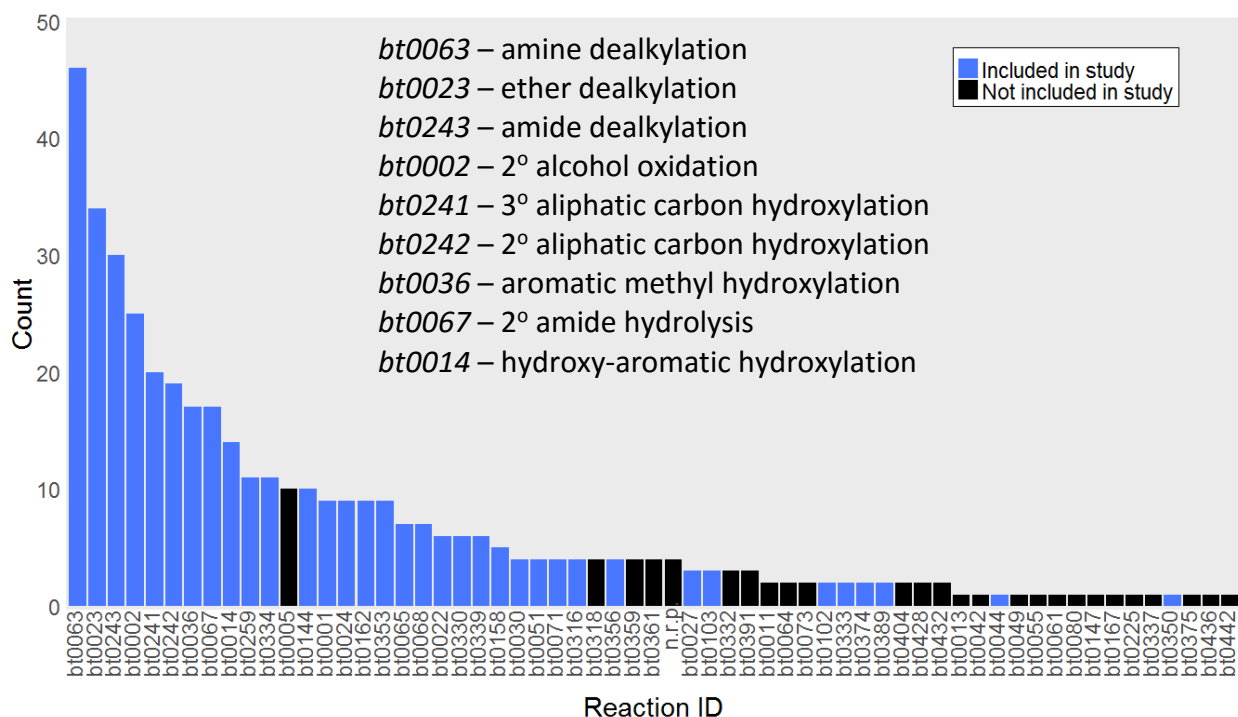


Figure 4: Total counts of unique biotransformation reactions predicted for 149 reference compounds. Predicted biotransformation reactions were obtained from EnviPath; a full description of each biotransformation reaction ID is available at www.envipath.org/rule. n.r.p = no reaction predicted.

Table 1: Micropollutants supplied to the biofilters and their classifications, uses, structures, predicted biotransformation reaction IDs, and physiochemical properties.

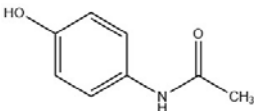
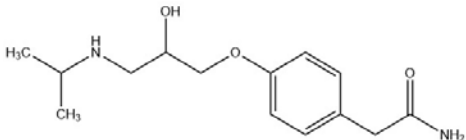
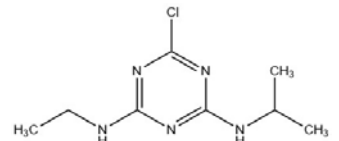
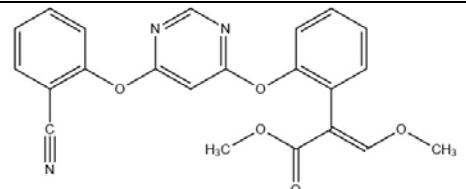
Micropollutant	Structure	Predicted Biotransformation Reaction ID(s)	Log D (pH = 7)	Henry's Law Constant (atm m ³ mole ⁻¹)	Water solubility (mg L ⁻¹)
Acetaminophen Pharmaceutical Analgesic		bt0067	0.91	1.27E-11	14000
Atenolol Pharmaceutical Beta-blocker		bt0002 bt0023 bt0027 bt0063	-2.14	3.93E-13	685
Atrazine Pesticide Herbicide		bt0330 bt0339	2.20	3.79E-08	35
Azoxystrobin Pesticide Fungicide		bt0024 bt0030	4.22	2.26E-11	10

Table 1 (continued)

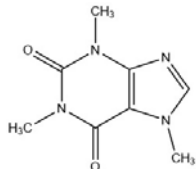
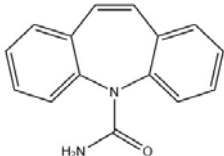
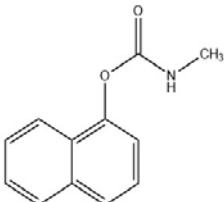
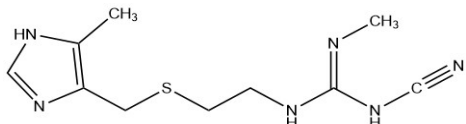
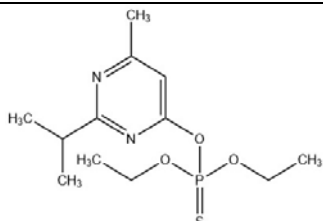
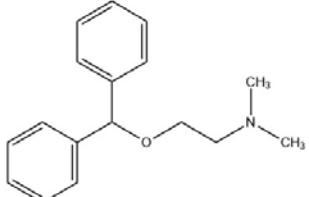
Caffeine Pharmaceutical Stimulant		bt0063 bt0243 bt0316	-0.55	7.12E-13	21600
Carbamazepine Pharmaceutical Anticonvulsant		bt0068	2.77	1.55E-09	18
Carbaryl Pesticide Insecticide		bt0389	2.46	3.39E-08	110
Cimetidine Pharmaceutical Antihistamine		bt0350	-0.34	6.22E-14	7426
Diazinon Pesticide Insecticide		bt0102 bt0103 bt0036	4.19	3.37E-06	40
Diphenhydramine Pharmaceutical Antihistamine		bt0023 bt0063	1.79	5.37E-09	3060

Table 1 (continued)

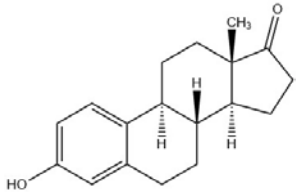
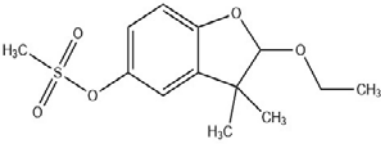
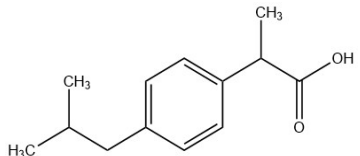
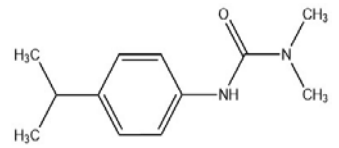
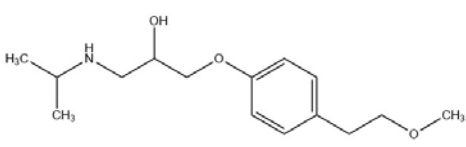
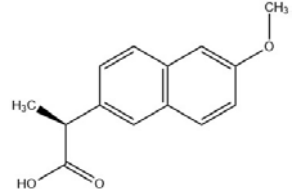
Estrone Pharmaceutical Hormone		bt0014 bt0071	4.31	1.23E-05	30
Ethofumesate Pesticide Herbicide		bt0023 bt0158	2.34	1.04E-09	50
Ibuprofen Pharmaceutical NSAID		bt0051 bt0241 bt0242 bt0333	1.71	1.23E-06	21
Isoproturon Pesticide Herbicide		bt0068 bt0241 bt0243	2.57	1.49E-08	65
Metoprolol Pharmaceutical Beta-blocker		bt0002 bt0023 bt0063	-0.81	2.12E-11	4777
Naproxen Pharmaceutical NSAID		bt0023 bt0241	0.25	2.66E-09	16

Table 1 (continued)

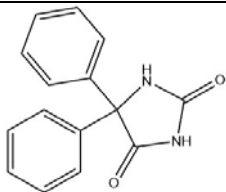
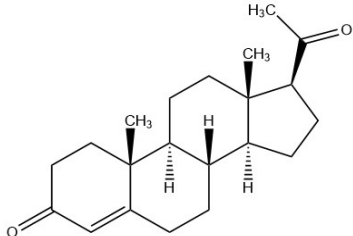
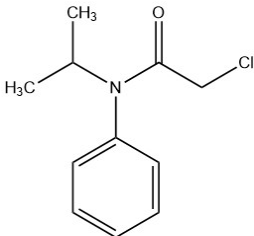
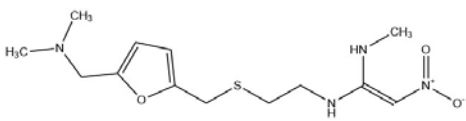
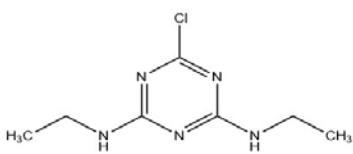
Phenytoin Pharmaceutical Anticonvulsant		bt0353	1.45	3.27E-14	32
Progesterone Pharmaceutical Hormone		bt0356	4.15	2.23E-07	9
Propachlor Pesticide Herbicide		bt0022 bt0065 bt0243	2.39	9.85E-08	700
Ranitidine Pharmaceutical Acid inhibitor		bt0063 bt0162 bt0259	0.13	2.35E-11	24660
Simazine Pesticide Herbicide		bt0330 bt0339	1.78	4.13E-09	6

Table 1 (continued)

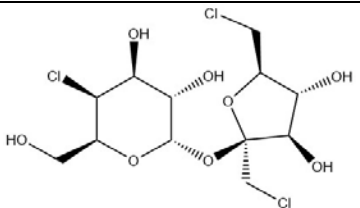
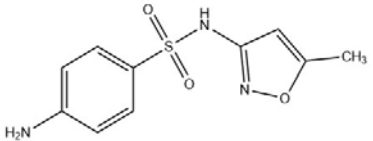
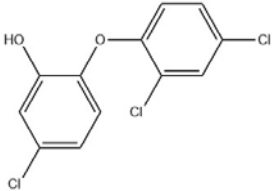
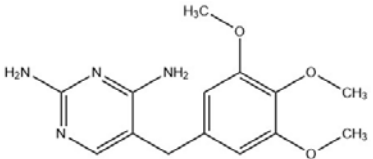
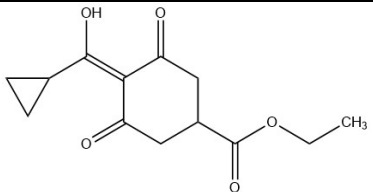
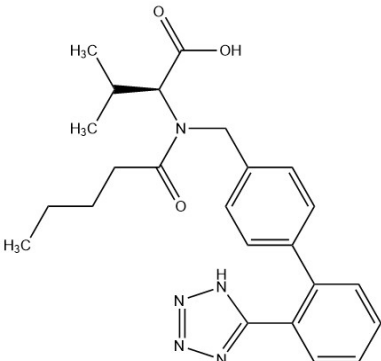
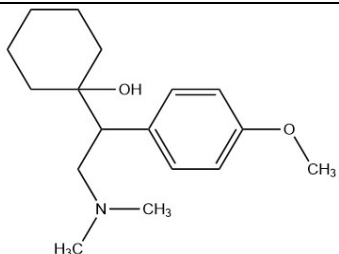
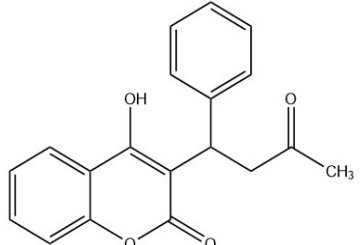
Sucralose Food additive Sweetener		bt0001 bt0002 bt0022 bt0023	-0.47	7.47E-19	22750
Sulfamethoxazole Pharmaceutical Antibiotic		bt0144	0.14	1.10E-11	610
Triclosan Biocide Antimicrobial		bt0374	4.90	3.83E-07	10
Trimethoprim Pharmaceutical Antibiotic		bt0023 bt0242	0.92	1.23E-12	400
Trinexepac-ethyl Pesticide Herbicide		bt0044	-2.37	4.23E-11	3

Table 1 (continued)

Valsartan Pharmaceutical Angiotensin receptor blocker		bt0051 bt0241 bt0242 bt0243 bt0334	0.43	3.33E-16	1
Venlafaxine Pharmaceutical Antidepressant		bt0023 bt0063 bt0241	0.84	3.37E-10	267
Warfarin Pharmaceutical Anticoagulant		bt0024	1.31	8.37E-14	17

Predicted biotransformation reactions were obtained from EnviPath; a full description of each biotransformation reaction ID is available at www.envipath.org/rule. Log D values were obtained through ChemAxon with JChem for Office (Excel). Henry's law constants and water solubilities were obtained through EPISuite at <http://www.chemspider.com>.

2.2.6 Micropollutant sampling and analysis

A 10 mL sample was collected from the inlet and outlet of each column and filtered to remove particulates (Acrodisc 25 mm syringe filter, 1 μ m glass fiber membrane, Sigma-Aldrich). Exactly 8 mL of the filtrate was transferred into 10 mL glass sample vials (Thermo Fisher Scientific) and stored at 4°C until analysis; all samples were analyzed within 24 hours of sampling. To quantify the MPs, a nine point calibration curve was created on the day of an analysis by diluting a stock mixture of pure reference standards with nanopure water. Both samples and calibration standards were spiked with 20 μ L of a mixture of isotopically labeled internal standards (see **Appendix E** for more details). A previously reported analytical method was used for the analysis of the MPs using high performance liquid chromatography (HPLC) coupled to high-resolution mass spectrometry (Helbling et al., 2010) and adjusted for large volume injections (see **Appendix C** for more details). After the MPs were quantified, the removal efficiency of each MP in each column was calculated using **Equation 4**. The removal efficiency describes only the loss of the parent compound and does not necessarily indicate complete mineralization.

$$\text{Removal efficiency (\%)} = \frac{C_i - C_e}{C_i} * 100 \quad \text{Equation 4}$$

where C_i and C_e are the influent and effluent MP concentrations, respectively.

Previous studies have shown that MP biotransformations occurring in steady-state biofilters can be modeled with pseudo-first-order kinetics (Bertelkamp et al., 2016a, 2015, 2014; Zearley and Summers, 2012). Pseudo-first-order rate constants (k') can be expressed by **Equation 5**.

$$k' = -\frac{\ln\left(\frac{C_e}{C_i}\right)}{EBCT} \quad \text{Equation 5}$$

To more accurately compare the performance of the biofilters, second-order rate constants (k_{bio}) were also calculated by means of **Equation 6**, which normalizes the pseudo-first-order rate constants by total biomass measurements (X_{tot}).

$$k_{bio} = -\frac{\ln\left(\frac{C_e}{C_i}\right)}{EBCT * X_{tot}} \quad \text{Equation 6}$$

2.2.7 Statistical analysis

All statistical analyses were performed using the R Statistical Software (R Core Team, 2016). Paired student's t-tests were conducted to assess the differences between duplicate biofilters. Tukey's honest significance difference tests (Tukey-HSD) were conducted to make pairwise comparisons across all column groups. For each MP, analysis of variance (ANOVA) was conducted to determine if removal was dependent on SV or the control filters vs the biofilters. The MP removal behavior was clustered using Ward's method (Murtagh and Legendre, 2014) to determine which MPs followed similar removal trends. Steady-state biomass is defined as the earliest time when both longitudinal dispersivity and surface biomass concentration are no longer changing with respect to time (one-way ANOVA). An alpha level of 0.05 was used to assess the significance of all statistical tests.

2.3 Results and Discussion

2.3.1 Spatial arrangement and concentration of biofilms

2.3.1.1 Longitudinal dispersivity

We used results from the carbamazepine tracer experiments to estimate the changes in longitudinal dispersivity in each of the biofilters at six time points throughout the experiment. Longitudinal dispersivity is a measure of the mechanical dispersion of a solute caused by variations in pore water velocity. Higher values of longitudinal dispersivity reflect more mechanical

dispersion and therefore more biomass growth. Changes in longitudinal dispersivity in the biofilters as a function of time are therefore indicative of biofilm growth. Results from tracer experiments and estimates of longitudinal dispersivity can be predictive of the extent of biological growth and the depth of the biological zone without the need to dismantle the columns to directly measure biomass concentrations (Seifert and Engesgaard, 2007; Suliman et al., 2006).

The results of the carbamazepine tracer studies are presented in **Figure 5**, where the estimated longitudinal dispersivity is presented for each filter group at days 1, 44, 105, 171, 241, and 297 of filter operation. The tracer breakthrough curves for days 44 and 241, modeled with **Equation 3**, are provided in **Appendix D (Figures D.1–D.4)**. The estimated longitudinal dispersivities for each pair of biofilters were not significantly different at any time point (paired t-tests, $p>0.05$), indicating that the rate of biological growth in duplicate experiments was consistent. The longitudinal dispersivity estimated among the control columns did not significantly change (t-test, $p>0.05$) from day 44 to 297, which confirms negligible biological growth throughout the experiment. At day 105, the estimated longitudinal dispersivity of biofilters B3a and B3ab (highest SV) increased significantly with respect to the control filters (Tukey-HSD, $p<0.05$). At day 171, the estimated longitudinal dispersivities of all of the biofilters were significantly greater than the control filters, and the estimated longitudinal dispersivities of the B3a group was significantly greater than the other biological column groups (Tukey-HSD, $p<0.05$). The estimated longitudinal dispersivity of the B3ab group was significantly less than the estimated longitudinal dispersivity of the B3a group, suggesting that there was less biological growth in the B3b group relative to the B3a group.

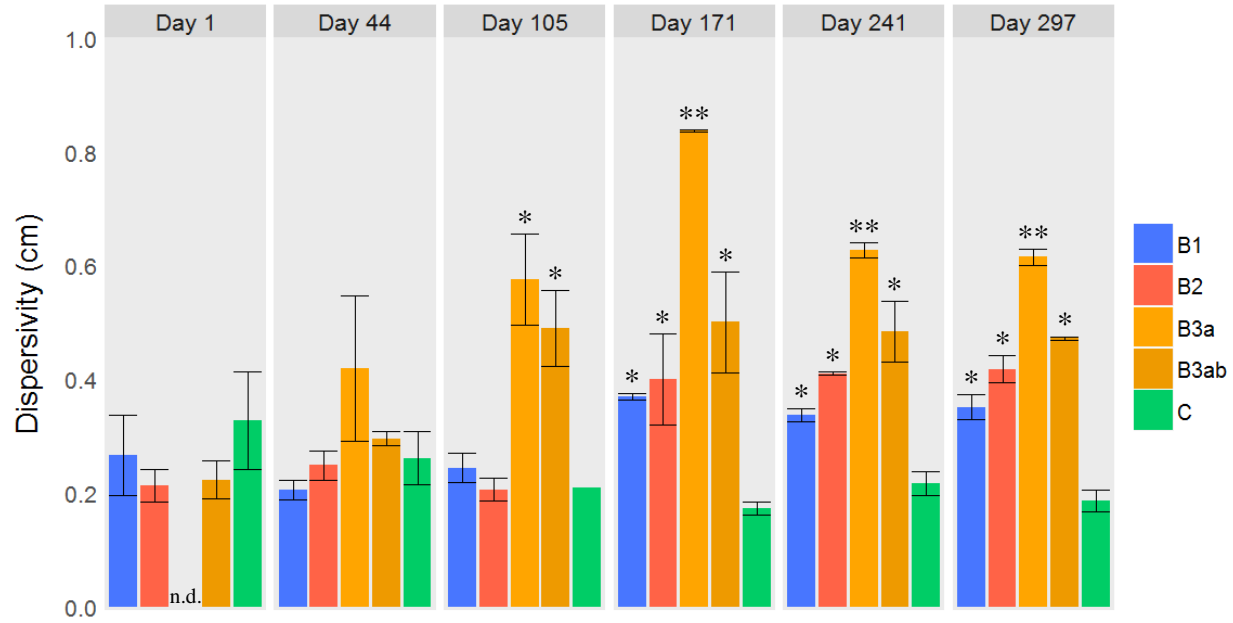


Figure 5: Average longitudinal dispersivity in each filter group for the duration of the experiment. For the biofilters (B1, B2, B3a, B3ab), error bars represent the values of duplicate measurements ($n=2$). For the control filters (C), error bars represent the standard deviation among the control filters ($n=4$). Bars denoted with one asterisk (*) are significantly different than the control groups, and bars denoted with two asterisks (**) are significantly different than all other groups (Tukey-HSD, $p<0.05$). Data is only shown for tracer studies where the mass recovery was greater than 85%. n.d. = no data.

Analysis of changes in longitudinal dispersivity with respect to time also provides insight on when the structure of the biofilm reaches a steady-state. We defined the time at which the biofilm structure attained a steady-state as the time when the longitudinal dispersivity was no longer changing with respect to time (one-way ANOVA, $p>0.05$). Based on this criterion, the B3a group reached steady-state at 105 days and the remaining biofilter groups reached steady-state at 171 days. Therefore, changes in MP removal performance from day 0 to day 171 could be attributed to the development of biomass, and changes in MP removal after day 171 could be attributed to changes in the activity of the microbial community. Subsequent analysis of MP removal focuses on data collected after day 171.

2.3.1.2 Surface biomass concentration

We used results from the total protein measurements from surface samples to approximate changes in surface biomass concentrations in each of the biofilters at ten time points throughout the experiment. Surface biomass concentrations provide a more direct measure of biological growth in the biofilters than longitudinal dispersivity, though these measurements were limited to surface samples whereas longitudinal dispersivity enables prediction of the extent of biological growth and the depth of the biological zone. We expected that surface biomass concentrations would increase as a function of time before reaching a steady-state concentration. Further, we expected that the time to reach a steady-state concentration and measured steady-state concentration would be a function of the hydrodynamics of the biofilter group.

The results of the total protein measurements are presented in **Figure 6**, where the estimated surface biomass concentration is presented for each filter group as a function of time. The estimated total protein measurements for each pair of biofilters were not significantly different at any time point (paired t-tests, $p > 0.05$), indicating that the rate of biological growth on the surface of each biofilter group was consistent. The surface biomass concentration in the control group had an average measured concentration of approximately $2.5 \mu\text{g protein per g dry sand}$ which represents the background level of the measurement. The initial surface biomass concentration in each of the biofilter groups was approximately $5.8 \pm 1.4 \mu\text{g protein per g dry sand}$ which is higher than the background level of the measurement and confirms the presence of microorganisms at the start of the experiment.

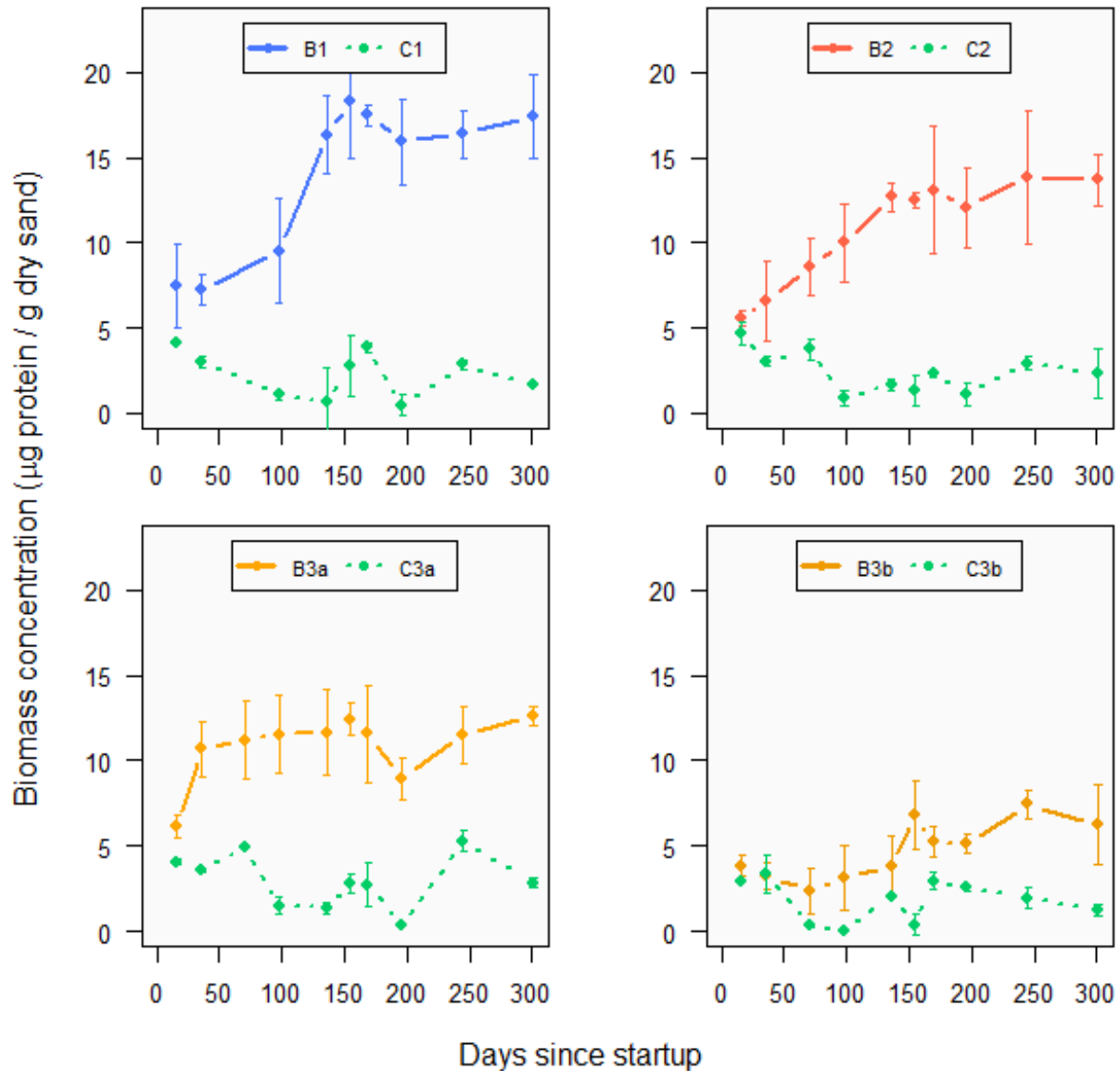


Figure 6: Average surface biomass concentration in each filter group for the duration of the experiment. For the biofilters (B1, B2, B3a, B3b), error bars represent the standard deviation between the duplicate biofilters and duplicate measurements (n=4). For the control filters (C1, C2, C3a, C3b), error bars represent the duplicate measurements (n=2).

The surface biomass concentration changed in each of the biofilter groups as a function of time, and the steady-state surface biomass concentration was clearly a function of the SV. The surface biomass concentration reached significantly greater levels in the B1 group (lowest SV) than in the other biofilter groups (Tukey-HSD, $p < 0.05$). The surface biomass concentration was also nominally greater in the B2 group (middle SV) than the B3a group (highest SV), though that

difference was not significant (Tukey-HSD, $p>0.05$). Surface biomass concentrations are controlled by the simultaneous growth and decay rates of the microbial communities and biofilm detachment. The negative association observed between maximum surface biomass concentration and SV in these experiments is likely due to more sloughing of biofilms at higher SVs. An investigation of two comparable full-scale biofiltration processes found more biomass at the surface of a full-scale biofilter operating at a SV of 0.05 m hr^{-1} compared to another full-scale biofilter operating at a SV of 0.10 m hr^{-1} and these differences were attributed to contact times influencing potential microbial growth in the biofilter beds (Collins et al., 1992). Finally, the B3b group had a significantly lower surface biomass concentration than the other biofilters (Tukey-HSD, $p<0.05$), suggesting that most of the primary substrate is utilized in the B3a group. Therefore, the B3b group is assumed to be an oligotrophic environment or otherwise carbon-limited environment. These data are corroborated by literature reports of decreasing biomass concentrations with biofilter bed depth (Bertelkamp et al., 2014; Carlson and Amy, 1998; Collins et al., 1992; Rauch-Williams et al., 2010; Urfer and Huck, 2001; Wang et al., 1995).

Analysis of changes in protein concentration with respect to time also provides insight on when the surface biomass concentration reaches a steady-state. We defined the time at which the surface biomass concentration attained a steady-state as the time when the protein concentration was no longer changing with respect to time (one-way ANOVA, $p>0.05$). Based on this criterion, the time required for the surface biomass concentrations to reach steady-state was significantly and negatively associated with SV. The B1 group reached steady-state in 135 days, the B2 group reached steady-state in 97 days, and the B3a group reached steady-state in 36 days. Other studies have shown that the time required for biomass concentrations at the tops of biofilters to reach steady-state is highly variable, ranging from a few weeks to several months (Liu, 2001; Urfer et

al., 1997; Urfer and Huck, 2001; Wang et al., 1995), though to the best of our knowledge, a clear association with SV has never been reported.

2.3.1.3 Total biomass

Because no differences in longitudinal dispersivity and surface biomass concentrations were observed between each pair of biofilters and because both measurements in all biofilter groups reached a steady-state by day 171, we sacrificed one of the duplicates from each biofilter group to measure total protein concentrations as a function of depth on day 301. Sand from each scarified biofilter was sampled at 1 cm intervals throughout the depth of the column. We expected these measurements to provide further evidence of the influence of the SV on the total biomass and the depth of the biological zone. The resulting profiles of biomass concentration as a function of filter depth are provided in **Figure 7**, where the concentrations are reported at the center of each segment of the sampled biofilter and the dashed vertical line represents the previously reported background level of the measurement. Biomass concentrations in the first segment agree with the steady-state surface biomass concentrations reported in **Figure 6**. The depth of the biological zone was deepest for the B3a group and shallowest for the B1 group (**Table 2**), reflecting a positive association between the depth of the biological zone and the SV at which the biofilter group was operated. These data are corroborated by literature reports showing that most of the biomass in full-scale biofiltration processes is in the top 5 cm of the filter bed (Collins et al., 1992; Urfer et al., 1997; Wang et al., 1995). These data also corroborate the conclusions made based on the longitudinal dispersivity measurements, demonstrating the value of tracer studies for predicting the depth of the biological zone. This positive association with SV has also been observed in biofilter groups operating at higher SVs (up to 9.7 m hr^{-1}) than this study (Carlson and Amy, 1998).

Higher SVs allow substrates to penetrate deeper into the filter bed and facilitate more microbial growth, thus increasing the depth of the biological zone.

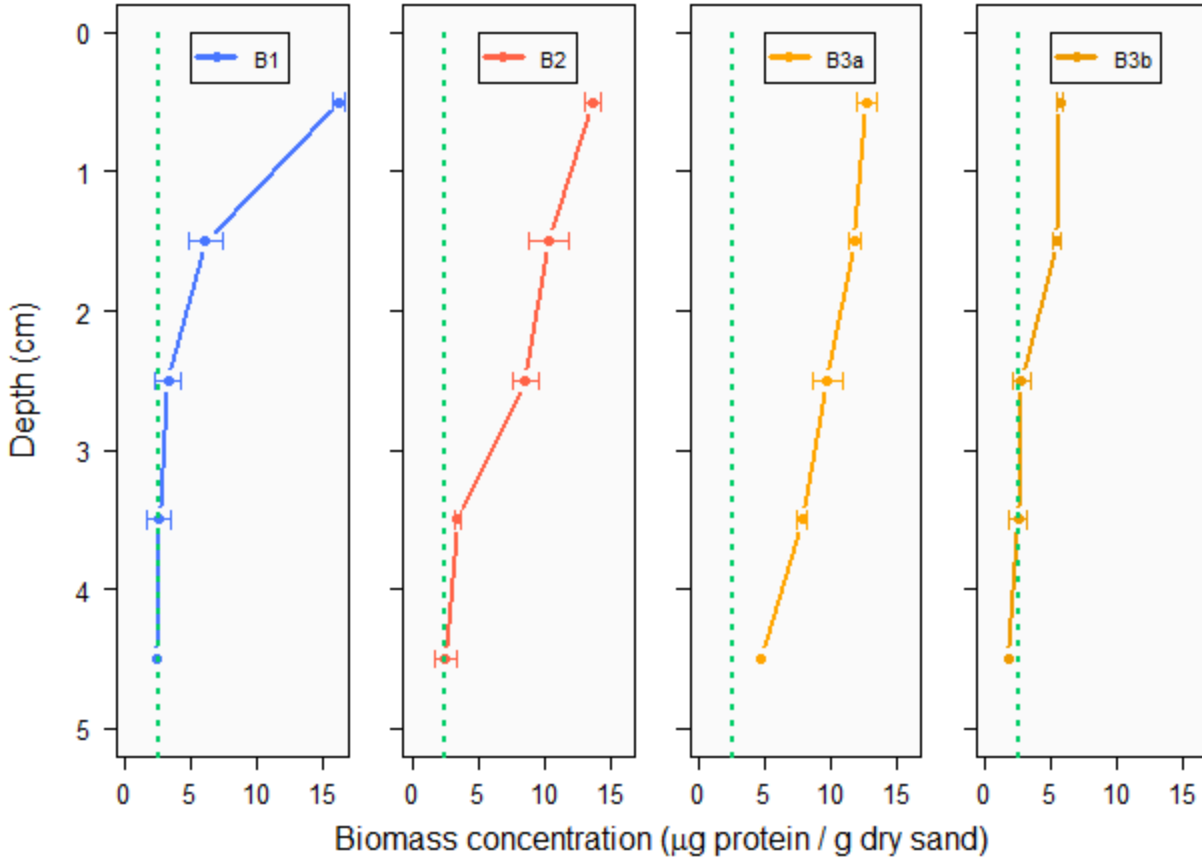


Figure 7: Biomass concentration profiles on day 301. For the biofilters (B1, B2, B3a, B3b), error bars represent duplicate measurements ($n=2$). The dashed line represents the average background level found in the abiotic control filters.

The biomass concentration profiles could also be used to estimate the total amount of biomass in each biofilter group. The biomass concentration profiles were integrated and the result was converted to total biomass using the dry density of the sand (1.47 g cm^{-3}) and the inner diameter of the columns (2.5 cm). The total biomass in each biofilter group is presented in **Table 2** and likewise reflects a positive association between the depth of the biological zone and SV. Greater organic loading rates caused by higher SVs likely attributed to this association by providing the biofilms with more substrates; although normalizing the total biomass in each

biofilter group by SV could not fully explain the differences in total biomass, as shown in **Table 2**. Although the B1 group had the highest surface biomass concentration, the B3a group had the highest total biomass. Based on these data, it could be expected that more MP removal would be observed for biofilters operated at higher SVs, though the reduced EBCT is a competing effect that could limit MP removal.

Table 2: Depth of the biological zone and total biomass found in each biofilter group.

Biofilter group	Superficial velocity, SV (cm hr ⁻¹)	Depth of the biological zone (cm)	Total biomass, X_{tot} (μg protein)	Normalized total biomass, X_{tot}/SV (μg protein hr m ⁻¹)
B1	10	2.5	131	13.1
B2	20	3.5	189	9.5
B3a	40	5.0	248	6.2
B3b	40	2.5	46	1.2
B3ab	40	7.5	294	7.4

2.3.2 Micropollutant removal

The primary objective of this work was to systematically explore SV to investigate the spatial arrangement and concentration of biofilms and how the consequent biofilm spatial arrangements of the biofilms affect MP biotransformation. The previous analyses demonstrate how different SVs influence the spatial arrangement of the biofilm—lower SVs lead to greater steady-state surface biomass concentrations, but shallower biological zones and lower total biomass. The consequences of these influences on MP removal in biofilters has not been systematically explored. We took samples from the influent and effluent of each filter over the duration of the experiment and measured the concentrations of 29 MPs to calculate removal efficiency (**Equation 4**). The removal efficiencies for each of the 29 MPs in each filter group as a function of time are presented in **Appendix F (Figures F.1–F.29)**. As observed with longitudinal dispersity and surface biomass concentrations, the calculated removal efficiencies of each MP for each pair

of biofilters were not significantly different at any time point (paired t-tests, $p>0.05$), indicating that performance of the biofilters was repeatable under each of the hydrodynamic regimes.

We aimed to characterize MP removal behavior in the biofiltration columns as a function of time. To do this, we used Ward's method to evaluate the similarity between removal efficiencies measured for each MP in both the biofilters and the control filters for the duration of the experiment as has been previously described for evaluating similar groups through a classical sum-of-squares criterion (Murtagh and Legendre, 2014). The resulting dendrogram is provided in **Figure 8**, which groups each of the MPs based on the similarity in which they are removed in each filter as a function of time. The clustering analysis suggests that the removal extent in the biofilters and the control filters is the dominant trend for grouping and not temporal patterns. The dendrogram reveals three distinct clusters at a height of approximately 600. Cluster A contains MPs that had no significant removal ($<10\%$ removal efficiency) in any filter throughout the duration of the experiment; these MPs are defined here as recalcitrant. Cluster B contains MPs that had low ($10\text{--}35\%$ removal efficiency) or moderate ($36\text{--}60\%$ removal efficiency) removal in some filters at some times throughout the duration of the experiment. Cluster C contains MPs that had high ($>60\%$ removal efficiency) removal in some filters at some times throughout the duration of the experiment. Additionally, clusters B and C could be divided further at a height of approximately 400 into groups that contain MPs that underwent abiotic removal (similar removal in the biofilters and abiotic control filters, one-way ANOVA, $p>0.05$) and biotic removal (significantly more removal in the biofilters than in the abiotic control filters, one-way ANOVA, $p<0.05$). **Table 3** summarizes the removal behaviors of the 29 MPs in our experiment and describes the removal efficiencies of these MPs found in several other studies which have examined similar biofiltration processes.

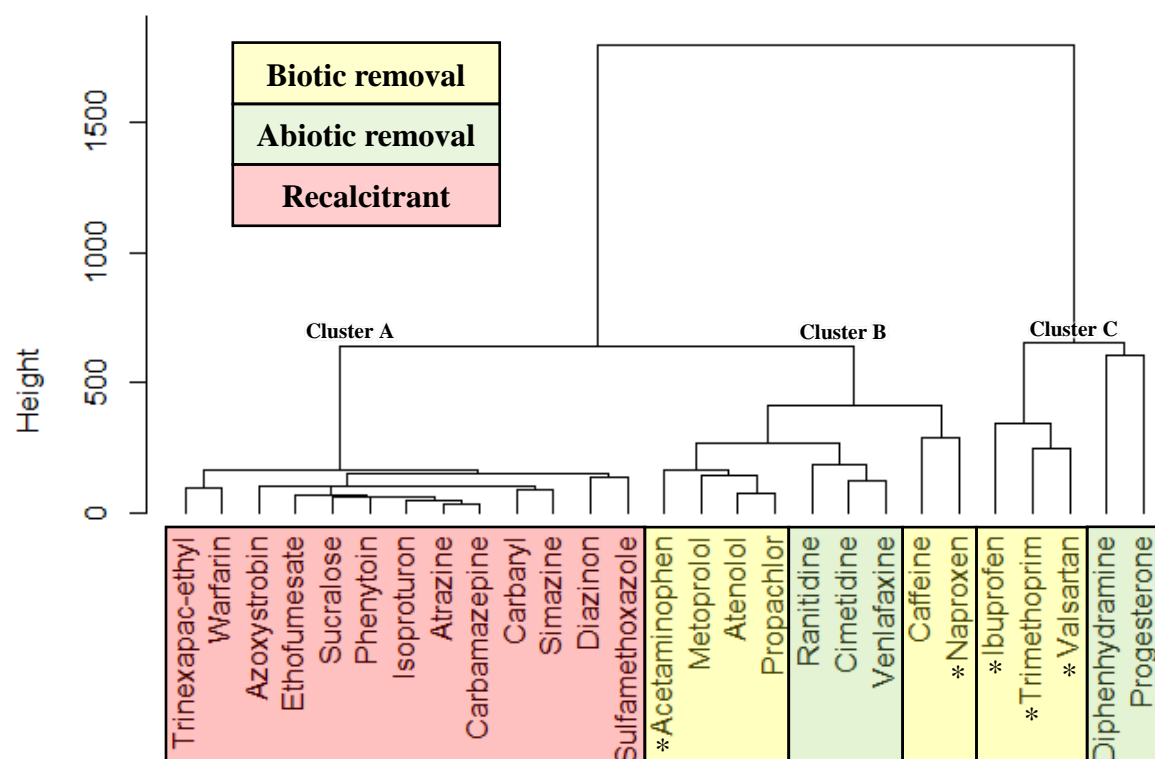


Figure 8: Dendrogram of micropollutant removal behavior for the duration of the experiment. Recalcitrant MPs have no significant removal in any filter. MPs with abiotic removal are removed in both the biofilters and abiotic control filters. MPs with biotic removal are removed significantly more in the biofilters than the control filters. Cluster A: no removal (<10%). Cluster B: low removal (10–35%) to moderate removal (35–60%). Cluster C: high removal (>60%). MPs with an asterisk (*) were removed (>10%) in the B3b group.

Table 3: Average removal efficiencies of micropollutants in biofiltration studies.

Micropollutant	Our Study		Other Studies		
	Removal behavior	Figure	Removal efficiencies (%)	Average removal ¹	Variability ²
Acetaminophen	Biotic (low)	Figure F.1	46 ^b , 91 ^g , 86–99 ^j , 59–79 ^k	High	High (n=18)
Atenolol	Biotic (low)	Figure F.2	10 ^g , 0 ⁱ , 68–99 ^j	High	High (n=7)
Atrazine	Recalcitrant	Figure F.3	0 ^b , 0 ^g , 2 ^{j1} , 1–13 ^j , 0.2–3 ^k	Recalcitrant	High (n=9)
Azoxystrobin	Recalcitrant	Figure F.4	n.d.	n.d.	n.d.
Caffeine	Biotic (moderate)	Figure F.5	29 ^b , 80 ^g , 33 ⁱ , 96–99 ^j , 67–80 ^{k1}	High	Moderate (n=10)
Carbamazepine	Recalcitrant	Figure F.6	1–4 ^a , 0 ^b , 0 ^g , 0 ⁱ , 0–10 ^j , 0.5–1.6 ^k	Recalcitrant	High (n=14)
Carbaryl	Recalcitrant	Figure F.7	3.3–17 ^k	Low	n.d. (n=2)
Cimetidine	Abiotic (low)	Figure F.8	17–97 ^j	High	Moderate (n=5)
Diazinon	Recalcitrant	Figure F.9	94 ^g , 12–40 ^k	Moderate	High (n=3)
Diphenhydramine	Abiotic (high)	Figure F.10	>99 ^j	High	Low (n=5)
Estrone	Biotic (high*)	Figure F.11	n.d.	n.d.	n.d.
Ethofumesate	Recalcitrant	Figure F.12	n.d.	n.d.	n.d.
Ibuprofen	Biotic (high)	Figure F.13	91–99 ^a , 43 ^b , 92–99 ^d , 97.2–99.7 ^e , 11–51 ^f , 95 ^g , 97–99 ^h , >95 ^k	High	Moderate (n=21)
Isoproturon	Recalcitrant	Figure F.14	n.d.	n.d.	n.d. (n=0)
Metoprolol	Biotic (low)	Figure F.15	5 ^b , 3 ^g , 8 ⁱ	Recalcitrant	Moderate (n=3)
Naproxen	Biotic (moderate)	Figure F.16	89–99 ^d , 23–99.1 ^e , 0–41 ^f , 60 ^g , 78–99 ^h , 72–86 ^k	High	High (n=17)
Phenytoin	Recalcitrant	Figure F.17	0 ^b , 5–15 ^f , 0 ^g , 19 ⁱ	Recalcitrant	High (n=7)
Progesterone	Abiotic (high)	Figure F.18	n.d.	n.d.	n.d. (n=0)
Propachlor	Biotic (low)	Figure F.19	n.d.	n.d.	n.d. (n=0)
Ranitidine	Abiotic (low)	Figure F.20	48 ⁱ	Moderate	n.d. (n=1)
Simazine	Recalcitrant	Figure F.21	6.8–8.2 ^k	Recalcitrant	n.d. (n=2)
Sucralose	Recalcitrant	Figure F.22	n.d.	n.d.	n.d. (n=0)

Table 3 (continued)

Sulfamethoxazole	Recalcitrant	Figure F.23	7–53 ^a , 0 ^b , 1 ^g , 0 ⁱ , 37–53 ^j , 2.4–4.4 ^k	Low	High (n=14)
Triclosan	Biotic (high*)	Figure F.24	93.5–95.5 ^e , 68–84 ^f , >90 ^k	High	Low (n=8)
Trimethoprim	Biotic (high)	Figure F.25	34 ^b , 5 ^g , 38 ⁱ , 11–87 ^j , 83–92 ^k	Moderate	High (n=10)
Trinexapac-ethyl	Recalcitrant	Figure F.26	n.d.	n.d.	n.d. (n=0)
Valsartan	Biotic (high)	Figure F.27	38 ^g	Moderate	n.d. (n=1)
Venlafaxine	Abiotic (low)	Figure F.28	0 ^g , 2 ⁱ	Recalcitrant	n.d. (n=2)
Warfarin	Recalcitrant	Figure F.29	39–68 ^k	Moderate	n.d. (n=2)

n.d. = no data; *removed below LOQs for the duration of the experiment; recalcitrant (<10% removal efficiency); low removal (10–35%); moderate removal (35–60%); high removal (>60%). ¹Average of all removal efficiency. ²Variability between reported removal efficiencies in all biotic columns (n>3) across all studies based on coefficient of variations: low variability (0–0.15); moderate variability (0.15–0.50); high variability (>0.50).

^a(Alidina et al., 2014) – estimated from bar chart; EBCT = 50 hours.

^b(Bertelkamp et al., 2014) – calculated from first-order rate constants; EBCT = 1 day.

^d(Krkošek et al., 2014) – EBCT = 17.7 hours.

^e(Onesios and Bouwer, 2012) – EBCT = 1 day.

^f(Onesios-Barry et al., 2014) – EBCT = 1 day.

^g(Rattier et al., 2014) – estimated from bar chart; EBCT = 8 minutes.

^h(Rauch-Williams et al., 2010) – calculated from influents and effluents; EBCT = 19 hours.

ⁱ(Reungoat et al., 2011) – estimated from bar chart; EBCT = 2 hours.

^j(Teerlink et al., 2012) – EBCT = 1–30 days.

^k(Zearley and Summers, 2012) – EBCT = 7.9–15.8 minutes.

2.3.2.1 Recalcitrance

Thirteen of the 29 MPs investigated were found to be recalcitrant in the biofilters throughout the duration of the experiment (atrazine, azoxystrobin, carbamazepine, carbaryl, ethofumesate, diazinon, isoproturon, phenytoin, simazine, sucralose, sulfamethoxazole, trinexapac-ethyl, and warfarin). To the best of our knowledge, the removal of azoxystrobin, ethofumesate, isoproturon, sucralose and trinexapac-ethyl in biofiltration processes has not previously been explored. Similar recalcitrant behaviors through biofiltration processes have been reported for atrazine, carbamazepine, carbaryl, phenytoin, and simazine, and is described in **Table 3**. These compounds were not removed in biofiltration processes with EBCTs ranging from 8 min to 30 days.

It is possible that removal efficiencies for some of these recalcitrant MPs are kinetically limited. For example, 53% removal of sulfamethoxazole was reported in biofiltration columns with EBCTs greater than 1 day (Alidina et al., 2014; Teerlink et al., 2012). However, our study and other studies involving similar biofiltration columns with short EBCTs (less than 2 hours) report less than 10% removal (Rattier et al., 2014; Reungoat et al., 2012; Zearley and Summers, 2012). This suggests that the biotransformation rate of sulfamethoxazole may be too small to observe removal in our study with EBCTs ranging from only 8–30 minutes. Additionally, variable removal behavior in biofiltration processes operating with similar EBCTs may be due to the absence or presence of specific microbial degraders. Up to 90% removal of diazinon and 68% removal of warfarin was reported in biofiltration columns with EBCTs of 8 min (Rattier et al., 2014; Zearley and Summers, 2012); however, these MPs are recalcitrant in our biofiltration system. The variable results between our study and the published literature could indicate that the bacteria capable of biotransforming diazinon and/or warfarin were not established in our biofilters.

2.3.2.2 Abiotic removal

Five MPs were removed to the same extent in both the biofilters and the abiotic control filters (cimetidine, diphenhydramine, progesterone, ranitidine, and venlafaxine). Possible abiotic removal mechanisms include photooxidation, hydrolysis, and adsorption. The columns were covered in aluminum foil to avoid potential photooxidation reactions, so those reactions are not likely to be important in this work. Furthermore, abiotic control experiments were conducted to decouple abiotic removal occurring in the feedwater (*e.g.* hydrolysis) and other abiotic removal mechanisms. See **Appendix B** for more details on the control experiments. The abiotic losses attributed to hydrolysis could be modeled assuming first-order kinetics and rate constants are less than 0.003 min^{-1} for all MPs. The average pseudo-first-order rate constants in the biofiltration columns for the abiotically removed MPs are at least an order of magnitude greater than those measured in the control experiments, suggesting abiotic hydrolysis of the MPs was negligible. Additionally, the estimated distribution coefficients ($\log D$, see **Table 1**) do not correlate with the abiotic removal in this system which suggests that adsorption may not be a major removal mechanism for these MPs. However, diphenhydramine has been previously found to be readily adsorbed to soils with over 90% of a solution containing 1 g L^{-1} diphenhydramine adsorbing to clay minerals within 15 minutes (Li et al., 2011). Diphenhydramine was also shown to be very persistent in different types of soils (loam, sandy loam, and clay loam)—50% dissipation times ranged from three months to a year (Topp et al., 2012). Progesterone has also been reported to be readily adsorbed to sand grains and silty loam with experimental K_d values of 33.3 and 207.2 L kg^{-1} , respectively (Sangster et al., 2015). Moreover, moderate to high removals of cimetidine and ranitidine has been reported in similar biofiltration processes; however, abiotic controls were not used in these studies and authors were unable to differentiate between biotic and abiotic

removal mechanisms (Reungoat et al., 2011; Teerlink et al., 2012). Venlafaxine has been reported to be recalcitrant in similar biofiltration processes (Rattier et al., 2014; Reungoat et al., 2011) but we observed low abiotic removal. Further investigation is needed to fully understand the abiotic removal occurring in this system.

2.3.2.3 Biotic removal

Eleven MPs underwent biotic removal in the biofilters (acetaminophen, atenolol, caffeine, estrone, ibuprofen, metoprolol, naproxen, propachlor, triclosan, trimethoprim, and valsartan). If any MP was removed below its limit of quantification (LOQ) on any particular sampling date, the LOQ was used as the effluent concentration in all subsequent calculations. **Table F.1** describes the average MP influent concentrations and the maximum recordable removal efficiencies based on the LOQs for each MP. For all biofilters, triclosan and estrone were removed below their respective LOQs for the duration of the experiment and therefore excluded from the subsequent analyses. To the best of our knowledge, the removals of estrone and propachlor in biofiltration processes have not previously been explored. Due to the low influent concentration of triclosan throughout the experiment, we were unable to accurately quantify the removal efficiencies; however, the high removal of triclosan has been reported in similar biofiltration processes (Onesios and Bouwer, 2012; Onesios-Barry et al., 2014; Zearley and Summers, 2012). The other compounds have been reported to undergo biotic removal in similar biofiltration processes as described in **Table 3**, but a systematic exploration of their removal based on hydrodynamics has not been reported. The reported removal efficiencies have considerable variability between studies and the following analyses were aimed to examine the effects of spatial arrangement of biomass and the biomass concentrations on MP removal.

2.3.2.4 Biotransformation extents and rates

We hypothesized that hydrodynamics influence the spatial arrangement and concentration of biofilms formed in biofiltration processes and consequently affect the biotransformation rates of MPs in different ways. The previous analyses demonstrate the effect of SV on the spatial arrangement and concentration of biofilms—higher SVs lead to lower steady-state surface biomass concentrations, but deeper biological zones and higher total biomass which we would expect to increase MP removal. However, higher SVs also result in shorter EBCTs which provides microbial communities less time to biotransform MPs and decreases MP removal. To investigate the consequences of the competing effects of EBCT and biomass on MP removal, we examined the average removal efficiencies, and pseudo-first-order and second-order rate constants in each biofilter group during steady-state total biomass conditions as determined through the estimated longitudinal dispersivities and surface biomass concentrations.

The average removal efficiencies, calculated with **Equation 4**, for the MPs that underwent biotic removal are presented in **Figure 9** for each group of biofilters between days 176–381 of filter operation. The removal efficiencies of acetaminophen, atenolol, trimethoprim, and valsartan were negatively associated with SV (one-way ANOVA, $p < 0.05$). In other words, the removal efficiencies of these compounds decrease with increasing SV and total biomass, and decreasing EBCT. This suggests that the effect of EBCT is more important than the effect of biomass for these compounds. A previous study showed the same correlation between removal efficiency and SV in wastewater biofiltration columns operated between 4–30 cm day⁻¹ for a subset of the MPs examined; higher removal efficiencies in the slower columns were attributed to increased contact time between the MPs and the biofilms (Teerlink et al., 2012). Conversely, the removal efficiencies of caffeine, ibuprofen, metoprolol, naproxen, and propachlor did not vary between hydrodynamic

regimes (B1, B2, and B3a) despite differences in EBCTs and biofilm spatial arrangements and concentrations (Tukey-HSD, $p>0.05$). This suggests that the competing effects of EBCT and biomass unexpectedly negate each other for these compounds. The higher SVs and organic loading rates applied to the B3ab group resulted in more total biomass than the B2 group despite being operated at the same EBCT (16 min) which lead to similar or greater removal efficiencies. A significant positive association between MP removal rates and organic loading rates was previously found in bench-scale microcosms simulating constructed wetlands (Sharif et al., 2014).

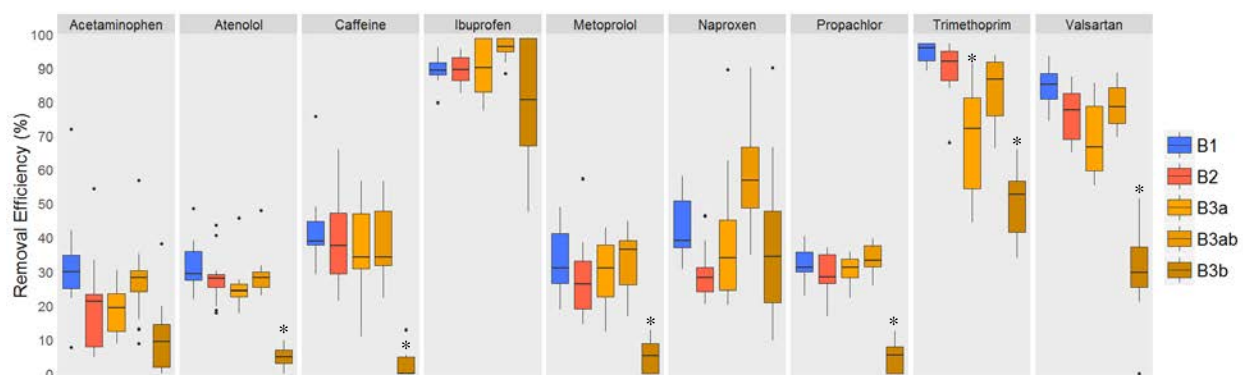


Figure 9: Average removal efficiencies of micropollutants that underwent biotic removal. Each box represents $n=14$ samples across days 171-381 of filter operation. Boxes denoted with an asterisk (*) are significantly different than all other groups (Tukey HSD, $p<0.05$).

Previous biofiltration studies have modeled MP removal with pseudo-first-order kinetics with the assumption of constant biomass concentrations (Bertelkamp et al., 2015, 2014; Zearley and Summers, 2012). The average pseudo-first-order rate constants, calculated with **Equation 5**, for the MPs that underwent biotic removal are presented in **Figure 10** for each group of biofilters between days 176–381 of filter operation. All of the pseudo-first-order biotransformation rate constants were positively associated with SV in the B1, B2, and B3a groups (one-way ANOVA, $p<0.05$), which confirms that the total active biomass is not constant between the biofilter groups. We previously demonstrated that the total biomass is not constant between the biofilter groups, as shown in **Table 2**.

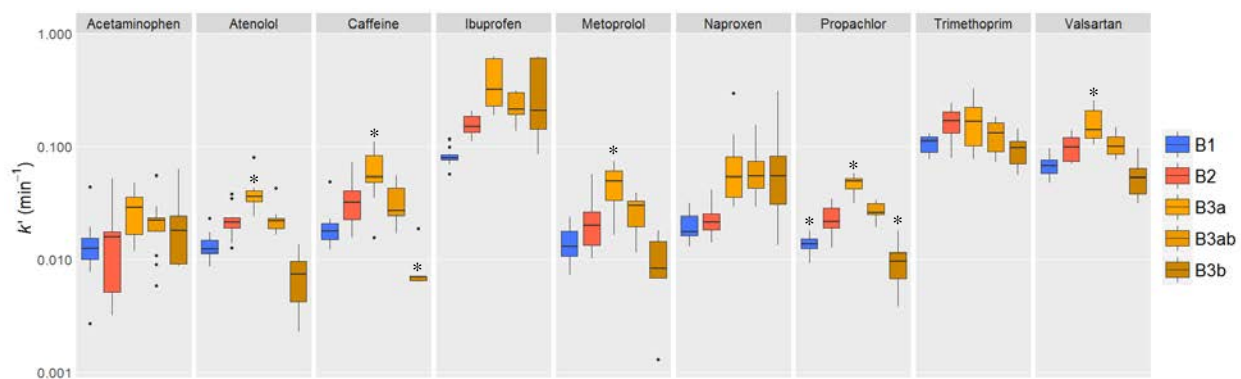


Figure 10: Average pseudo-first-order rate constants of micropollutants that underwent biotic removal. Each box represents n=14 samples across days 171–381 of filter operation. Boxes denoted with an asterisk (*) are significantly different than all other groups (Tukey HSD, $p < 0.05$).

Lastly, we examined the second-order rate constants, which effectively normalizes the pseudo-first-order rate constants by the total biomass measured in the biofilters. The average second-order rate constants, calculated with **Equation 6**, for the MPs that underwent biotic removal are presented in **Figure 11** for each group of biofilters between days 176–381 of filter operation. Second-order biotransformation rate constants were not significantly different between the B1, B2, and B3a groups (Tukey-HSD, $p > 0.05$). This analysis confirms that MP removal is a second-order process that is dependent on the total biomass. We measured total biomass using total protein concentrations throughout the depth of the biofilters, which seems to be a useful surrogate measure of active biomass in the biofiltration columns throughout the experiment. Additionally, the active fraction of the biomass must be consistent among the biofilter groups, suggesting that sloughing at higher SVs does not remove active biomass preferentially. Finally, it is clear that using pseudo-first order estimates of MP rate constants may misrepresent performance estimates when applied in practice.

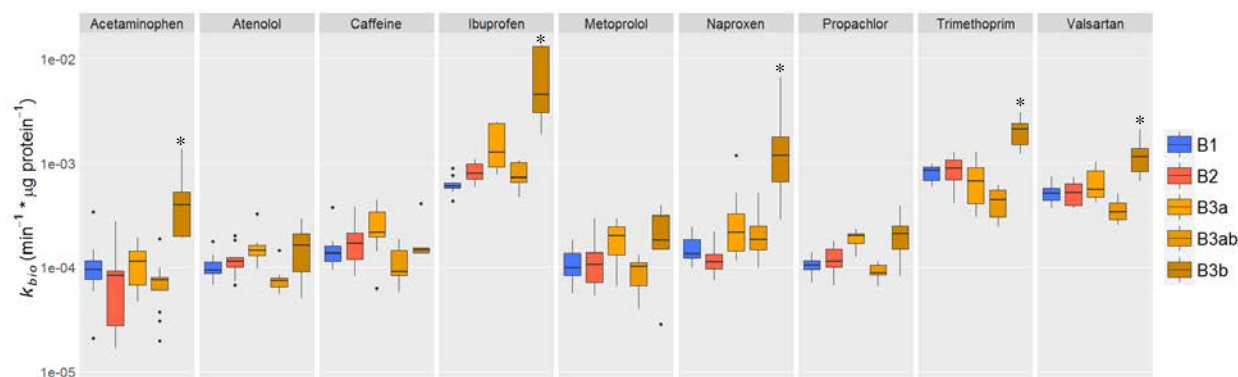


Figure 11: Average second-order rate constants of micropollutants that underwent biotic removal. Each box represents n=14 samples across days 171-381 of filter operation. Boxes denoted with an asterisk (*) are significantly different than all other groups (Tukey HSD, $p < 0.05$).

2.3.2.5 Oligotrophic environments

As shown in **Figure 7**, the B3b group was characterized as having low total biomass and is assumed to be an oligotrophic or otherwise carbon-limited environment. Nevertheless, significant removal (>10% removal efficiency) of acetaminophen, ibuprofen, naproxen, trimethoprim, and valsartan was observed in these columns, as shown in **Figure 9**. We also observed significantly greater second-order rate constants for these MPs in the B3b group (Tukey-HSD, $p < 0.05$), as shown in **Figure 11**. This suggests either an increase in microbial activity towards these MPs or an increase in the active fraction of the biomass in oligotrophic or carbon-limited environments. Additionally, we investigated if the significantly greater second-order rate constants in the B3b group were a consequence of an absolute error in the total protein measurements. The total biomass would need to be at least three times the measured amount for these second-order rate constants to be similar across the biofilter groups; however, the second-order rate constants of the other MPs would now be significantly less in the B3b group than the other biofilter groups. Therefore, it is unlikely that errors in the biomass measurements occurred to this extent.

Biofilters with oligotrophic or carbon-limited environments are characterized as having low biomass concentrations but have been previously observed to have greater microbial activity towards MPs. Biofiltration columns operated under low biodegradable organic carbon conditions promoted less biomass growth but led to similar or higher removal efficiencies of MPs when compared to columns supplied with higher substrate concentrations (Bertelkamp et al., 2016a; Hoppe-Jones et al., 2012; Rauch-Williams et al., 2010). Additionally, higher humic acid content and lower biodegradable organic carbon concentrations promoted more biodiverse microbial communities in soil columns and more biodiverse communities were found at deeper filter bed depths (D. Li et al., 2014). A recent study showed a significant positive association between biodiversity and the collective rate of multiple MP biotransformations (Johnson et al., 2015a). In our study, each of the biofilters received the same feedwater but an oligotrophic environment likely developed at deeper biofilter depths where there was less primary substrate available. Oligotrophic environments can lead to mixed-substrate utilization and the potential for more microbial activity and enzyme production capable of performing more diverse biotransformation reactions (Daughton and Ternes, 1999; Egli, 2010, 1995). The normalized biomass activity to amount of viable biomass has also been shown to increase with filter bed depth by up to two orders of magnitude (Urfer and Huck, 2001). We hypothesize that the microbial communities in the B3b group are either expressing different types of enzymes than the microbial communities in the other biofilter groups or are over-expressing the same enzymes, resulting in higher second-order rate constants. We can assess this hypothesis by examining the types of biotransformation reactions occurring in the biofilters.

2.3.2.6 Transformation product formation

We aimed to characterize the influence of hydrodynamics on the types of biotransformation reactions that are occurring by identifying TPs in the biofilter effluents. The analytical methods used to analyze and confirm the TPs are summarized in **Appendix G**. A list of 53 TPs for the 11 MPs that underwent biotic removal was compiled from the literature and predicted using EnviPath. We confirmed the presence of 15 TPs for 8 different parent MPs. The identified TPs are provided in **Appendix G (Figures G.1–G.15)** where chromatographic peaks, mass spectra, and MS/MS fragments are reported for each TP. All TPs are reported with a confidence of Level 1 (confirmed structure by reference standard) or Level 2 (probable structure by library/diagnostic evidence) as described in Schymanski et al., 2014.

The different hydrodynamic regimes did not have a significant impact on the formation of the TPs nor the types of biotransformation reactions occurring. A variety of biotransformation reaction types were observed including amide dealkylation, amide hydrolysis, ether dealkylation, glutathione coupling, and hydroxylation of aliphatics and aromatics. However, all of the identified TPs were found in the effluent of each biofilter group (B1, B2, B3a, and B3b). It is likely that the range of SVs examined did not have an influence on the microbial community composition of each biofilter. Additionally, we also previously demonstrated that the biofilters with oligotrophic or carbon-limited environments had significantly greater second-order rate constants towards some MPs and hypothesized that either different reactions were occurring due to new enzyme production or the same reactions were occurring at higher rates due to enzyme over-expression. We identified multiple TPs for trimethoprim, propachlor, and valsartan. The relative distribution of the various TPs formed in each biofilter is shown in **Figure 12**, where the average of triplicate chromatographic peak areas normalized to the sum of the peak areas for all TPs are shown for each

biofilter group and for each parent MP. The relative distributions did not significantly differ between biofilter groups (multiple t-tests, $p>0.05$) which suggests that there is not a shift of the preferred or utilized microbial pathways. The oligotrophic environment non-selectively increased the activity of the microbial communities and did not influence the types of reactions occurring.

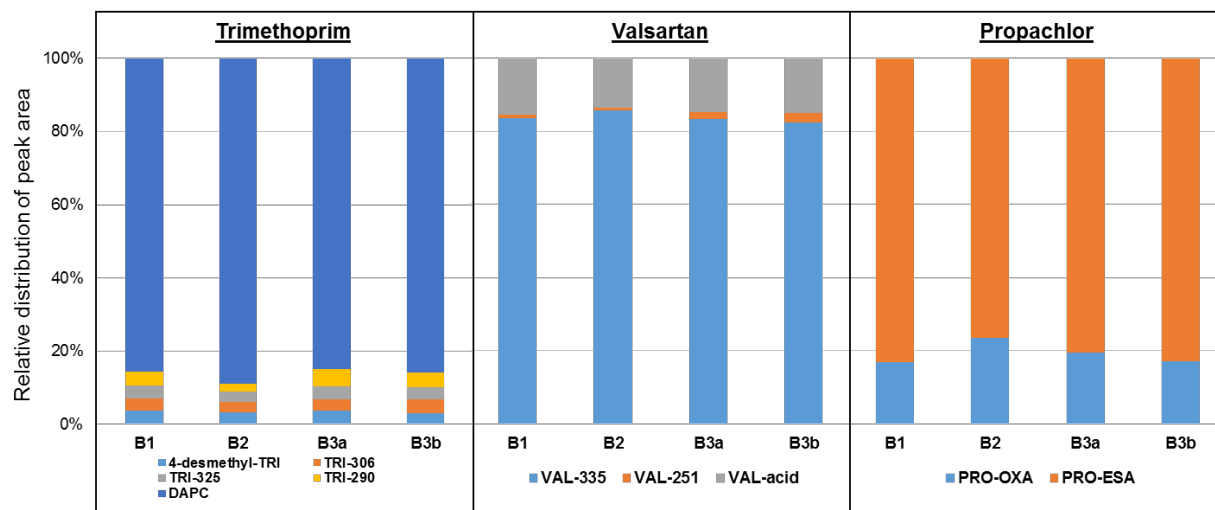


Figure 12: Relative distributions of transformation products formed in each biofilter. The relative distribution of the TPs represent the average of triplicate chromatographic peak areas normalized to the sum of the peak areas for all TPs in each biofilter group and for a parent MP.

Our analyses showed that the role of hydrodynamics in biofiltration processes is important for MP removal. First, we demonstrated that the SV at which a biofilter is operated is negatively associated with surface biomass, but positively associated with the depth of the biological zone and total biomass. Deeper biofilter bed depths (represented by the B3b group) were characterized as having low total biomass, and are assumed to be oligotrophic or otherwise carbon-limited environments. Second, we demonstrated that MP removal is a second-order process that is dependent on the total biomass and that certain MPs had significantly higher second-order rate constants in the B3b group. Finally, this TP analysis suggests that the microbial communities are likely over-expressing the same enzymes that are produced in shallower biofilter bed depths and are not preferential towards any type of biotransformation reaction.

2.4 Conclusions

- The hydrodynamics of the biofiltration columns altered the spatial arrangement and concentration of biofilms formed on the filter media. We observed that higher superficial velocities, within the range examined ($0.1\text{--}0.4\text{ m h}^{-1}$), led to less concentrated surface biomass but a deeper biological zone and more total biomass.
- Different hydrodynamic regimes resulted in similar removal efficiencies for caffeine, ibuprofen, metoprolol, naproxen, and propachlor which indicates that any potential effects of hydrodynamics were negated. However, the removal efficiencies of acetaminophen, atenolol, trimethoprim, and valsartan were negatively associated with SV which suggests that the effect of EBCT is more important than the effect of total biomass for these compounds.
- All of the pseudo-first-order rate constants for the MPs that underwent biotic removal were significantly and positively associated with SV and total biomass in the B1, B2, and B3a groups. Second-order rate constants for all MPs were not significantly different across the B1, B2, and B3a groups which indicates that MP removal in biofiltration columns is second-order overall with respect to concentration and biomass, and is best modeled by second-order rate constants.
- Additional removal of acetaminophen, ibuprofen, naproxen, trimethoprim, and valsartan was observed in oligotrophic or carbon-limited environments found at deeper biofilter depths. We observed that the sparser microbial communities found deeper in the biofilter beds were contributing to MP biotransformations at greater second-order rates than the higher biofilm concentration biofilters which indicates that deeper biofilms have greater microbial activity towards some MPs than the biofilms found in shallower filter depths.

- The identification of 15 TPs in the effluents of all biofilter groups indicates that the different hydrodynamic regimes did not have a significant impact on the formation of the TPs nor the types of biotransformation reactions occurring. The relative distribution of the TPs formed in each biofilter did not significantly differ between biofilter groups which suggests that the oligotrophic environment non-selectively increased the activity of the B3b group microbial communities.

CHAPTER 3: Future work

We must continue to improve our understanding of biofiltration processes through research to garner widespread acceptance and usage. Among responses from a biofiltration process survey sent to water utility managers, regulators, academics, and other professional groups, MP removal was the most popular research priority (Evans et al., 2010). Biofiltration is an exciting solution for MP removal during drinking water production with broad appeal for its sustainable advantages.

The data presented in this thesis demonstrate that biofiltration processes are capable of biotransforming multiple MPs and that the biotransformation rates of select MPs are dependent on the hydrodynamics of the system. We also demonstrated that MP removal is a second-order process that is dependent on the concentration of biomass. It is also clear that using pseudo-first-order estimates of MP rate constants may misrepresent performance estimates when applied in practice and future studies should report second-order rate constants for more direct comparisons between different biofilters and across different studies.

Estimates of longitudinal dispersity from tracer studies and surface biomass measurements can be used to assess total biomass. In our study, steady-state total biomass is defined as the earliest time when both longitudinal dispersivity and surface biomass concentration are no longer changing with respect to time. However, the biofilters had to be disassembled to measure the total biomass by total protein measurements through the depth of the biofilters. Future studies should examine ways to mathematically relate results from tracer studies and surface biomass measurements to total biomass to enable estimates of second-order rate constants without sacrificing the biofilters.

In addition to examining the biomass concentrations, it is important to consider the formation of TPs through biofiltration processes. To the best of our knowledge, no other

continuously operated biofiltration study has examined the formation of TPs. The development of high-resolution mass spectrometry has allowed researchers to supplement their targeted analysis with suspect and non-target screening methods (Schymanski et al., 2015). These methods have been applied to examine MPs in surface waters (Ruff et al., 2015) and wastewater effluents (Singer et al., 2016), as well as for the elucidation of TPs in activated sludge processes (Gulde et al., 2016; Helbling et al., 2010). The identification of TPs is essential to improving our understanding of biofiltration processes. TP analyses can provide insights into the types of biotransformation reactions that are occurring through inference of relevant reaction pathways. Subsequent predictions about how other MPs might biotransform in the same system can be made. This type of analysis can also be used to determine what types of biotransformation reactions are not commonly occurring in biofiltration systems. MPs that are predicted to undergo biotransformation reactions that are not commonly occurring in biofiltration systems are unlikely to be removed through biofiltration processes. Additionally, TP analyses are important because the disappearance of MPs may not coincide with decreases in toxicity. Biofilter effluents may retain toxic activity if MPs are not mineralized and/or the biotransformation reactions produce toxic TPs. Therefore, future research should focus on identifying the relevant types of biotransformation reactions that are contributing to MP removal in biofiltration processes.

Future research should continue to focus on ways to improve MP removal. Thirteen of the 29 MPs examined in our study were removed by less than 10%. A recent study showed a significant positive association between biodiversity in activated sludge processes and the collective rate of multiple MP biotransformations (Johnson et al., 2015a). The relationship between biodiversity and biotransformation rates should also be explored for biofiltration processes as both processes rely on microbial communities to biotransform MPs. One recent biofiltration study showed that less

biodegradable organic carbon concentrations promoted more biodiverse microbial communities and more biodiverse communities were found at deeper filter bed depths (D. Li et al., 2014). However, our results indicated no changes in the types of biotransformation reactions occurring at deeper filter bed depths. Other factors should be explored to increase the biodiversity of the microbial communities while maintaining sufficient total biomass and EBCTs to effectively remove MPs during drinking water production. For example, previous biofiltration studies have focused on the associations between the amount and type of carbon substrates added (Bertelkamp et al., 2016a; D. Li et al., 2014; Onesios and Bouwer, 2012; Rauch-Williams et al., 2010); however, the activity and diversity of a microbial community can be determined by the amount and type of carbon and nitrogen substrates available in the environment (Johnson et al., 2015b). Therefore, future investigations should also include supplemental nitrogen substrates to identify conditions that support the growth of more diverse microbial communities that consequently perform more types of MP biotransformations.

The focus of the experiments presented in this thesis was on sand biofiltration for drinking water treatment applications. Additional types of biofiltration should be explored to expand our knowledge of biofiltration processes from engineered DWTP applications to natural environmental applications. For example, most biofiltration studies are conducted with clean sand, but there has been recent interest in soil biofiltration studies using soils sampled from field sites (*e.g.* Bertelkamp et al., 2015) to more accurately replicate field conditions in the laboratory. For example, the leach fields associated with onsite wastewater treatment systems such as septic tanks are underexplored biofiltration processes. Leach fields are expected to harbor microbial communities that perform important environmental services, through their role in MP attenuation from septic leachate is poorly understood. Septic systems are used by approximately 20-25% of

U.S. households (Vedachalam et al., 2015) and can contribute to MP loading in groundwater (Del Rosario et al., 2014; Hinkle et al., 2005; Phillips et al., 2015) and surface water (Fairbairn et al., 2015; Karpuzcu et al., 2014; Schenck et al., 2015). However, the factors controlling MP loading from septic systems to receiving waters are mostly unknown.

Future studies aimed at improving our understanding of biofiltration processes will allow us to optimize their design and operation. The work presented in this thesis explored the consequences of changing SV on biomass formation and MP removal in biofiltration processes for drinking water production. Continued research and discussion will help broaden the acceptance and usage of biofiltration processes and will enable their optimization for MP removal.

APPENDICES

TABLE OF CONTENTS

Appendix A: Filter design and column setup	64
Appendix B: Control experiments.....	65
Appendix C: Analytical methods	68
Appendix D: Tracer experiments.....	72
Appendix E: Micropollutant information.....	74
Appendix F: Micropollutant removal	84
Appendix G: Transformation product identification	115

Appendix A: Filter design and column setup

Table A.1: Target and actual filter flow rates, empty bed contact times, and superficial velocities for each column for the duration of the experiment.

Column group	Filter	Target			Actual*		
		Flow (mL hr ⁻¹)	EBCT (min)	SV (cm hr ⁻¹)	Flow (mL hr ⁻¹)	EBCT (min)	SV (cm hr ⁻¹)
Group 1	B1-1	48	31	10	52 ± 1	28.6 ± 0.6	10.5 ± 0.2
	B1-2				51 ± 3	29.0 ± 1.6	10.4 ± 0.5
	C1				51 ± 2	28.9 ± 1.3	10.4 ± 0.5
Group 2	B2-1	95	16	20	97 ± 4	15.2 ± 0.6	19.8 ± 0.9
	B2-2				97 ± 5	15.2 ± 0.8	19.8 ± 1.0
	C2				100 ± 4	14.8 ± 1.3	20.3 ± 0.8
Group 3a & Group 3b	B3-1a B3-1b	190	8	40	191 ± 7	7.7 ± 0.3	38.9 ± 1.4
	B3-2a B3-1b				193 ± 8	7.7 ± 0.3	39.2 ± 1.7
	C3a C3b				197 ± 9	7.5 ± 0.3	40.1 ± 1.8
Group 3ab	B3-1ab	190	16	40	191 ± 7	15.4 ± 0.6	38.9 ± 1.4
	B3-2ab				193 ± 8	15.3 ± 0.7	39.2 ± 1.7
	C3ab				197 ± 9	15.0 ± 0.6	40.1 ± 1.8

*Measured average and standard deviation data are based on n=20 measurements over the 381 day experiment.

Appendix B: Control experiments

Control experiments were conducted to assess the stability of the micropollutants (MPs) in the MP and acetate stock solution between weekly replenishing. Three reactors (50 mL erlenmeyer flasks) wrapped in aluminum foil each received 20 mL of nanopure water spiked with MPs at a target concentration of $50 \mu\text{g L}^{-1}$ and sodium acetate at 70 mg L^{-1} . Seven samples were taken over the course 8 days, diluted with nanopure, and analyzed as described in **Appendix C**. Results indicate minimal losses over the course of 8 days and follow first-order kinetics. Samples were always taken from the columns within 24 hours of replenishing the MP and acetate stock solution to maintain constant influent concentrations. First-order abiotic transformation rate constants (k_{stock}) were estimated by semi-logarithmic plots and presented in **Table B.1**.

Similarly, abiotic control experiments were carried out to examine the abiotic transformation rates of the MPs in the feedwater. Briefly, 100 mL of autoclaved tap water supplemented with 1 mg L^{-1} acetate and 2 mg L^{-1} sodium metabisulfite was added to triplicate reactors (250 mL erlenmeyer flasks) and wrapped in aluminum foil. Then, MPs were spiked into each reactor at $1 \mu\text{g L}^{-1}$, sampled at seven time points within 120 minutes, and analyzed as described in **Appendix C**. Results indicate no to minimal losses of MPs and follow first-order kinetics. First-order abiotic transformation rate constants (k_a) were estimated by semi-logarithmic plots and presented in **Table B.1**.

Table B.1: Results of the micropollutant control experiments.

Micropollutant	Stock solution stability			Abiotic processes		
	t = 0 days ^a (ng L ⁻¹)	t = 8 days ^a (ng L ⁻¹)	k _{stock} (day ⁻¹)	t = 0 min ^a (ng L ⁻¹)	t = 120 min ^a (ng L ⁻¹)	k _a (min ⁻¹)
Acetaminophen	1536 ± 60	1609 ± 53	0	1072 ± 87	1127 ± 96	0
Atenolol	1359 ± 19	1328 ± 25	0.004	1029 ± 20	1055 ± 32	0
Atrazine	1377 ± 23	1392 ± 35	0	1089 ± 10	1109 ± 27	0
Azoxystrobin	1502 ± 94	1443 ± 59	0	1195 ± 64	1212 ± 69	0
Caffeine	1366 ± 28	1417 ± 32	0	1073 ± 62	1069 ± 37	0
Carbamazepine	1370 ± 51	1368 ± 38	0	1065 ± 11	1068 ± 26	0
Carbaryl	1288 ± 138	956 ± 43	0.021	1021 ± 56	860 ± 114	0.002
Cimetidine	1331 ± 9	1251 ± 10	0.009	1030 ± 26	959 ± 164	0.001
Diazinon	1241 ± 43	1140 ± 7	0.009	1097 ± 33	1027 ± 77	0
Diphenhydramine	1381 ± 10	841 ± 157	0.069	956 ± 54	775 ± 137	0.003
Estrone	1280 ± 195	1240 ± 95	0	1217 ± 48	1178 ± 27	0
Ethofumesate	1403 ± 28	1332 ± 41	0.004	1094 ± 16	1081 ± 65	0
Ibuprofen	1348 ± 38	1340 ± 31	0	1069 ± 16	1088 ± 51	0
Isoproturon	1356 ± 13	1355 ± 30	0	1060 ± 10	1080 ± 37	0
Metoprolol	1016 ± 89	984 ± 49	0	952 ± 190	896 ± 164	0
Naproxen	1344 ± 54	1258 ± 20	0	1070 ± 45	1050 ± 51	0
Phenytoin	1327 ± 78	1330 ± 45	0	940 ± 179	884 ± 195	0
Progesterone	1114 ± 94	990 ± 71	0.006	1209 ± 173	1311 ± 224	0

Table B.1 (continued)

Propachlor	1354 ± 40	1331 ± 79	0	1063 ± 31	1079 ± 36	0
Ranitidine	830 ^b ± 63	718 ± 129	0.018	1044 ± 29	988 ± 156	0.001
Simazine	1215 ± 63	1251 ± 63	0	931 ± 60	968 ± 46	0
Sucralose	1373 ± 27	1302 ± 42	0.004	1247 ± 32	1170 ± 48	0
Sulfamethoxazole	1354 ± 12	1363 ± 12	0	1037 ± 17	1043 ± 20	0
Triclosan	1322 ± 97	1329 ± 19	0	1292 ± 183	1405 ± 196	0
Trimethoprim	1093 ± 34	799 ± 26	0.049	1004 ± 37	1010 ± 12	0
Trinexapac-ethyl	1417 ± 19	1397 ± 115	0.003	966 ± 35	979 ± 36	0
Valsartan	1158 ± 41	1066 ± 60	0.007	1351 ± 75	1398 ± 14	0
Venlafaxine	1418 ± 26	1378 ± 53	0.002	1124 ± 47	1066 ± 54	0
Warfarin	1334 ± 94	1233 ± 156	0.007	1196 ± 56	1224 ± 36	0

^aAverage ± standard deviation. ^bDay 0 concentrations were excluded.

Appendix C: Analytical methods

Analysis of carbamazepine for the tracer experiments

Concentrations of carbamazepine were measured using a high performance liquid chromatography (HPLC) system coupled to an UltiMate 3000 RS Variable Wavelength Detector (Thermo Fisher Scientific). All data acquisition and processing was conducted using Dionex Chromeleon 7.2 (Thermo Fisher Scientific). The mobile phase consisted of HPLC-grade methanol (OmniSolv, VWR, Radnor, PA) and HPLC-grade water (OmniSolv, VWR). To quantify carbamazepine, a nine point calibration was prepared by diluting a stock mixture of pure carbamazepine (Sigma-Aldrich) with nanopure water. Standards and samples were injected at 20 μL into an Acclaim 120 C-18 analytical column (4.6 x 100 mm, particle size 5 μm , Thermo Fisher Scientific) with a mobile phase of 30:70 water:methanol and elution was achieved with an isocratic flow at 0.600 mL min^{-1} . The wavelength detector was set to the peak absorbance of carbamazepine, 285 nm. A full spectrum scan of carbamazepine is provided in **Figure C.1**. The retention time (RT) of carbamazepine was 3.9 min.

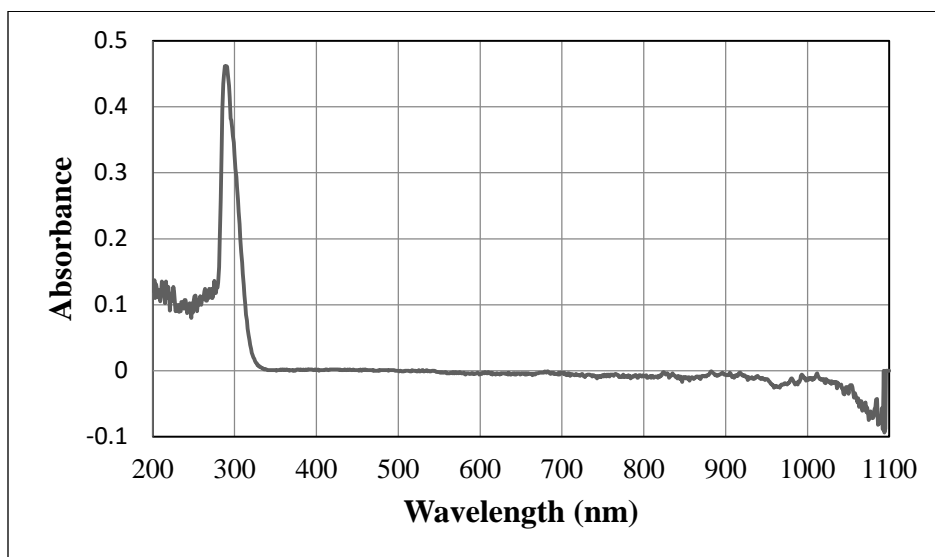


Figure C.1: Full spectrum scan of carbamazepine at 10 mg L^{-1} .

Analysis of micropollutants

A previously reported analytical method was used for the analysis of the MPs using HPLC coupled to high-resolution mass spectrometry, and adjusted for large volume injections (Helbling et al., 2010). Briefly, we used an HPLC system coupled to a QExactive quadrupole-orbitrap mass spectrometer (Thermo Fisher Scientific, Waltham, MA). The mobile phase consisted of HPLC-grade water (OmniSolv, VWR) and HPLC-grade methanol (OmniSolv, VWR), each supplemented with 0.1% formic acid (98-100%, Thermo Fisher Scientific) by volume. Mobile phase was pumped at 1 mL min⁻¹ via a low-pressure loading pump into an XBridge C-18 trap column (2.1 x 20 mm, particle size 5 µm, Waters, Milford, MA). Samples were injected at 5 mL into the trap column using an isocratic flow of 98:2 water:methanol; the complete loading pump gradient is provided in **Table C.1**. Elution from the trap column was achieved with a high pressure elution pump delivering an initial mobile phase of 90:10 water:methanol at 0.200 mL min⁻¹. Separation of analytes occurred on an XBridge C-18 analytical column (2.1 x 50 mm, particle size 3.5 µm) at 25°C following the gradient provided in **Table C.2**.

All data acquisition and processing was conducted using XCalibur v3.1 (Thermo Fisher Scientific). The mass spectrometer was equipped with a heated electrospray ionization source and was used in both positive and negative modes. Mass calibrations and mass accuracy checks were conducted prior to each analysis. The scan range was set to 100–500 mass-to-charge (m/z) and the resolution was set to 70,000. Data dependent MS/MS was acquired at the exact mass of the dominant adduct for each analyte. The limit of quantification (LOQ) of each analyte was determined by the lowest concentration point in a matrix matched calibration row with a peak at the correct RT containing at least five MS scans and at least one matching MS/MS product ion. Analytes were quantified using internal calibration standards (isotopically labeled), based on the

ratio of the analyte to the internal standard area responses, and by 1/x weighted linear least-squares regression. For reference standard ionization behaviors, adduct m/z, retention times, LOQs, and internal standard assignments, see **Appendix E**.

Table C.1: Loading pump gradient for micropollutant analyses.

Retention time (min)	Flow (mL/min)	%A (HPLC-grade water with 0.1% formic acid)	%B (HPLC-grade methanol with 0.1% formic acid)
0	1.000	98	2
5.1	1.000	98	2
5.11	0.000	98	2
30.2	0.000	98	2
30.3	1.000	2	98
34.3	1.000	2	98
34.4	1.000	98	2
35.6	1.000	98	2

Table C.2: Elution pump gradient for micropollutant analyses.

Retention time (min)	Flow (mL/min)	%A (HPLC-grade water with 0.1% formic acid)	%B (HPLC-grade methanol with 0.1% formic acid)
0	0.200	90	10
5.1	0.200	90	10
9.1	0.200	50	50
22.1	0.200	5	95
30.1	0.200	5	95
30.2	0.200	90	10
35.6	0.200	90	10

Analysis of transformation products

A previously reported analytical method was adapted for the identification of candidate transformation products (TPs) using HPLC coupled to high-resolution mass spectrometry (Gulde et al., 2016). Briefly, the same mass spectrometry instrument, HPLC system, and mobile phase as previously described in this section was used. However, samples were injected at 20 μL into an Atlantis T3 analytical column (3.0 x 150 mm, particle size 3 μm , Waters) and separation of analytes was achieved by following the extended gradient provided in **Table C.3**. The mass spectrometer was used with heated electrospray ionization and samples were analyzed separately in positive and negative modes. The scan range was set to 100–1000 m/z and the resolution was set to 140,000. Data dependent MS/MS was acquired for all suspect TPs.

Table C.3: Elution pump gradient for transformation product analyses.

Retention time (min)	Flow (mL/min)	%A (HPLC-grade water with 0.1% formic acid)	%B (HPLC-grade methanol with 0.1% formic acid)
0	0.300	90	10
10	0.300	90	10
31.25	0.300	5	95
37	0.300	5	95
40	0.300	90	10
50	0.300	90	10

Appendix D: Tracer experiments

The analytical solution to the 1-D advection-dispersion equation with asymmetric boundary conditions was used to determine the longitudinal dispersivity (α_L) of each column (Ogata and Banks, 1961):

$$\frac{C(x, t)}{C_0} = \frac{1}{2} \left\{ \operatorname{erfc} \left(\frac{x - ut}{\sqrt{4Dt}} \right) + \exp \left(\frac{ux}{D} \right) \operatorname{erfc} \left(\frac{x + ut}{\sqrt{4Dt}} \right) \right\}$$

Equation D.1

$$\text{Boundary conditions: } \begin{cases} C(0, t) = C_0; t \geq 0 \\ C(x, 0) = 0; x \geq 0 \\ C(\infty, t) = 0; t \geq 0 \end{cases}$$

where $C(x, t)$ is the concentration at depth x , and time t , C_0 is the concentration of the conservative solute injected into the porous media, u is the average pore water velocity, and D is the dispersion coefficient. The longitudinal dispersivity is defined as:

$$D = \alpha_L u + D^*$$

Equation D.2

where D^* is the diffusion coefficient for carbamazepine, $2.73 \times 10^{-4} \text{ cm}^2 \text{ min}^{-1}$ (Bertelkamp et al., 2015). The diffusion coefficient was negligible when compared to the effects of dispersion, and was therefore ignored. The cumulative fractional tracer breakthrough curves, $F(t)$, were calculated using data from the tracer experiments (as described in *Section 2.2.3* in the main text) and by:

$$F(t) = \frac{C(t)}{C_0} = \frac{C_{e,avg,i} \Delta t_i Q}{M}$$

Equation D.3

where $C_{e,avg,i}$ is the average effluent concentration and Δt_i is the time difference between time step i and $i-1$, Q is the flow through the column, and M is the mass of tracer injected. Solving for D and plugging **Equations D.2 and D.3** into **Equation D.1**, and setting x equal to the length of the column, L , yields the equation presented in the main text for the analytical solution to the 1-dimensional advection-diffusion equation:

$$F(t) = \frac{1}{2} \left\{ \operatorname{erfc} \left(\frac{L - ut}{\sqrt{4 \alpha_L ut}} \right) + \exp \left(\frac{L}{\alpha_L} \right) \operatorname{erfc} \left(\frac{L + ut}{\sqrt{4 \alpha_L ut}} \right) \right\} \quad \text{Equation D.4}$$

Details for two tracer experiments are provided in **Table D.1** and the breakthrough curves are presented in **Figures D.1 –D.4**. The breakthrough curves are normalized to account for differences in flow rates between experiments by:

$$\text{Filter bed volumes} = \frac{t}{EBCT} \quad \text{Equation D.5}$$

Table D.1: Breakthrough curve results for days 44 and 241.

Column	Day 44			Day 241		
	Dispersivity (cm)	R ²	Mass recovery (%)	Dispersivity (cm)	R ²	Mass recovery (%)
B1-1	0.22	0.996	99%	0.35	0.991	89%
B1-2	0.19	0.999	103%	0.33	0.991	86%
C1	0.29	0.997	99%	0.18	0.998	104%
B2-1	0.22	0.996	96%	0.41	0.980	86%
B2-2	0.27	0.995	99%	0.41	0.996	95%
C2	0.19	0.994	95%	0.23	0.997	105%
B3-1a	0.29	0.998	101%	0.64	0.984	90%
B3-2a	0.55	0.995	107%	0.61	0.990	96%
C3a	0.31	0.994	97%	0.24	0.988	109%
B3-1ab	0.28	0.998	100%	0.43	0.997	96%
B3-2ab	0.31	0.996	102%	0.54	0.991	93%
C3ab	0.26	0.999	101%	0.21	0.997	106%

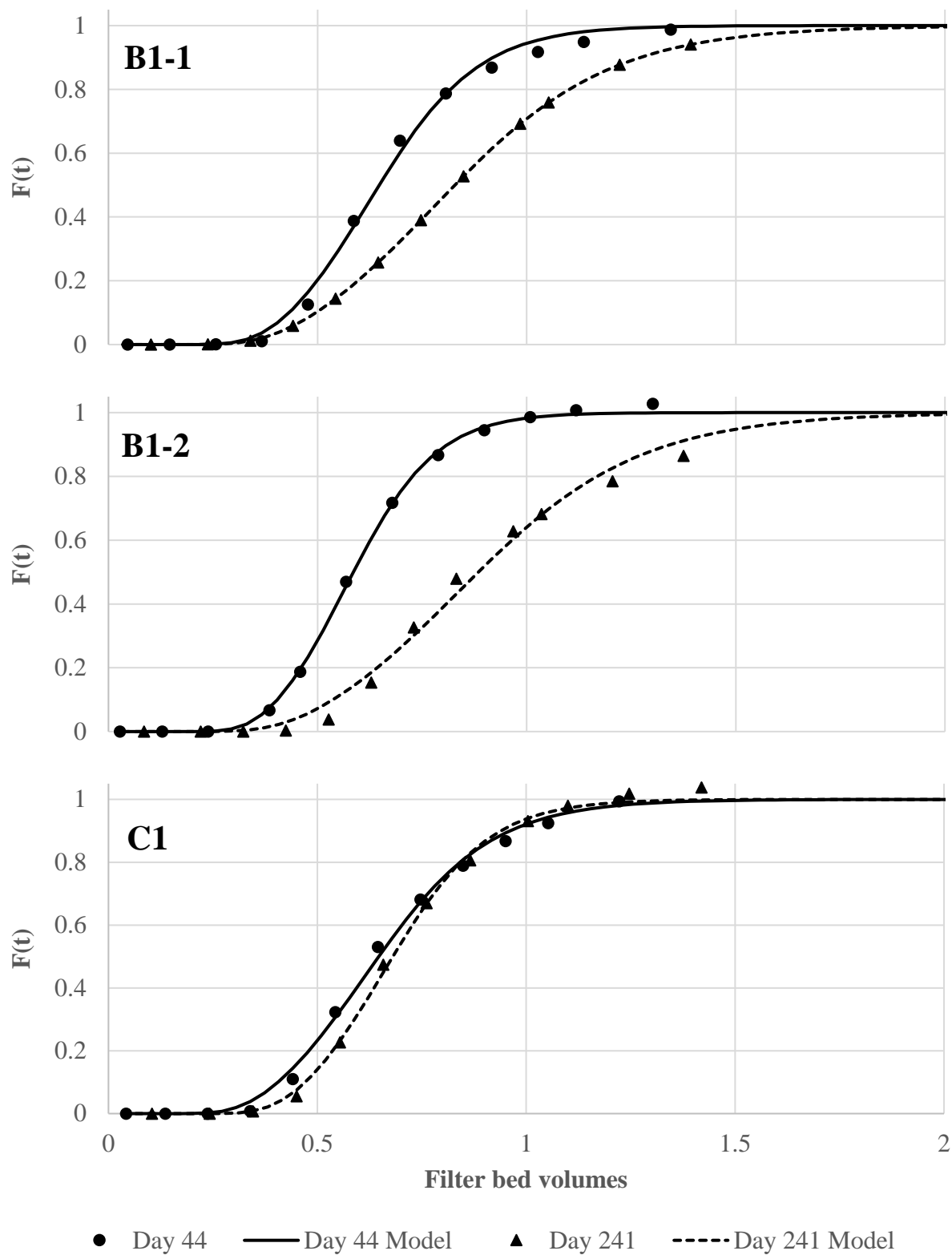


Figure D.1: Cumulative fractional tracer breakthrough curves for filter group 1.

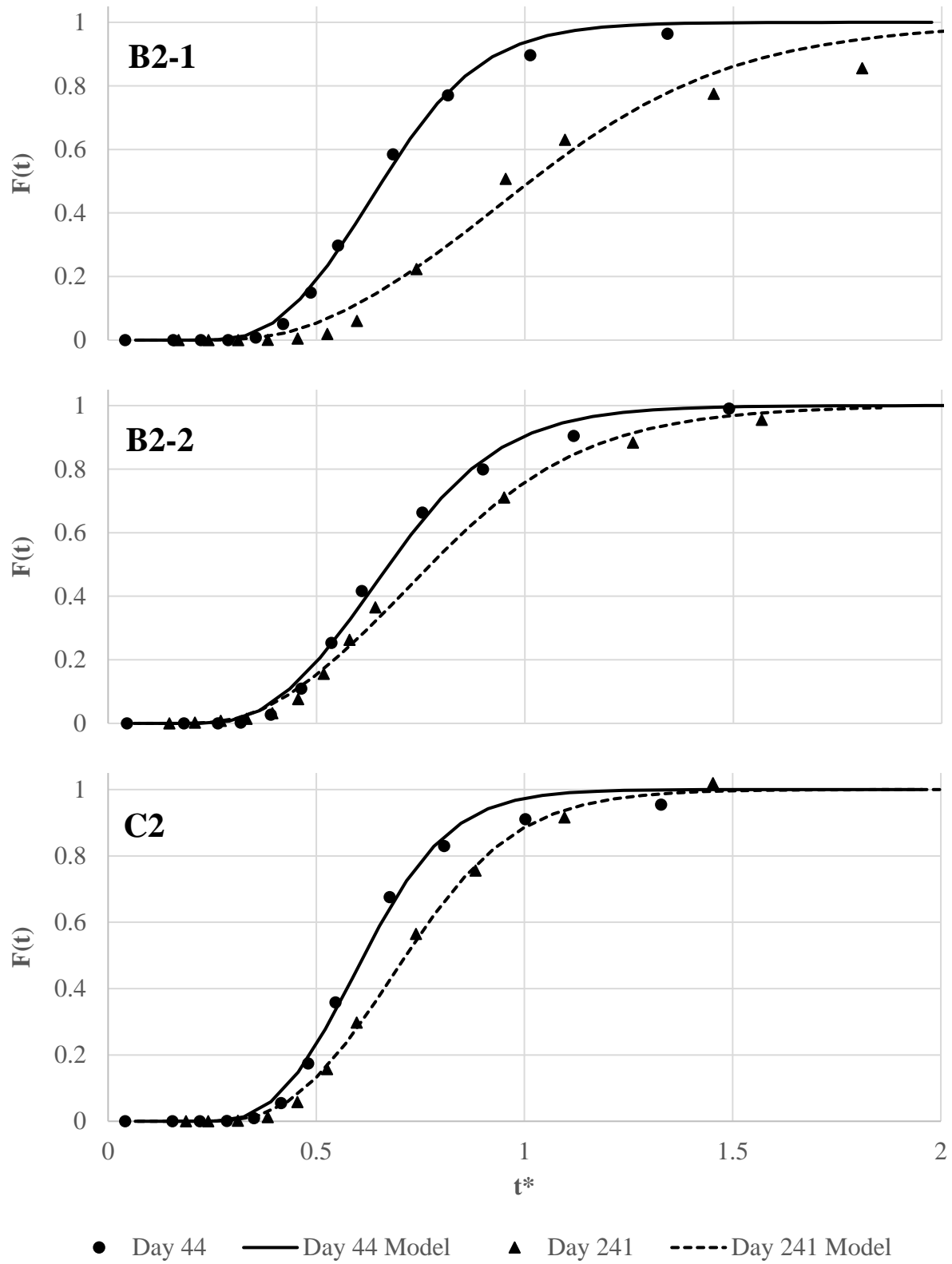


Figure D.2: Cumulative fractional tracer breakthrough curves for filter group 2.

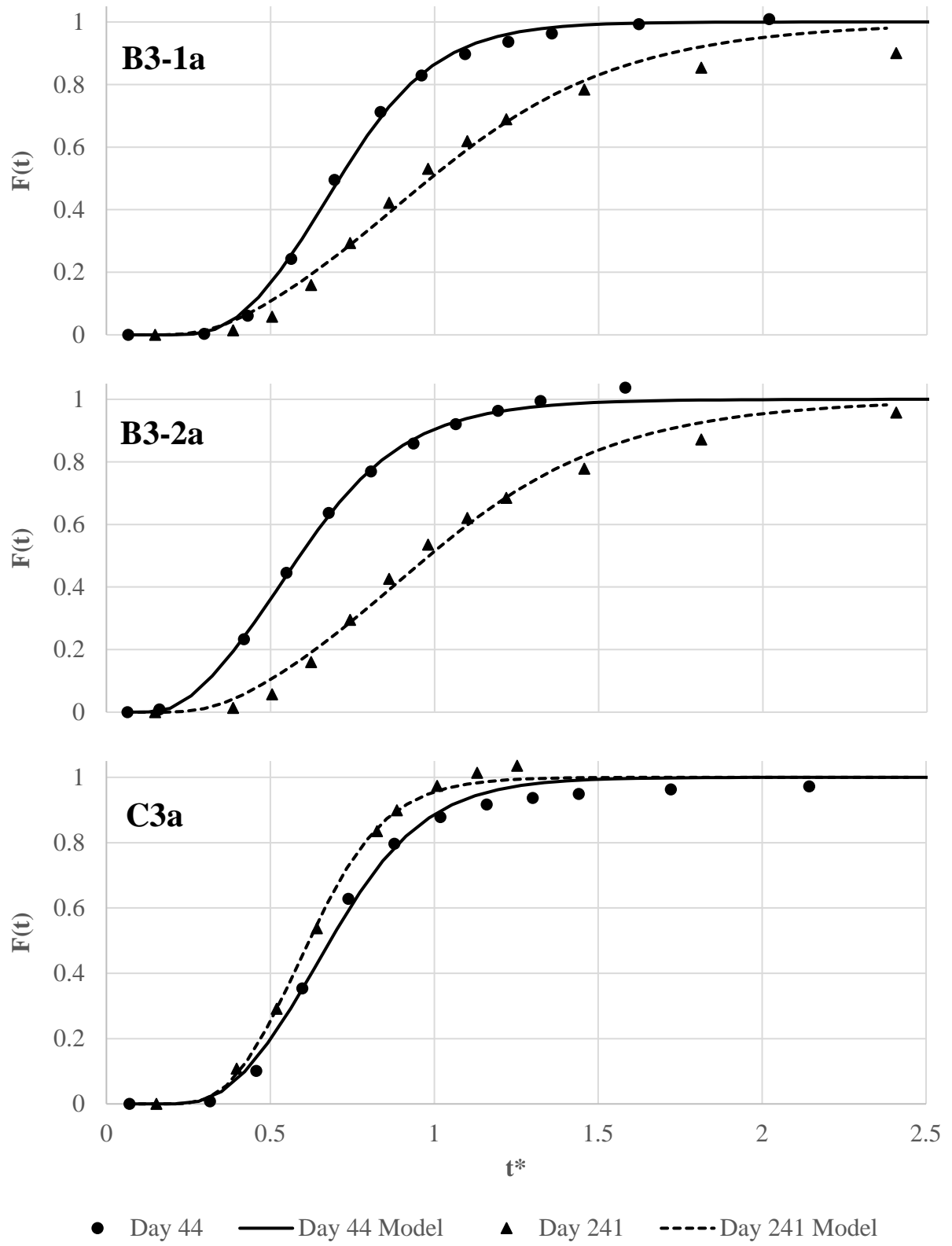


Figure D.3: Cumulative fractional tracer breakthrough curves for filter group 3a.

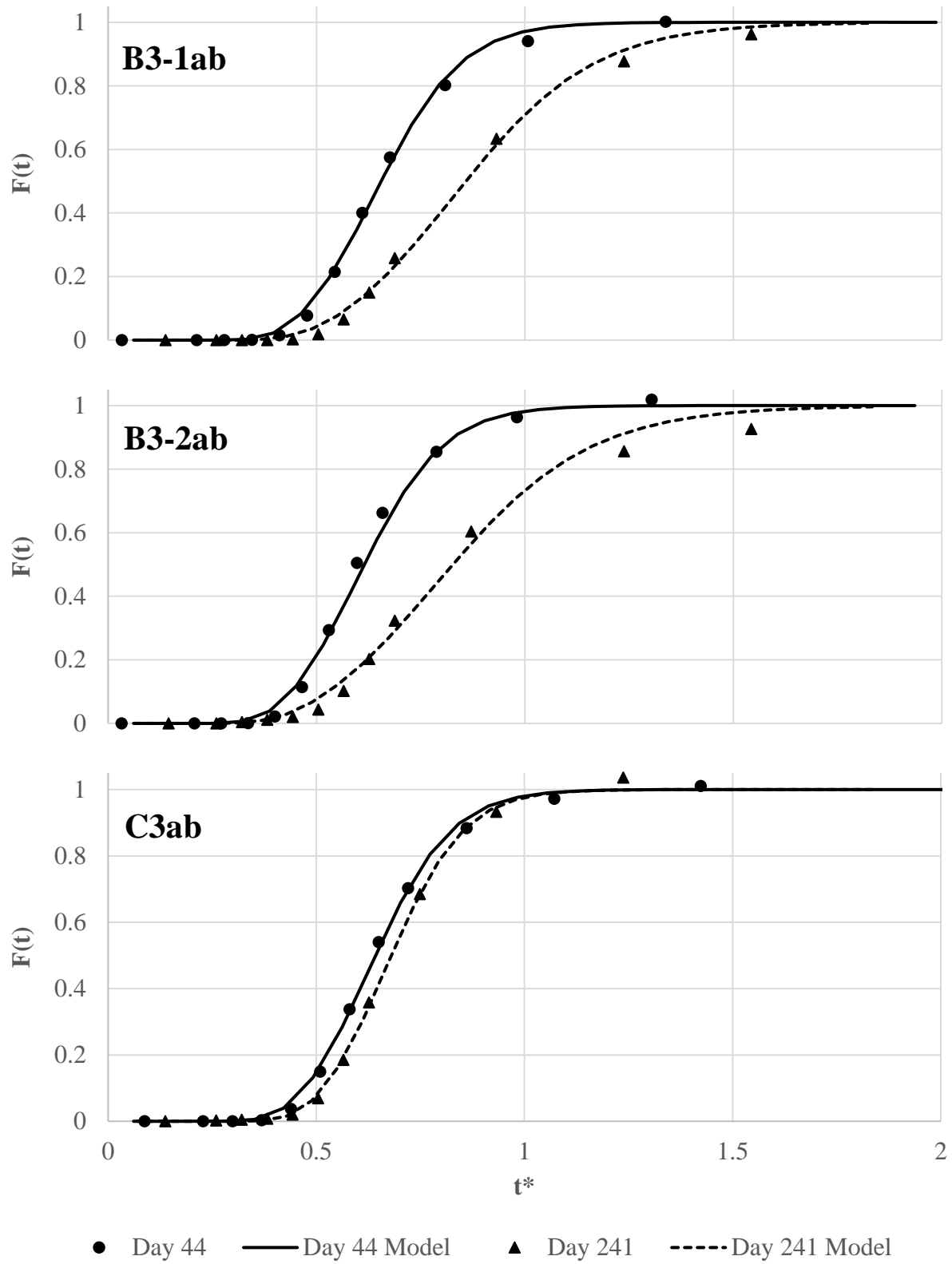


Figure D.4: Cumulative fractional tracer breakthrough curves for filter group 3ab.

Appendix E: Micropollutant information

Stock solutions of pure reference standards and pure isotopically labeled reference standards were prepared at 1 g L^{-1} in either HPLC-grade methanol, chloroform, or acetone and stored at -20°C . A mixture of all reference standards was created in nanopure water at 10 mg L^{-1} and stored at 4°C until needed. Furthermore, the mixture was diluted to 100, 10, and $1 \text{ }\mu\text{g L}^{-1}$ in nanopure water to create a calibration curve for the micropollutant analyses at 0, 10, 50, 100, 200, 500, 750, 1000, 1500, 2000 ng L^{-1} . Similarly, a mixture of all isotopically labeled reference standards was created in nanopure water at 10 mg L^{-1} and stored at 4°C until needed. The mixture was diluted to $200 \text{ }\mu\text{g L}^{-1}$ in nanopure water, and was spiked into each calibration standard and sample at 500 ng L^{-1} . Internal standard assignments for compounds without exact matches were based on structural similarity, ionization behavior, and retention time. A complete list of reference standard information is provided in **Table E.1**. Isotopically labeled internal reference standard structures are provided in **Table E.2**, and a complete list of information is provided in **Table E.3**.

Table E.1: Reference standard information

Micropollutant	CAS Number	Adduct	Exact Mass (m/z)	RT (min)	Product Ion (m/z)	LOQ (ng/L)	Internal Standard Assignment
Acetaminophen	103-90-2	[M+H] ⁺	152.0706	8.2	110.06	200	Acetaminophen-ring-d ₄
Atenolol	29122-68-7	[M+H] ⁺	267.1703	8.1	190.09	50	Atenolol-d ₇
Atrazine	1912-24-9	[M+H] ⁺	216.1010	13.1	174.05	10	Atrazine-d ₅
Azoxystrobin	131860-33-8	[M+H] ⁺	404.1241	14.5	372.10	10	Azoxystrobin-d ₄
Caffeine	58-08-2	[M+H] ⁺	195.0876	9.4	138.07	50	Caffeine- ¹³ C ₃
Carbamazepine	298-46-4	[M+H] ⁺	237.1022	12.5	194.10	10	Carbamazepine- ¹³ C ₆
Carbaryl	63-25-2	[M+H] ⁺	202.0862	12.4	132.03	10	Carbaryl-d ₇
Cimetidine	51481-61-9	[M+H] ⁺	253.1230	8.2	95.06	50	Cimetidine-d ₃
Diazinon	333-41-5	[M+H] ⁺	305.1083	17.3	169.08	10	Naproxen-methoxy-d ₃
Diphenhydramine	58-73-1	[M+H] ⁺	256.1696	11.7	167.09	10	Venlafaxine-d ₆
Estrone	53-16-7	[M+H] ⁺	271.1692	14.9	159.08	200	Estrone-d ₂
Ethofumesate	26225-79-6	[M+H] ⁺	287.0947	14.7	121.06	50	Naproxen-methoxy-d ₃
Ibuprofen	51146-56-6	[M+Na] ⁺	229.1199	17.7	159.12	10	Ibuprofen-d ₃
Isoproturon	34123-59-6	[M+H] ⁺	207.1492	13.4	165.10	10	Isoproturon-d ₆
Metoprolol	56392-17-7	[M+H] ⁺	268.1907	10.1	159.08	10	Atenolol-d ₇
Naproxen	22204-53-1	[M+H] ⁺	231.1015	14.7	185.10	100	Naproxen-methoxy-d ₃
Phenytoin	57-41-0	[M+H] ⁺	253.0971	12.3	182.10	50	Carbaryl-d ₇
Progesterone	57-41-1	[M+H] ⁺	315.2318	17.2	170.09	10	Carbaryl-d ₇

Table E.1 (continued)

Propachlor	1918-16-7	[M+H] ⁺	212.0836	13.3	152.03	10	Isoproturon-d ₆
Ranitidine	66357-59-3	[M+H] ⁺	315.1485	8.1	176.05	100	Ranitidine-d ₆
Simazine	122-34-9	[M+H] ⁺	202.0854	11.9	132.03	10	Atrazine-d ₅
Sucralose	56038-13-2	[M-H+FA] ⁻	441.0117	9.9	395.01	200	Sucralose-d ₆
Sulfamethoxazole	723-46-6	[M+H] ⁺	254.0594	9.9	156.01	10	Sulfamethoxazole-phenyl- ¹³ C ₆
Triclosan	723-46-7	[M-H] ⁻	286.9428	19.3	218.98	50	Triclosan-d ₃
Trimethoprim	738-70-5	[M+H] ⁺	291.1451	9.2	261.10	10	Trimethoprim-d ₉
Trinexepac-ethyl	95266-40-3	[M+H] ⁺	253.1070	13.7	69.03	10	Isoproturon-d ₆
Valsartan	137862-53-4	[M+H] ⁺	436.2343	15.5	235.10	10	Isoproturon-d ₆
Venlafaxine	99300-78-4	[M+H] ⁺	278.2114	11.2	58.07	10	Venlafaxine-d ₆
Warfarin	81-81-2	[M+H] ⁺	309.1121	15.2	251.07	10	Isoproturon-d ₆

Table E.2: Isotopically labeled internal reference standard structures

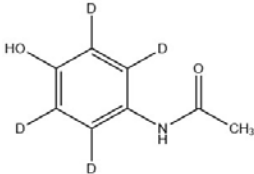
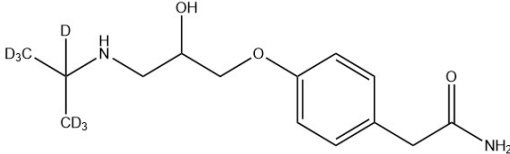
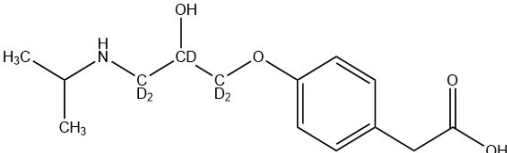
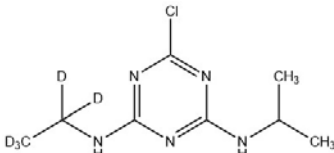
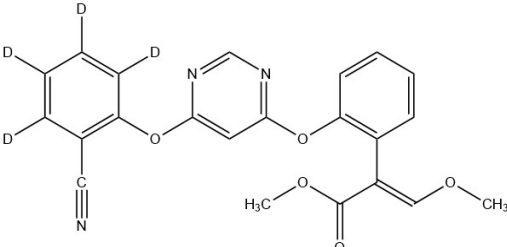
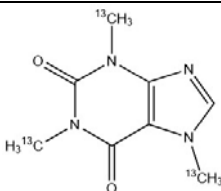
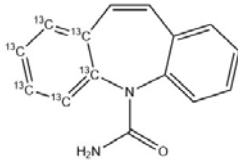
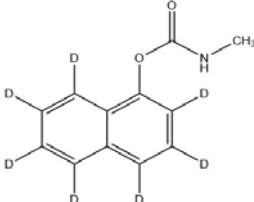
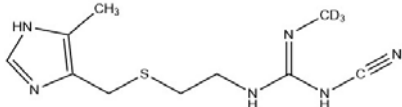
Labeled reference standard	Structure
Acetaminophen-ring-d ₄	
Atenolol-d ₇	
Atenolol Acid-d ₅	
Atrazine-d ₅	
Azoxystrobin-d ₄	
Caffeine- ¹³ C ₃	
Carbamazepine- ¹³ C ₆	
Carbaryl-d ₇	
Cimetidine-d ₃	

Table E.2 (continued)

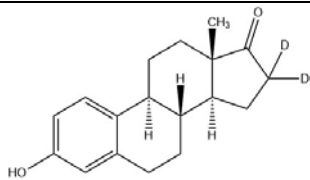
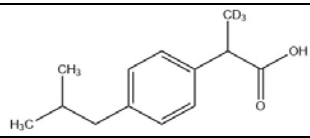
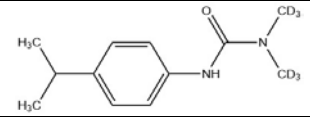
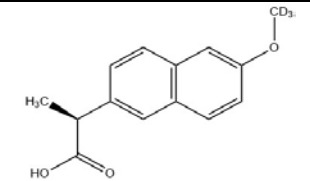
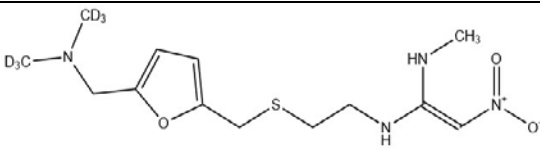
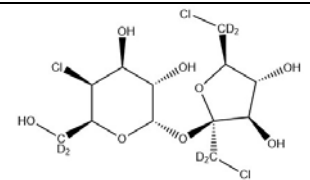
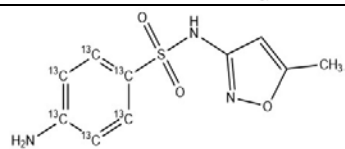
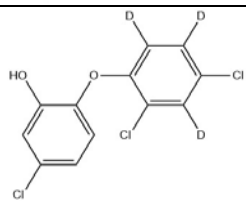
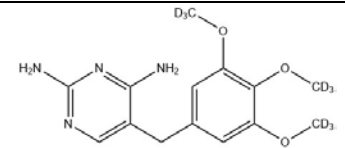
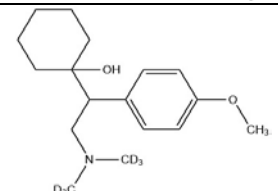
Estrone-d ₂	
Ibuprofen-d ₃	
Isoproturon-d ₆	
Naproxen-methoxy-d ₃	
Ranitidine-d ₆	
Sucralose-d ₆	
Sulfamethoxazole-phenyl- ¹³ C ₆	
Triclosan-d ₃	
Trimethoprim-d ₉	
Venlafaxine-d ₆	

Table E.3: Isotopically labeled internal reference standard information.

Micropollutant	CAS Number	Supplier	Adduct	Adduct m/z	RT (min)
Acetaminophen-ring-d ₄	64315-36-2	Sigma-Aldrich	[M+H] ⁺	156.0957	8.2
Atenolol-d ₇	1202864-50-3	Sigma-Aldrich	[M+H] ⁺	274.2142	8.1
Atenolol Acid-d ₅	1215404-47-9	TRC	[M+H] ⁺	273.1857	9.2
Atrazine-d ₅	163165-75-1	Sigma-Aldrich	[M+H] ⁺	221.1324	13.1
Azoxystrobin-d ₄	1346606-39-0	TRC	[M+H] ⁺	408.1492	14.5
Caffeine- ¹³ C ₃	200-659-6	Sigma-Aldrich	[M+H] ⁺	198.0977	9.4
Carbamazepine- ¹³ C ₆	n.a.	Sigma-Aldrich	[M+H] ⁺	243.1224	12.5
Carbaryl-d ₇	362049-56-7	TRC	[M+H] ⁺	209.1302	12.4
Cimetidine-d ₃	1185237-29-9	TRC	[M+H] ⁺	256.1418	8.2
Estrone-d ₂	1219799-27-5	TRC	[M+H] ⁺	273.1818	14.9
Ibuprofen-d ₃	121662-14-4	Sigma-Aldrich	[M+Na] ⁺	232.1388	17.7
Isoproturon-d ₆	217487-17-7	Sigma-Aldrich	[M+H] ⁺	213.1868	13.4
Naproxen-methoxy-d ₃	958293-79-3	Sigma-Aldrich	[M+H] ⁺	234.1204	14.7
Ranitidine-d ₆	1185238-09-8	TRC	[M+H] ⁺	321.1862	8.1
Sucralose-d ₆	1459161-55-7	TRC	[M-H+FA] ⁻	447.0494	9.9
Sulfamethoxazole-phenyl- ¹³ C ₆	1196157-90-0	Sigma-Aldrich	[M+H] ⁺	260.0795	9.9
Triclosan-d ₃	1020719-98-5	TRC	[M-H] ⁻	289.9616	19.3
Trimethoprim-d ₉	1189460-62-5	Sigma-Aldrich	[M+H] ⁺	300.2016	9.2
Venlafaxine-d ₆	1062606-12-5	Sigma-Aldrich	[M+H] ⁺	284.2491	11.2

TRC = Toronto Research Chemicals

Appendix F: Micropollutant removal

Table F.1: Average micropollutant influent concentrations and maximum recordable removal efficiencies based on individual limits of quantification.

Micropollutant	Average influent ^a (ng L ⁻¹)	Maximum recordable removal efficiency	Removal behavior	Figure
Acetaminophen ^b	1041 ± 234	81%	Biotic (low)	Figure F.1
Atenolol	1172 ± 190	96%	Biotic (low)	Figure F.2
Atrazine	966 ± 156	99%	Recalcitrant	Figure F.3
Azoxystrobin	557 ± 421	98%	Recalcitrant	Figure F.4
Caffeine ^d	942 ± 415	95%	Biotic (moderate)	Figure F.5
Carbamazepine ^d	969 ± 159	99%	Recalcitrant	Figure F.6
Carbaryl	913 ± 230	99%	Recalcitrant	Figure F.7
Cimetidine	1016 ± 249	95%	Abiotic	Figure F.8
Diazinon ^d	635 ± 283	99%	Recalcitrant	Figure F.9
Diphenhydramine ^c	607 ± 269	98%	Abiotic	Figure F.10
Estrone ^{b,c}	357 ± 146	44%	Biotic (high*)	Figure F.11
Ethofumesate	1083 ± 289	95%	Recalcitrant	Figure F.12
Ibuprofen ^c	930 ± 212	99%	Biotic (high)	Figure F.13
Isoproturon	1017 ± 163	99%	Recalcitrant	Figure F.14
Metoprolol	583 ± 127	98%	Biotic (low)	Figure F.15
Naproxen ^c	1027 ± 176	90%	Biotic (moderate)	Figure F.16
Phenytoin	747 ± 163	93%	Recalcitrant	Figure F.17
Progesterone ^c	562 ± 262	98%	Abiotic	Figure F.18
Propachlor	791 ± 177	99%	Biotic (low)	Figure F.19
Ranitidine ^b	847 ± 241	88%	Abiotic	Figure F.20
Simazine	619 ± 153	98%	Recalcitrant	Figure F.21
Sucralose ^d	1438 ± 403	86%	Recalcitrant	Figure F.22
Sulfamethoxazole ^d	1185 ± 232	99%	Recalcitrant	Figure F.23
Triclosan ^{b,c}	91 ± 49	45%	Biotic (high*)	Figure F.24
Trimethoprim ^c	376 ± 120	97%	Biotic (high)	Figure F.25
Trinexapac-ethyl	824 ± 190	99%	Recalcitrant	Figure F.26
Valsartan	1167 ± 240	99%	Biotic (high)	Figure F.27
Venlafaxine	1078 ± 219	99%	Abiotic	Figure F.28
Warfarin	682 ± 157	99%	Recalcitrant	Figure F.29

*removed below LOQs for the duration of the experiment; low removal (10–35%); moderate removal (36–60%); high removal (61–100%). ^aAverage ± standard deviation for 10 sampling events across 9 columns and 2 sampling events across 6 columns over the 381 day experiment. ^bAt least one influent sample was below LOQ and not included. ^cAt least one effluent sample was below LOQ and reported as maximum removal. ^dAt least one sample was above the highest calibration point and not included.

Figures F.1-F.29 show the average removal efficiencies for the duration of the experiment for each MP. The average influent concentration and maximum recordable removal efficiencies for each MP is provided in **Table F.1**. The first 10 sampling events were conducted between 30-295 days of filter operation and for the biofilters (B1, B2, B3a, and B3b), and error bars represent the duplicate biofilters (n=2). There were two additional sampling events (days 337 and 381) after we sacrificed one of the duplicate biofilters from each biofilter group on day 301.

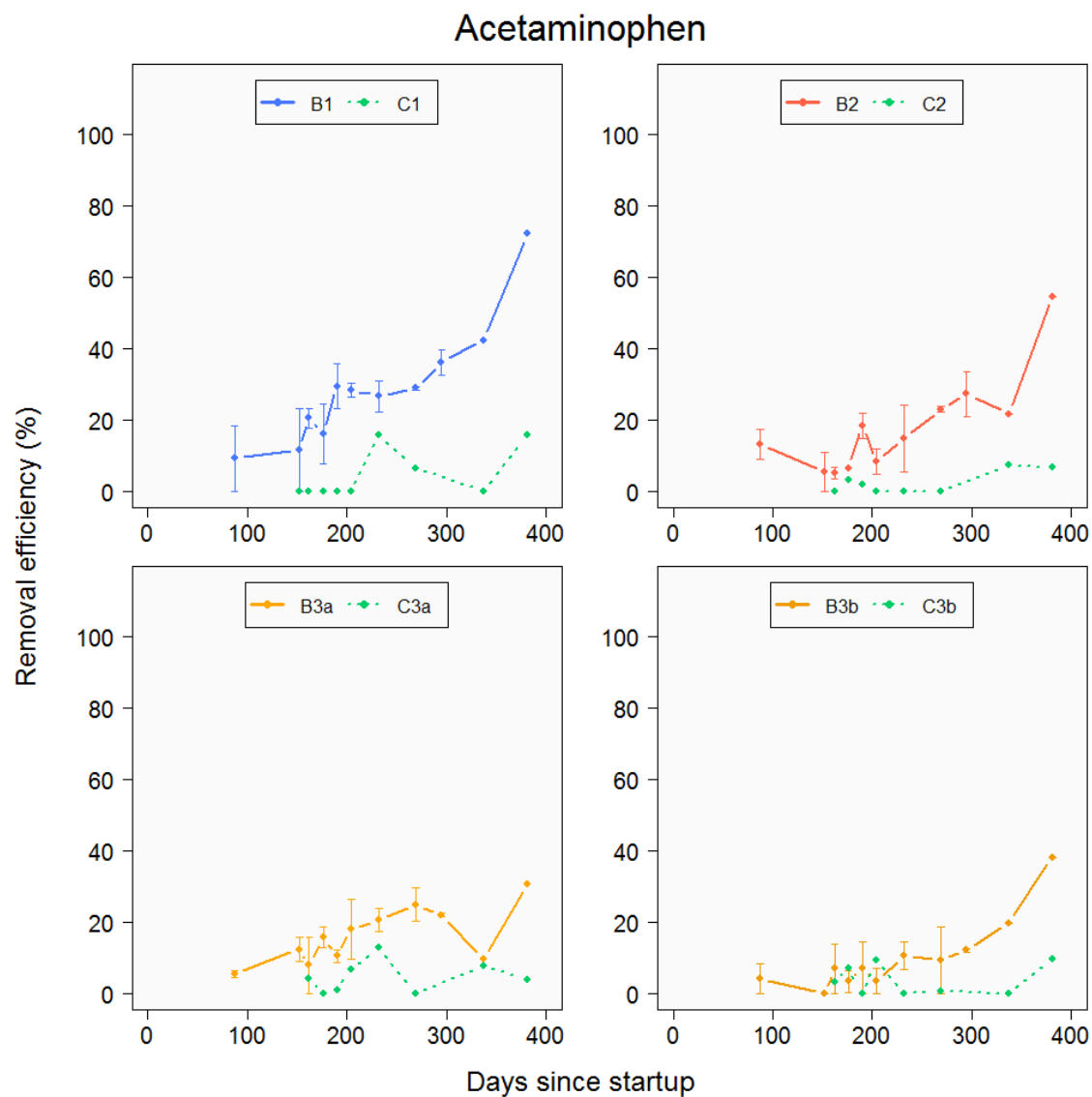


Figure F.1: Removal efficiency of acetaminophen for the duration of the experiment.

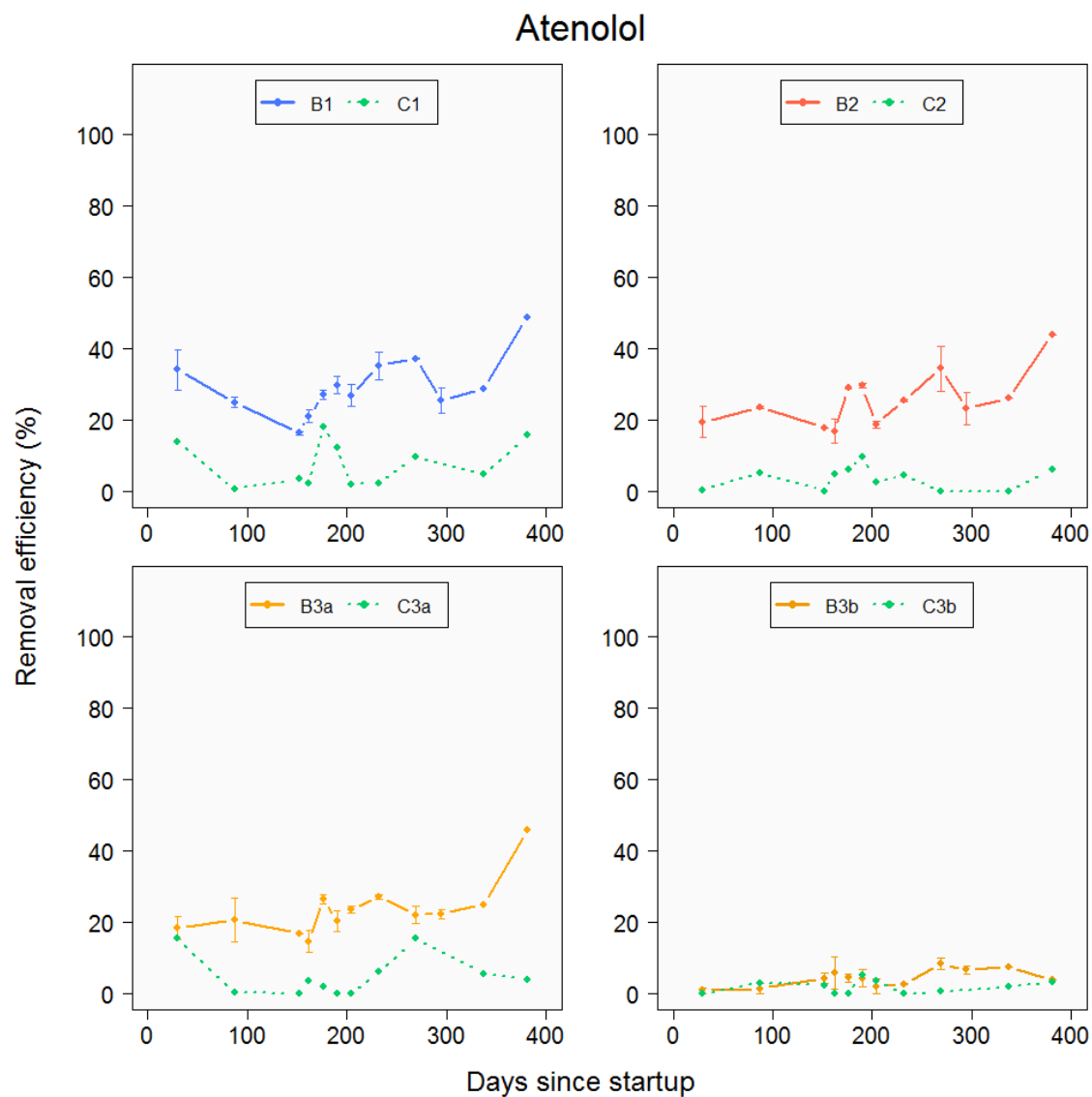


Figure F.2: Removal efficiency of atenolol for the duration of the experiment.

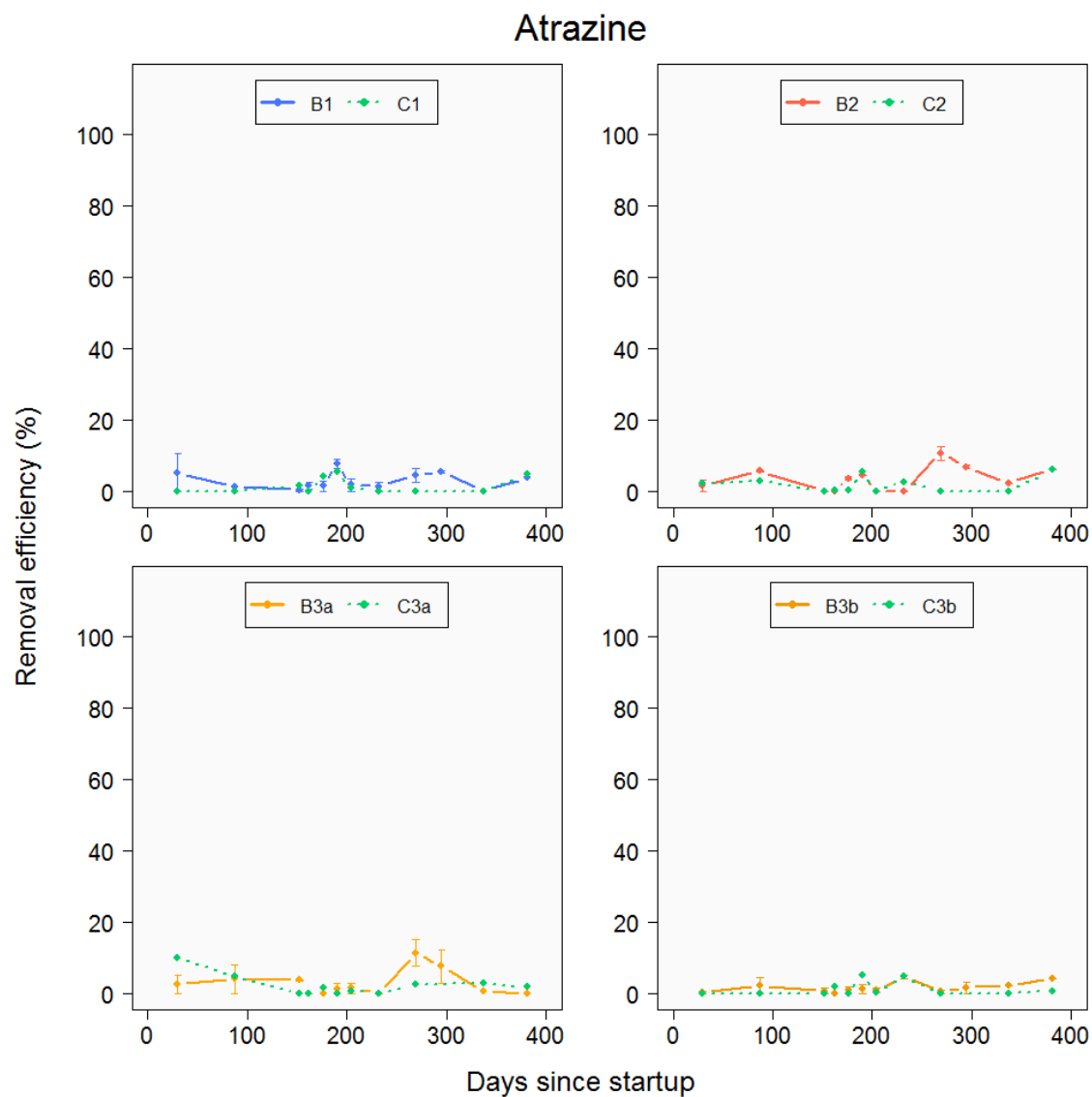


Figure F.3: Removal efficiency of atrazine for the duration of the experiment.

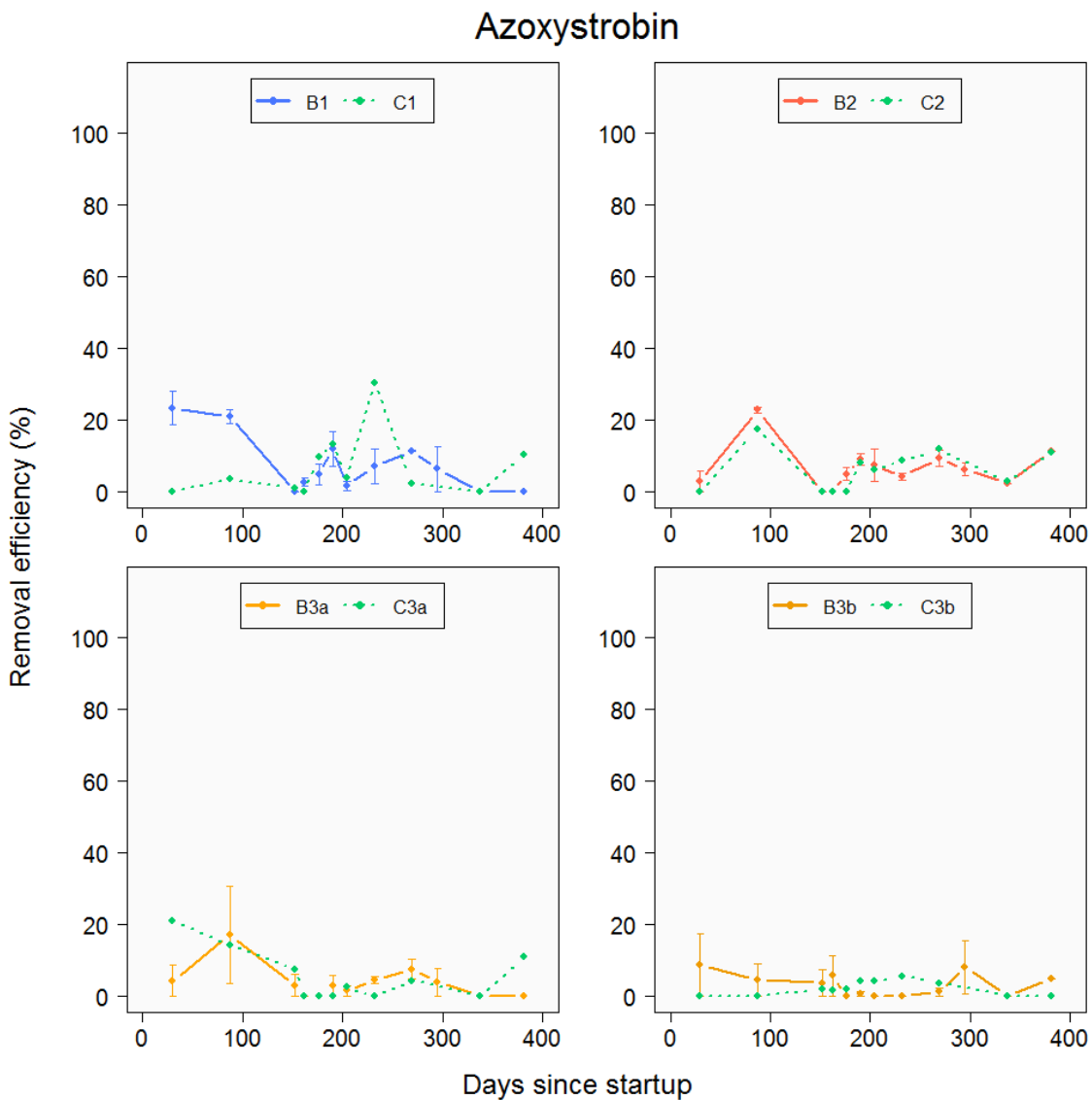


Figure F.4: Removal efficiency of azoxystrobin for the duration of the experiment.

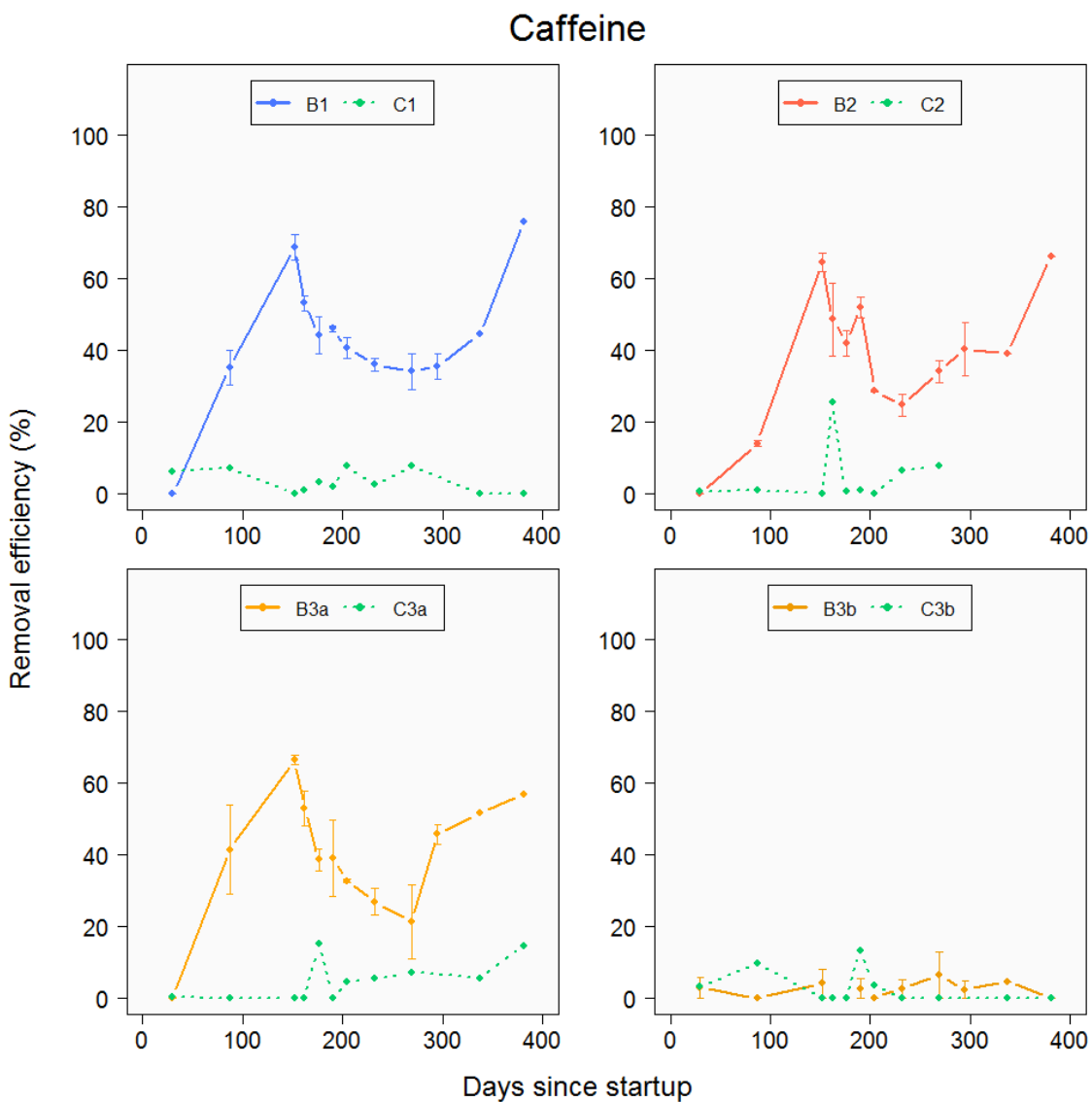


Figure F.5: Removal efficiency of caffeine for the duration of the experiment.

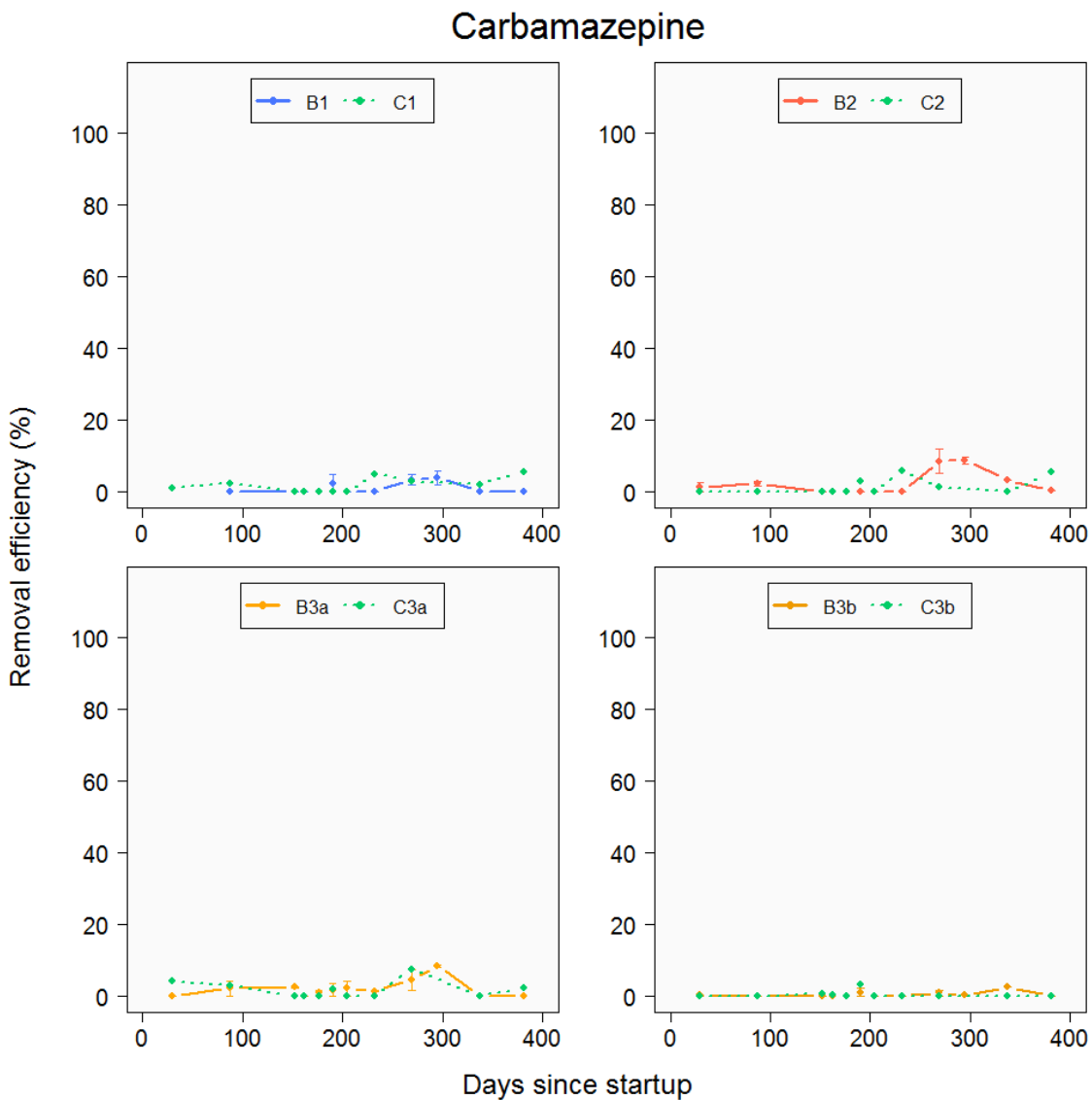


Figure F.6: Removal efficiency of carbamazepine for the duration of the experiment.

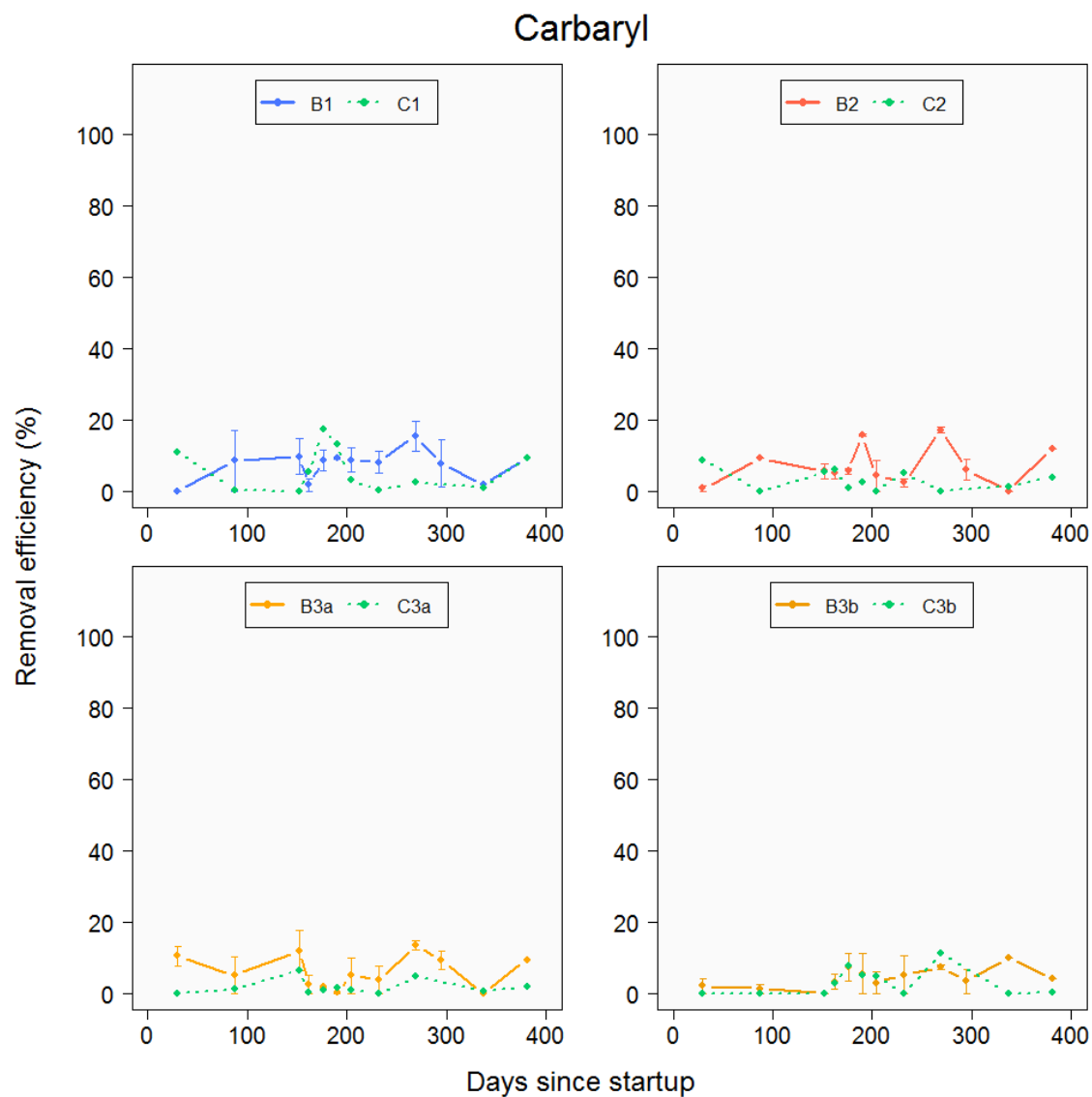


Figure F.7: Removal efficiency of carbaryl for the duration of the experiment.

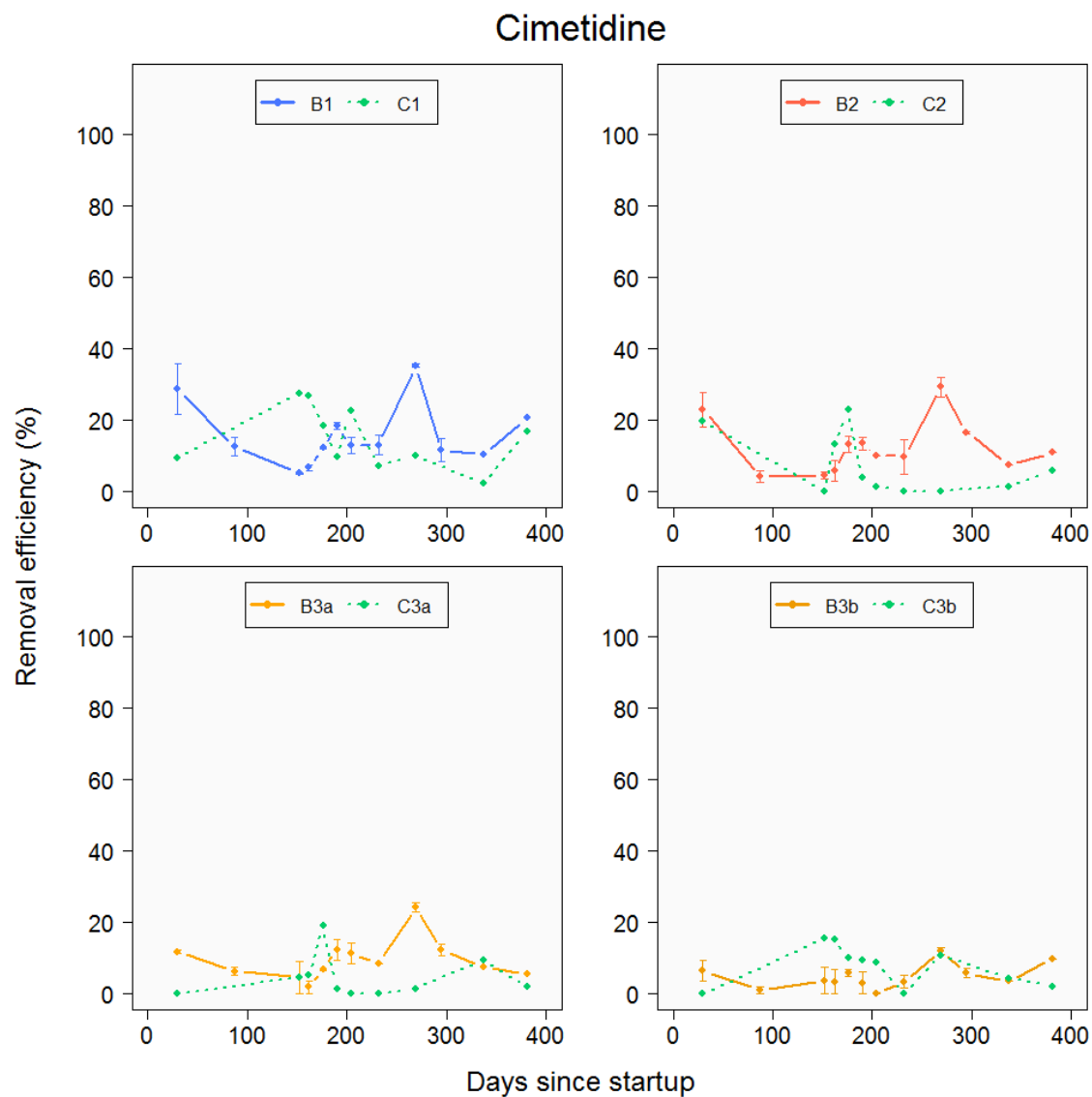


Figure F.8: Removal efficiency of cimetidine for the duration of the experiment.

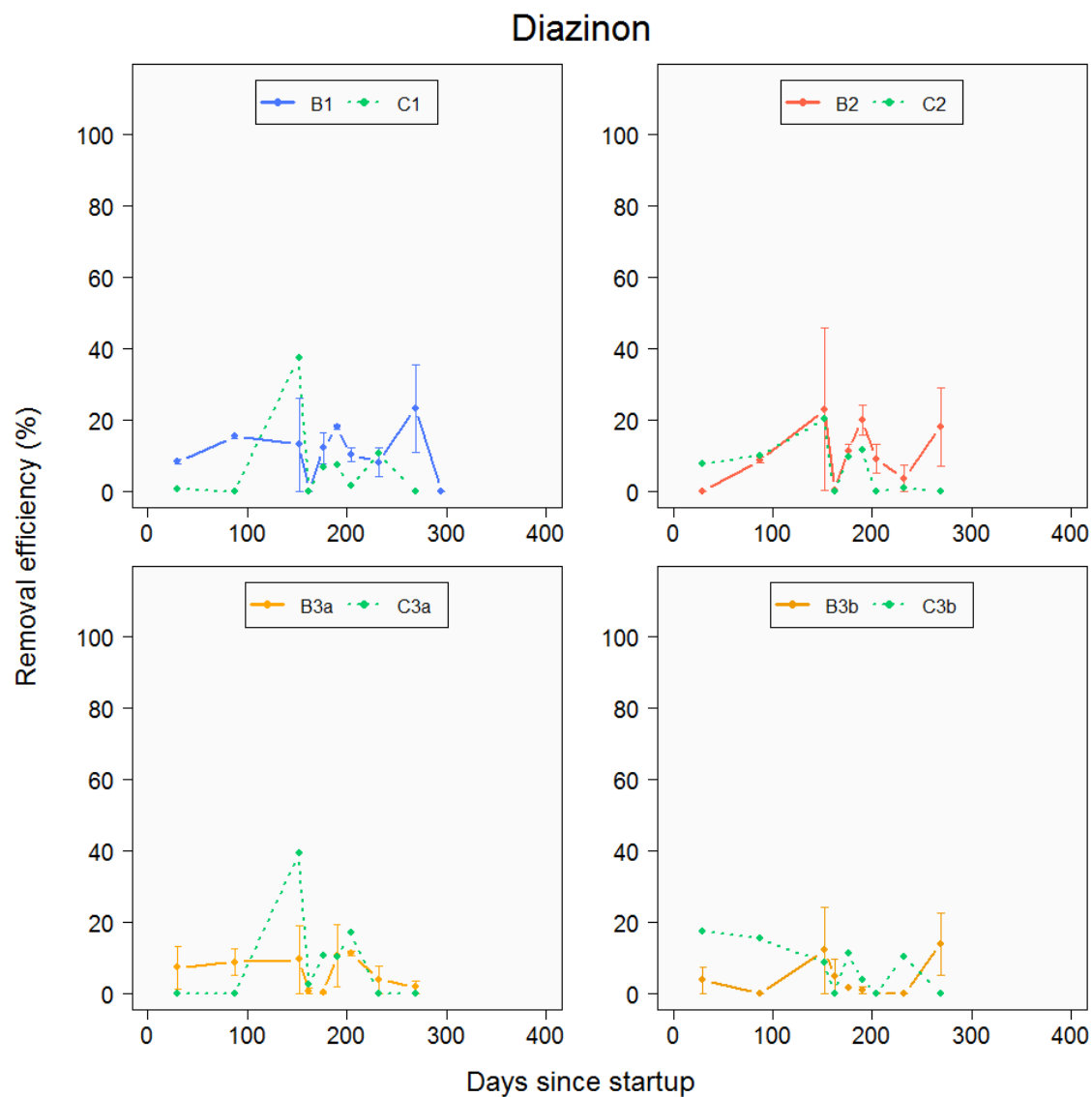


Figure F.9: Removal efficiency of diazinon for the duration of the experiment.

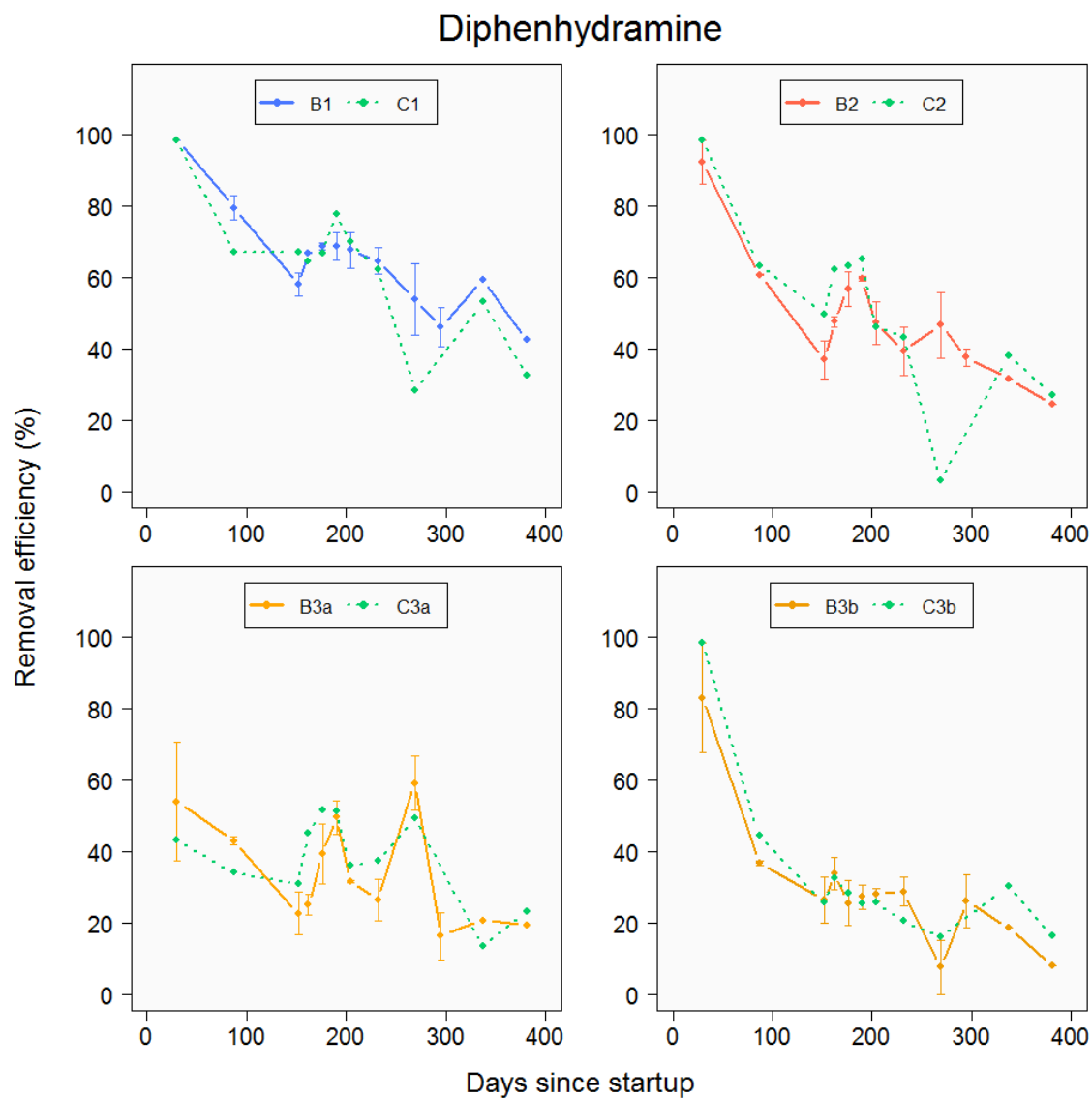


Figure F.10: Removal efficiency of diphenhydramine for the duration of the experiment.

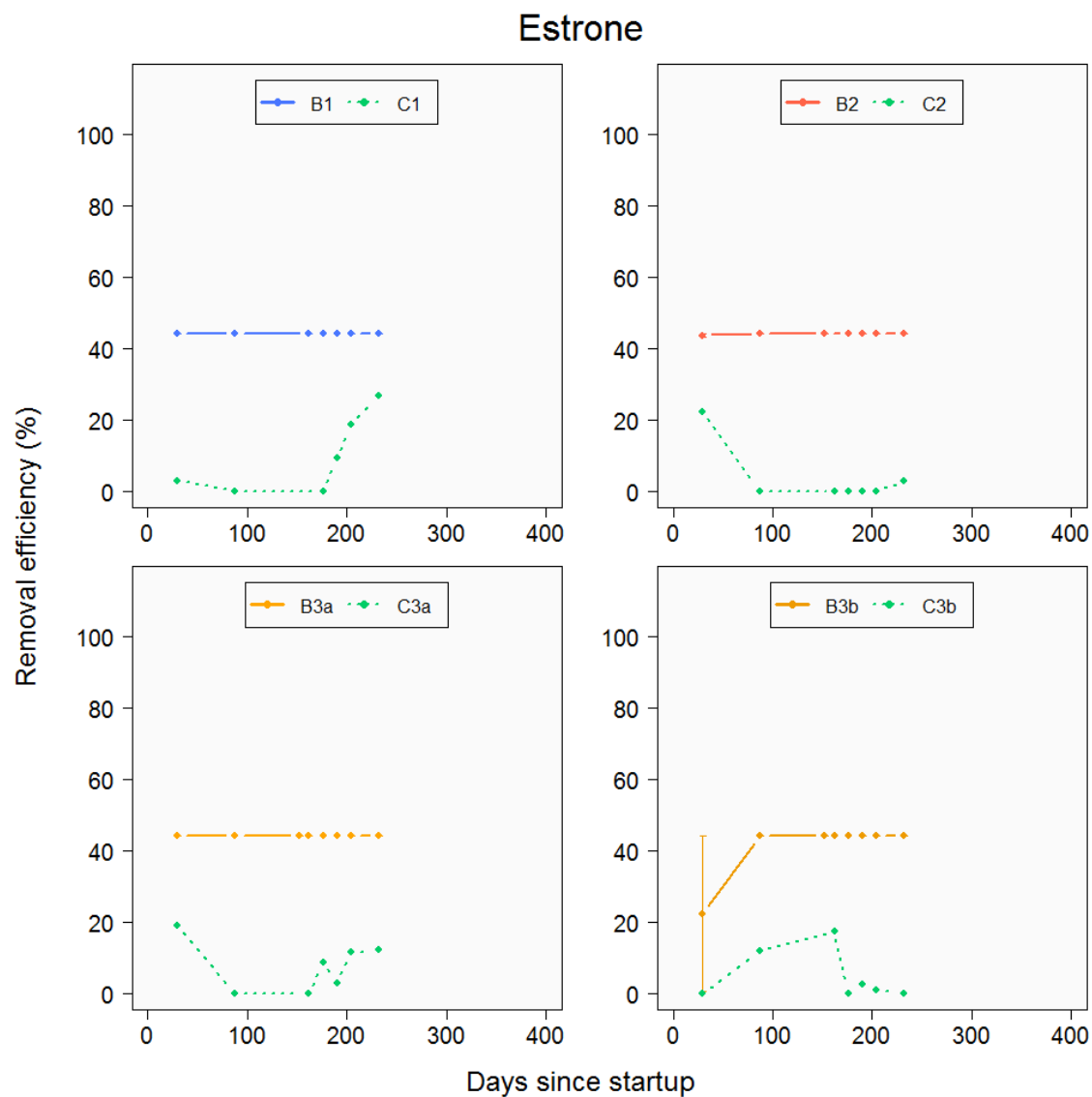


Figure F.11: Removal efficiency of estrone for the duration of the experiment.

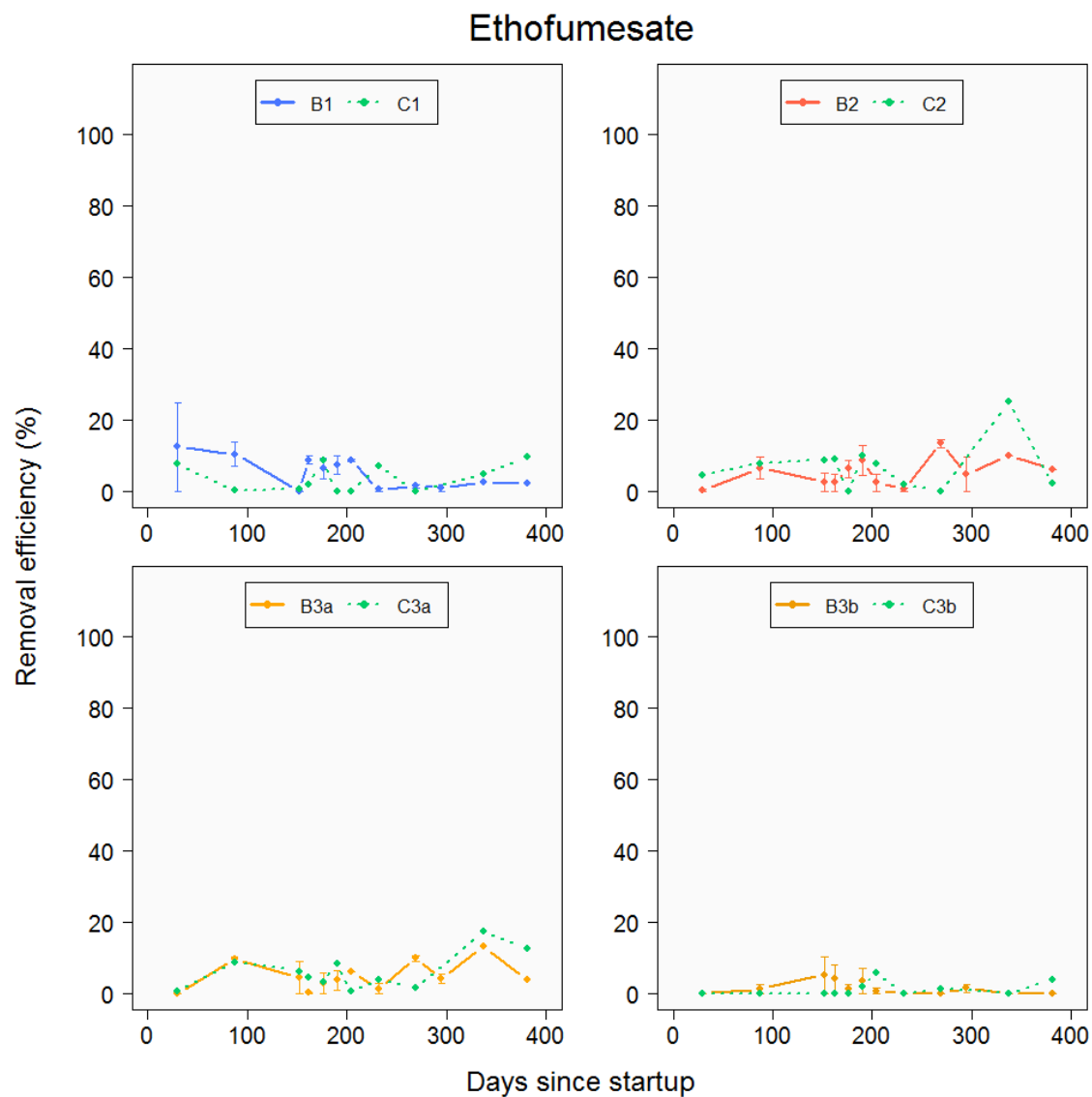


Figure F.12: Removal efficiency of ethofumesate for the duration of the experiment.

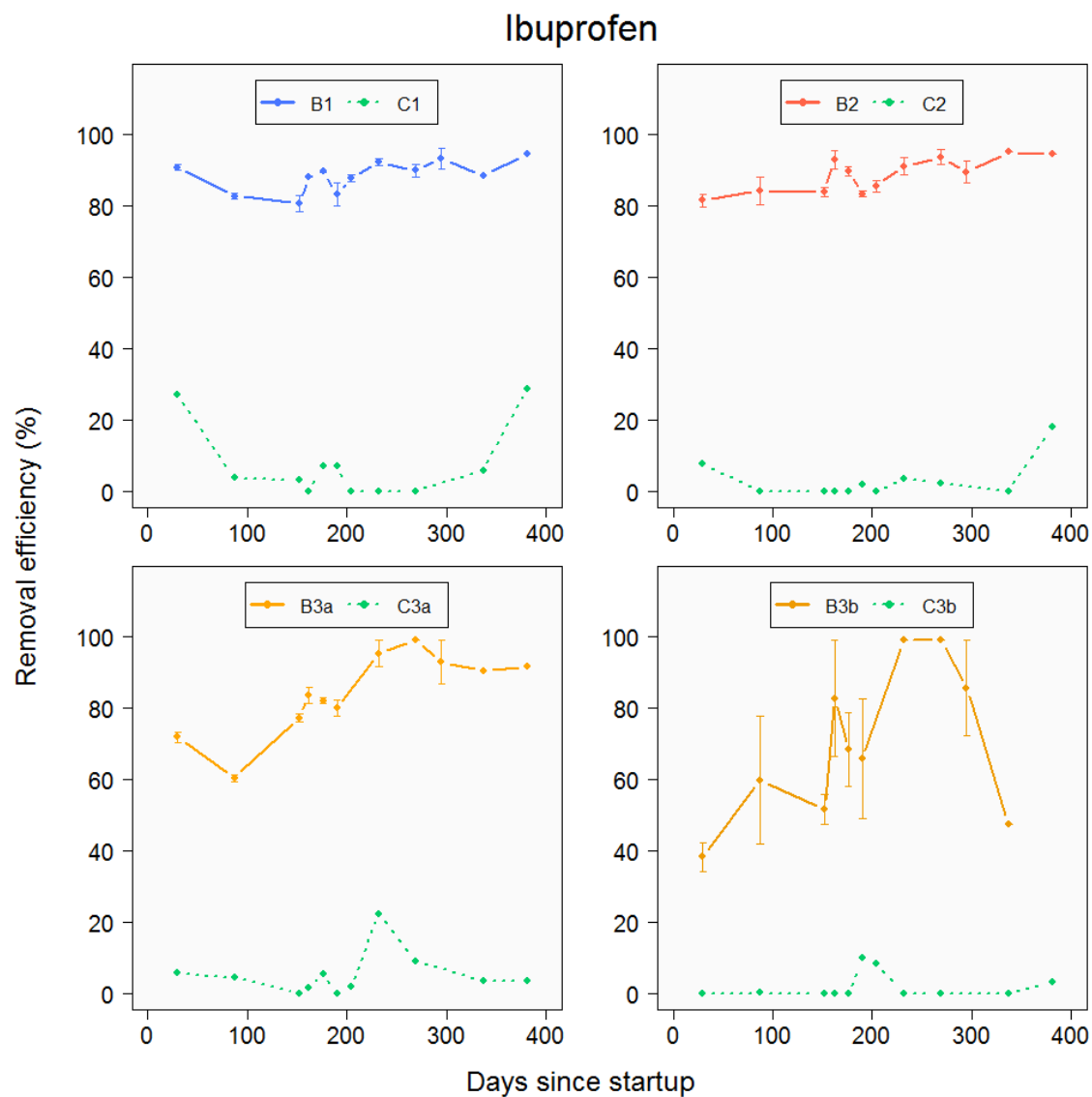


Figure F.13: Removal efficiency of ibuprofen for the duration of the experiment.

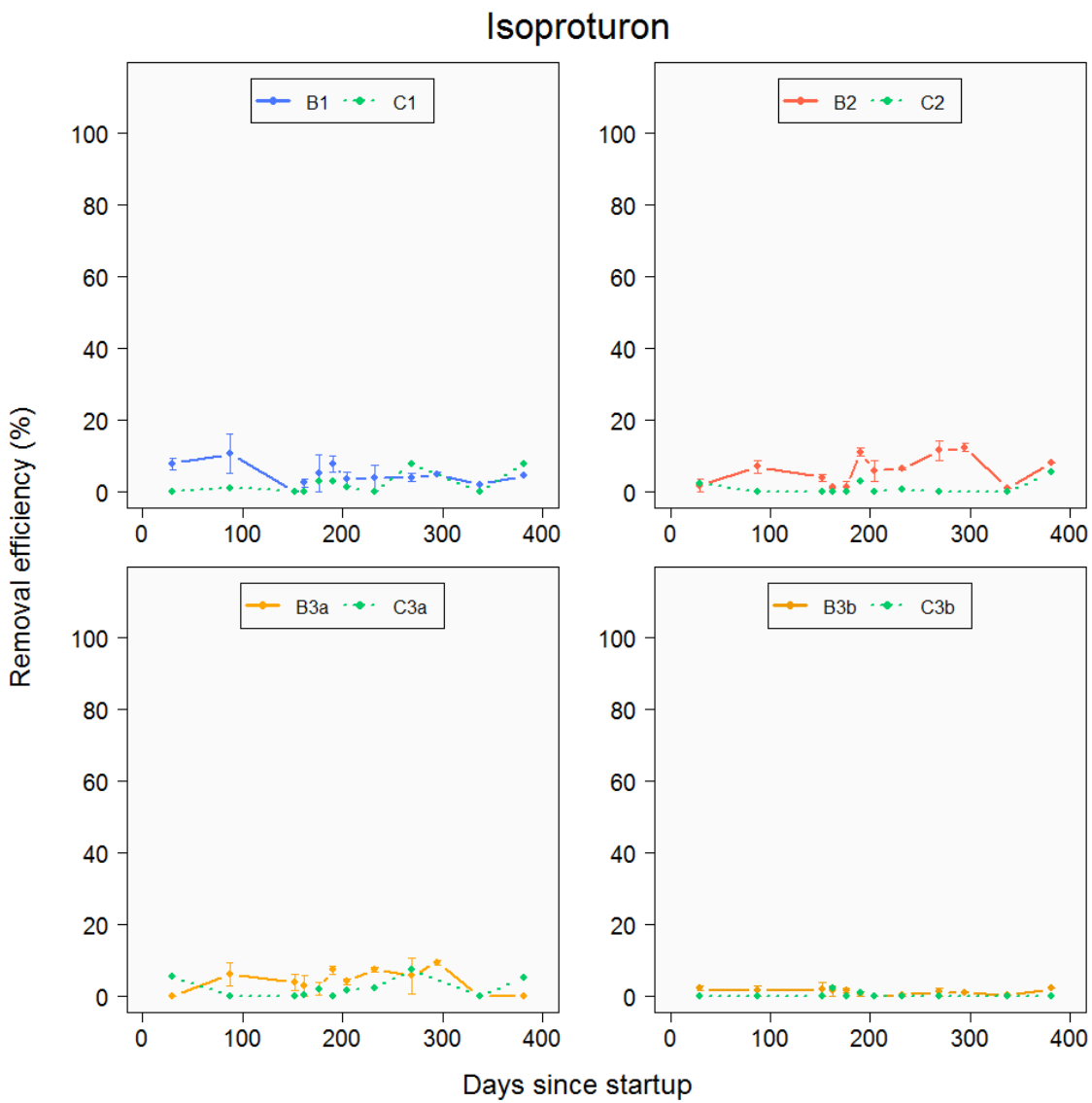


Figure F.14: Removal efficiency of isoproturon for the duration of the experiment.

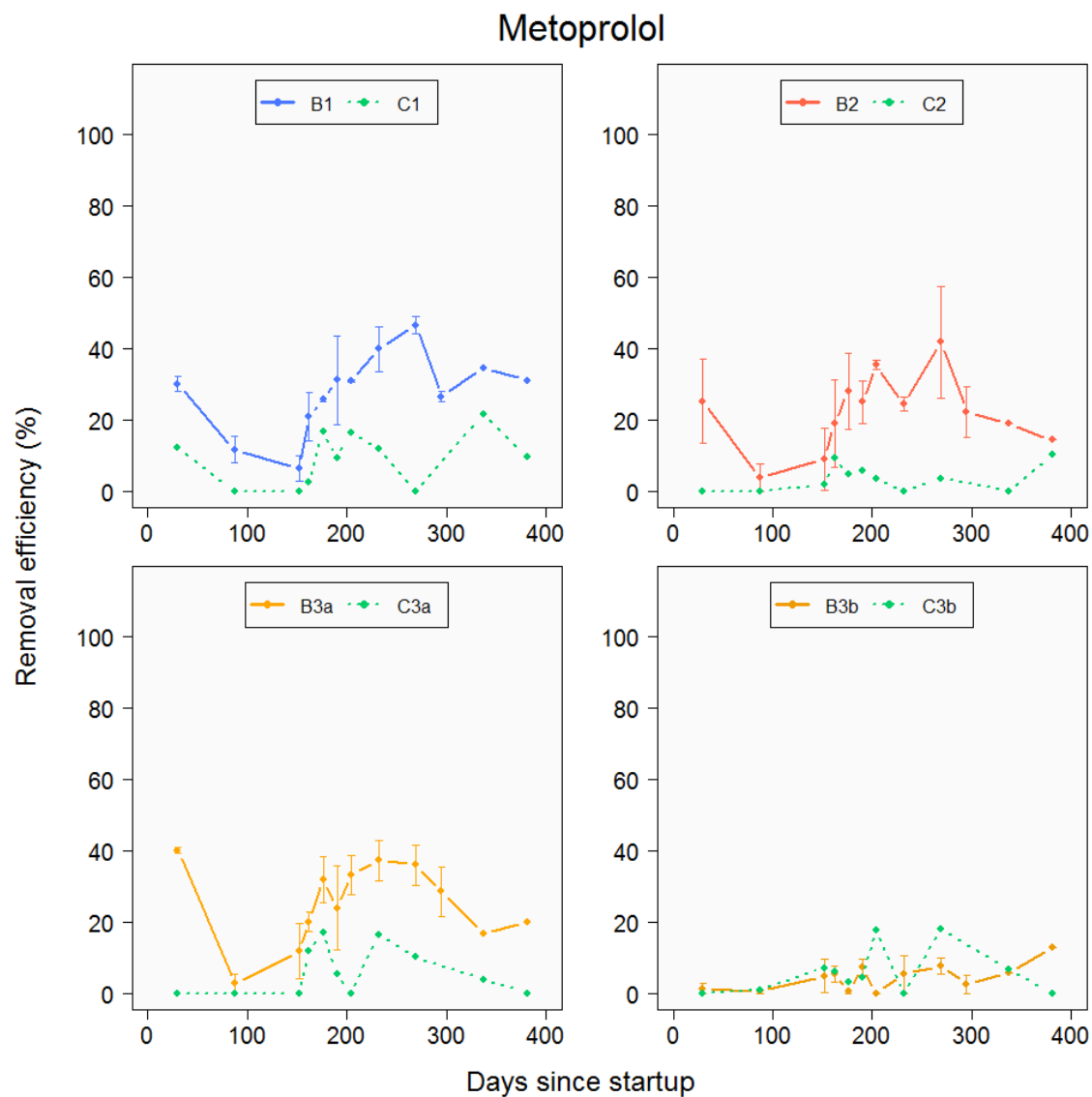


Figure F.15: Removal efficiency of metoprolol for the duration of the experiment.

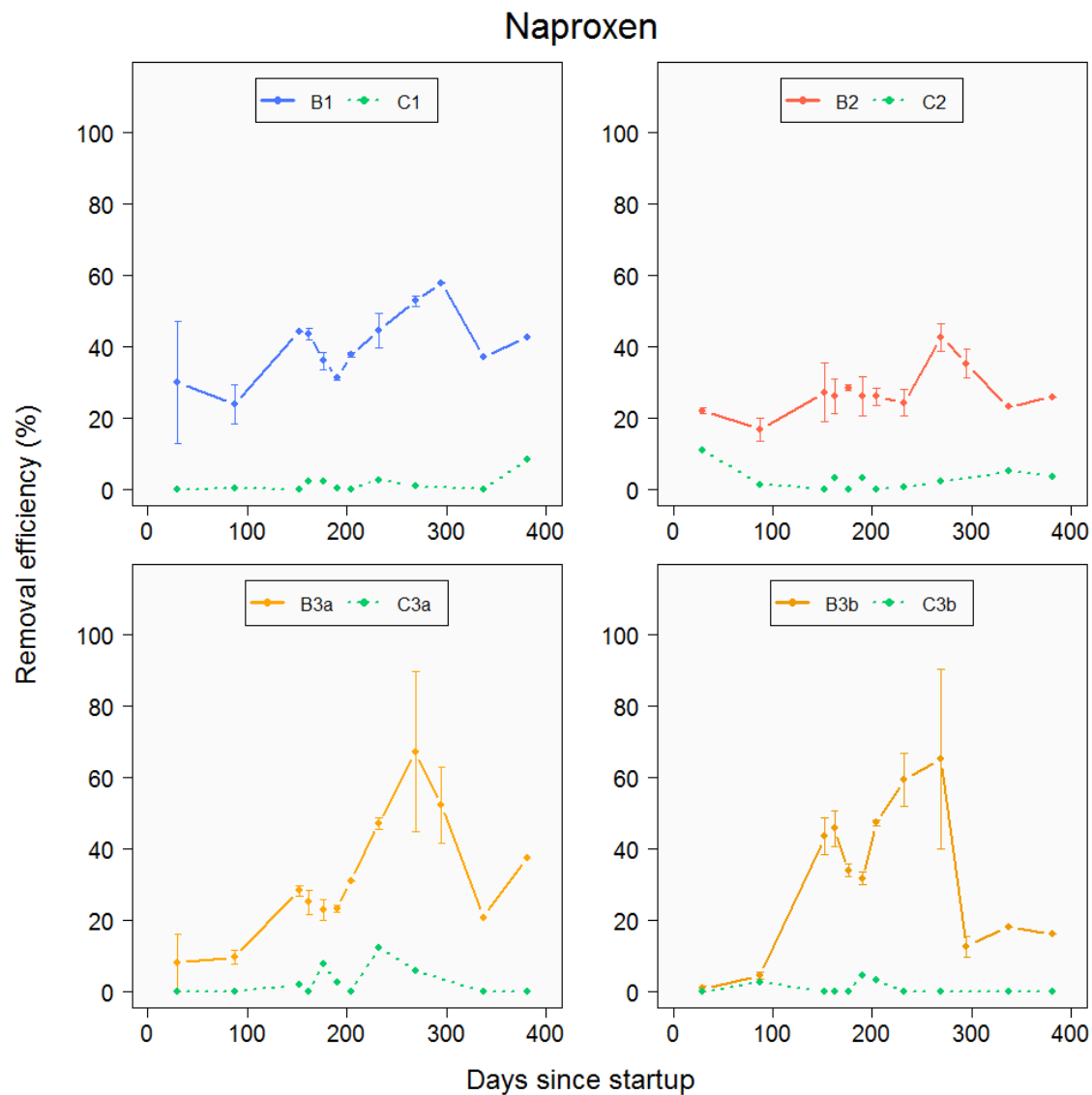


Figure F.16: Removal efficiency of naproxen for the duration of the experiment.

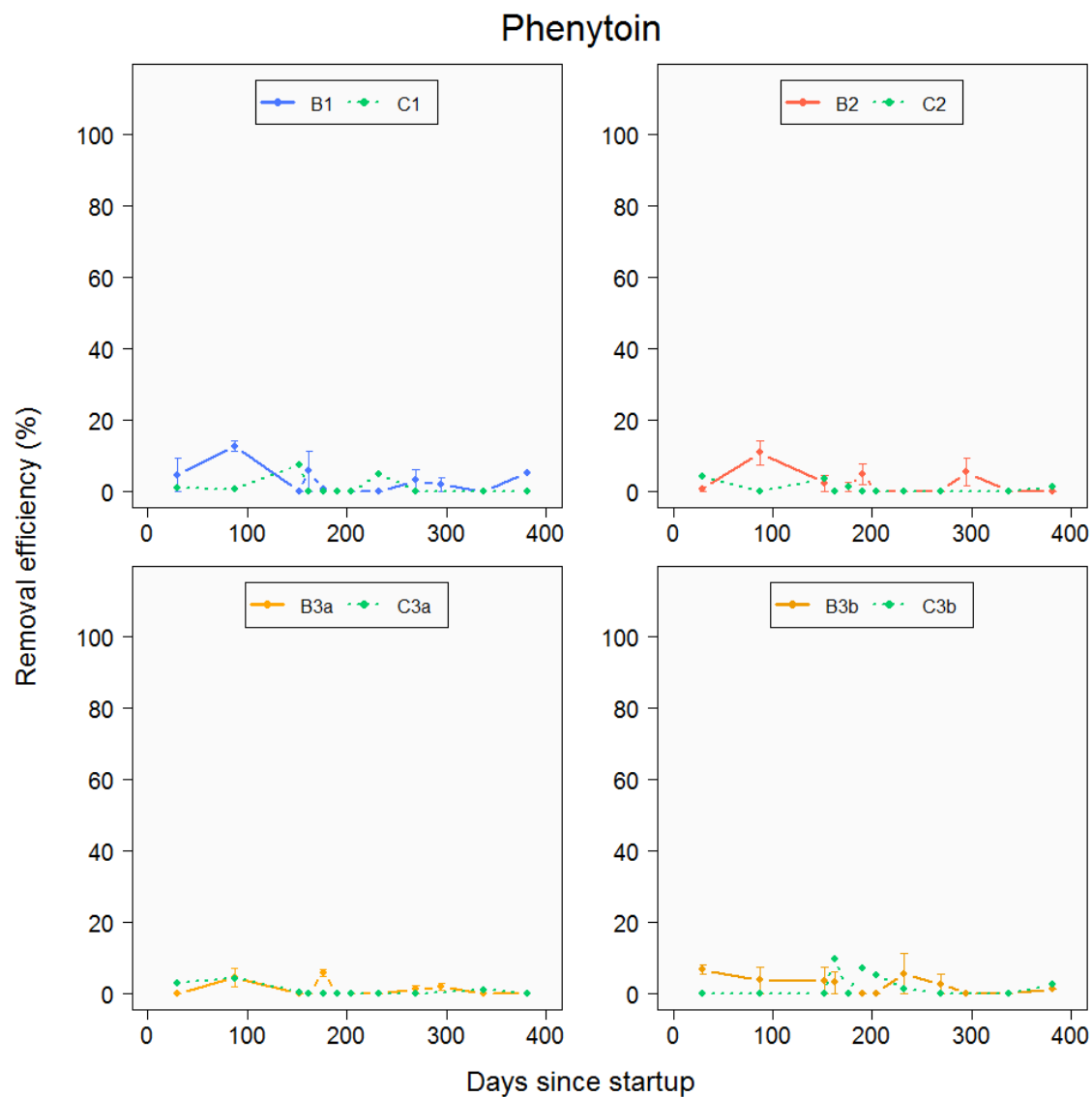


Figure F.17: Removal efficiency of phenytoin for the duration of the experiment.

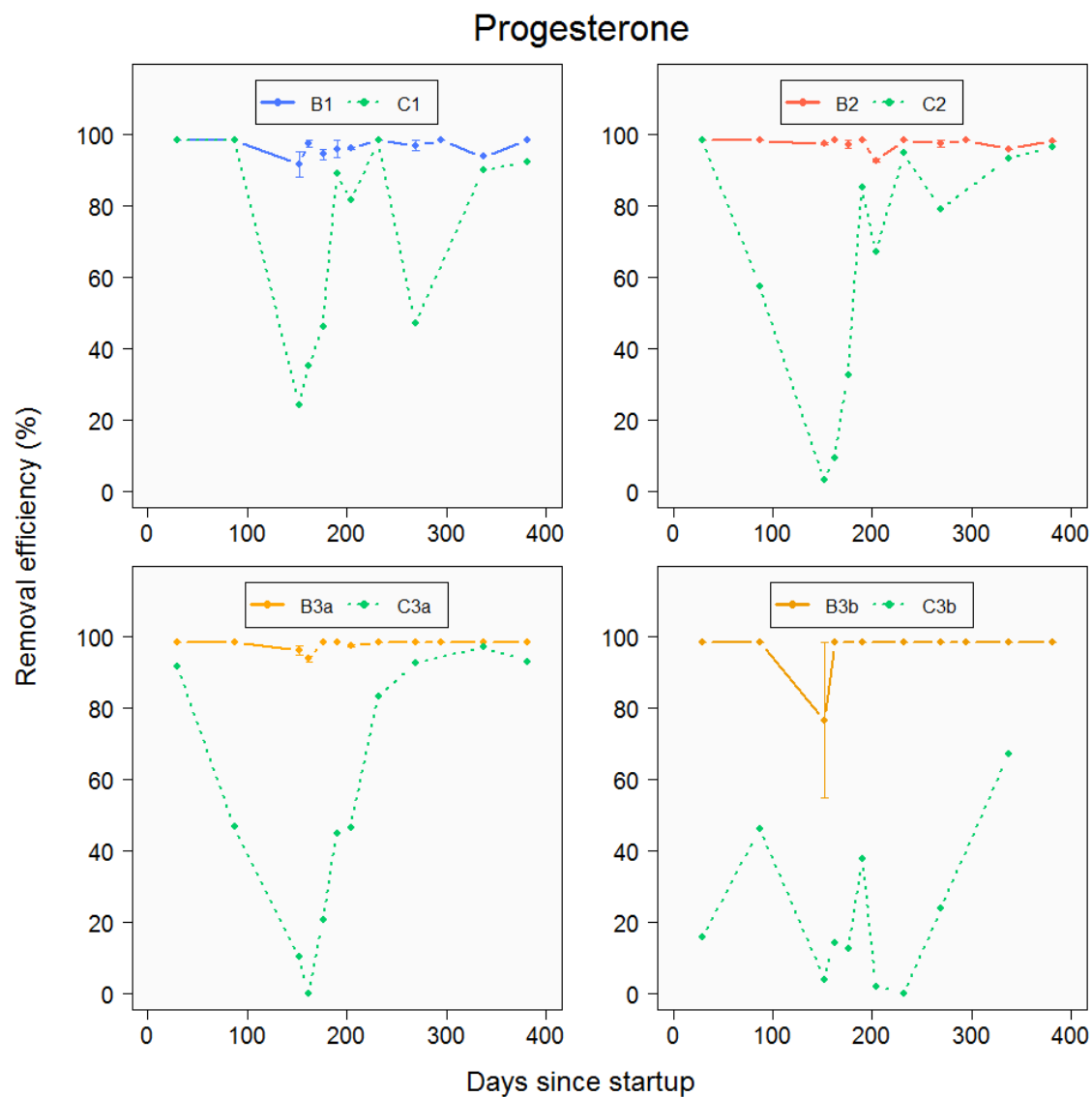


Figure F.18: Removal efficiency of progesterone for the duration of the experiment.

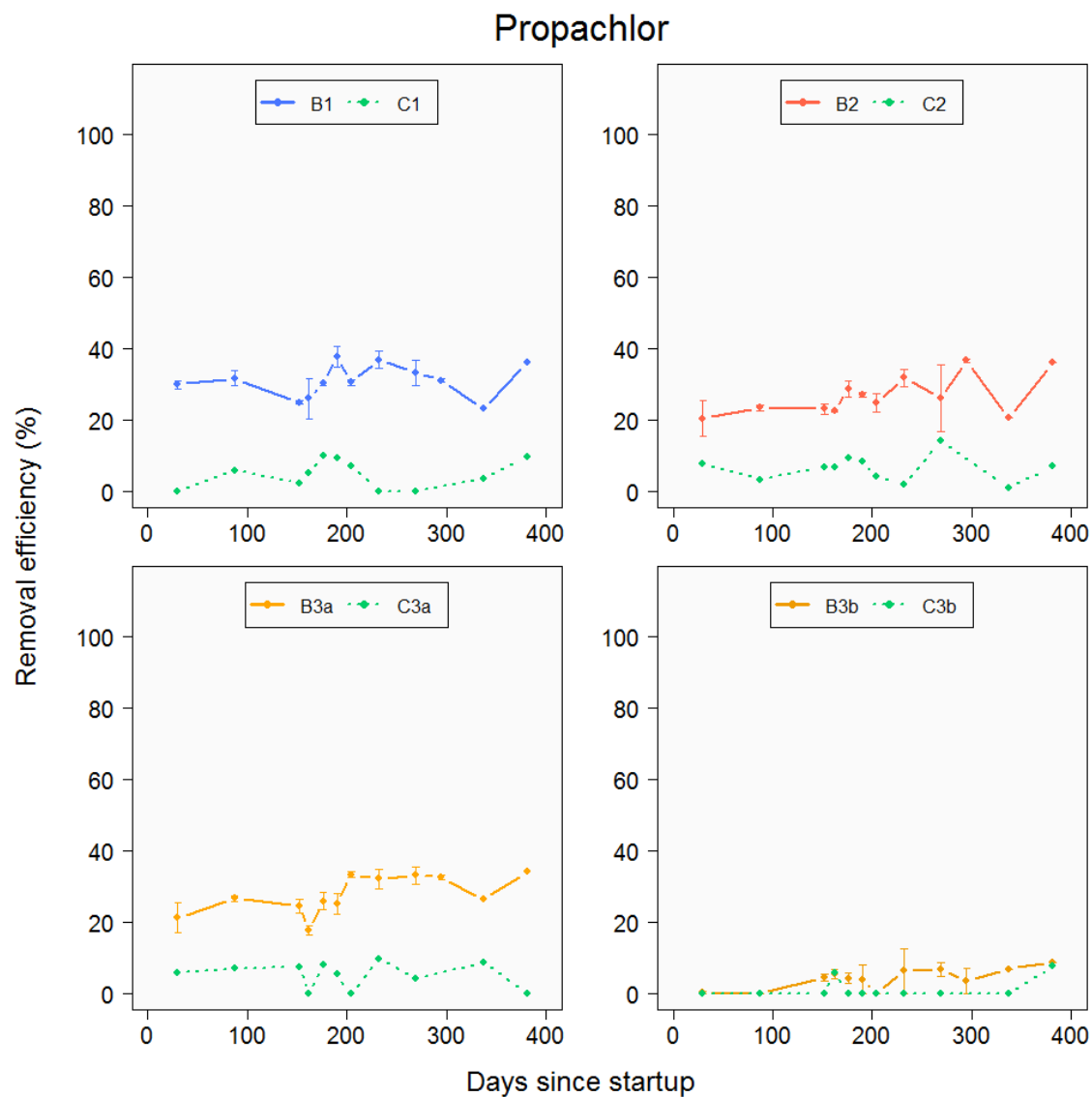


Figure F.19: Removal efficiency of propachlor for the duration of the experiment.

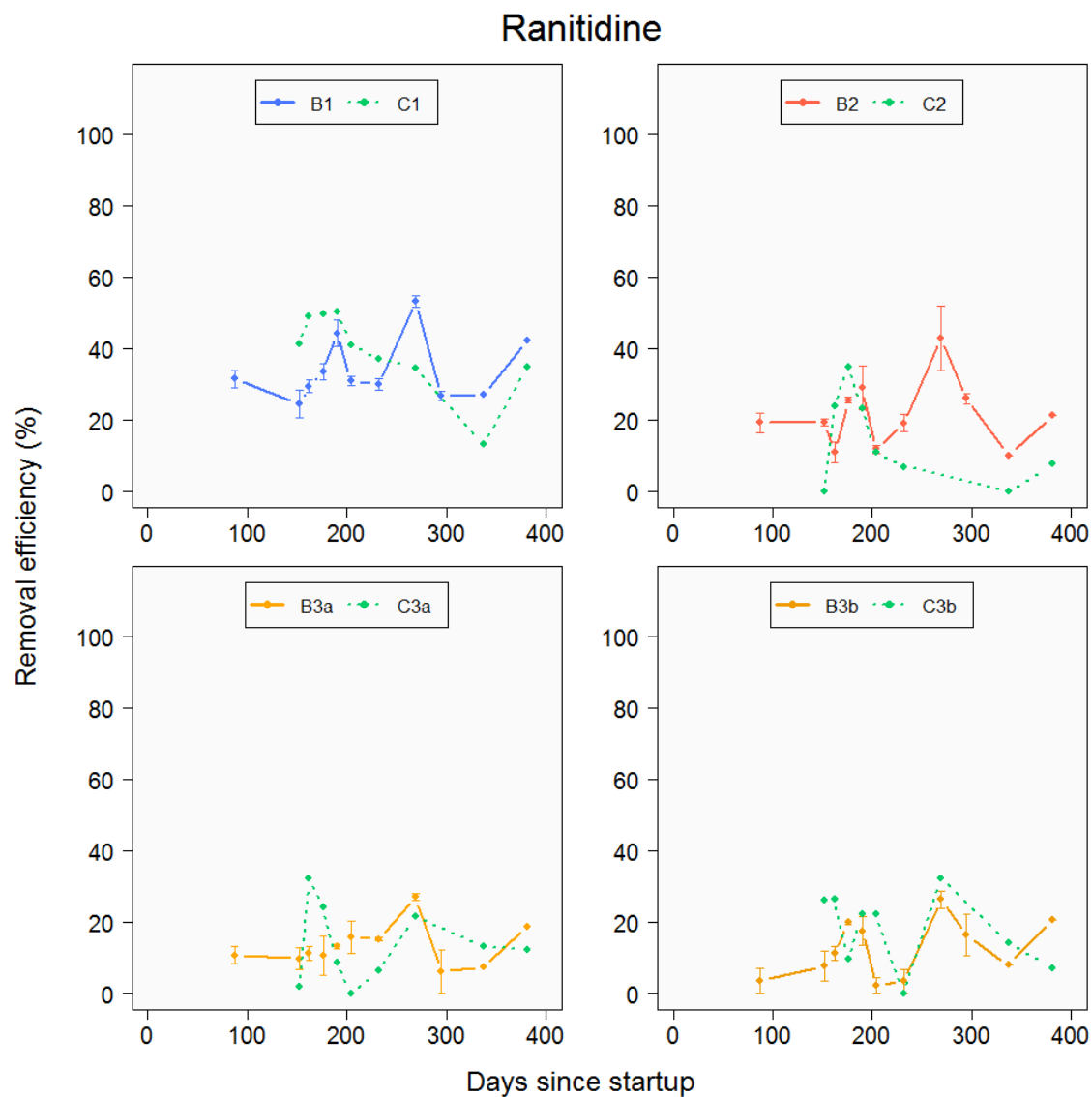


Figure F.20: Removal efficiency of ranitidine for the duration of the experiment.

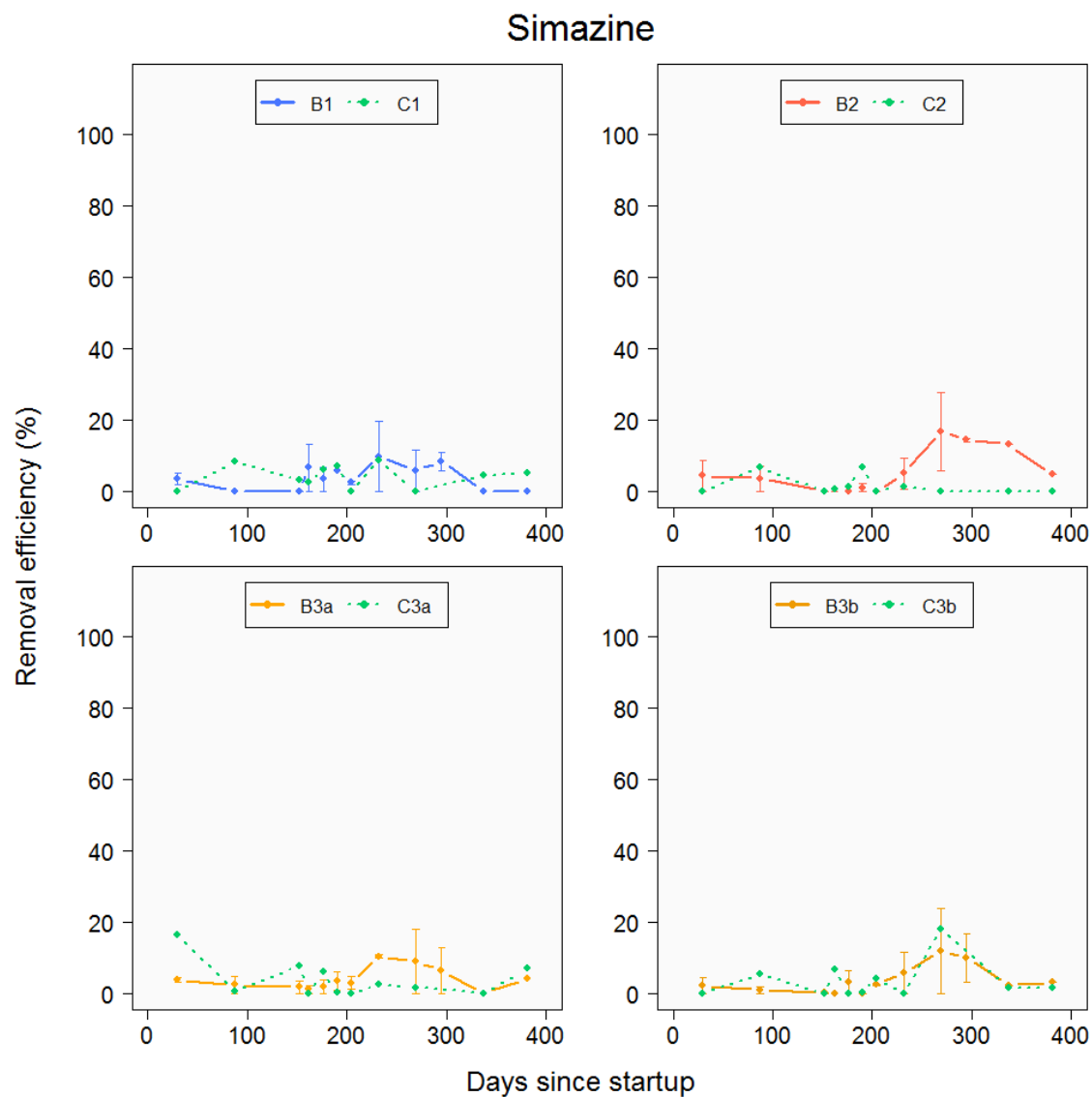


Figure F.21: Removal efficiency of simazine for the duration of the experiment.

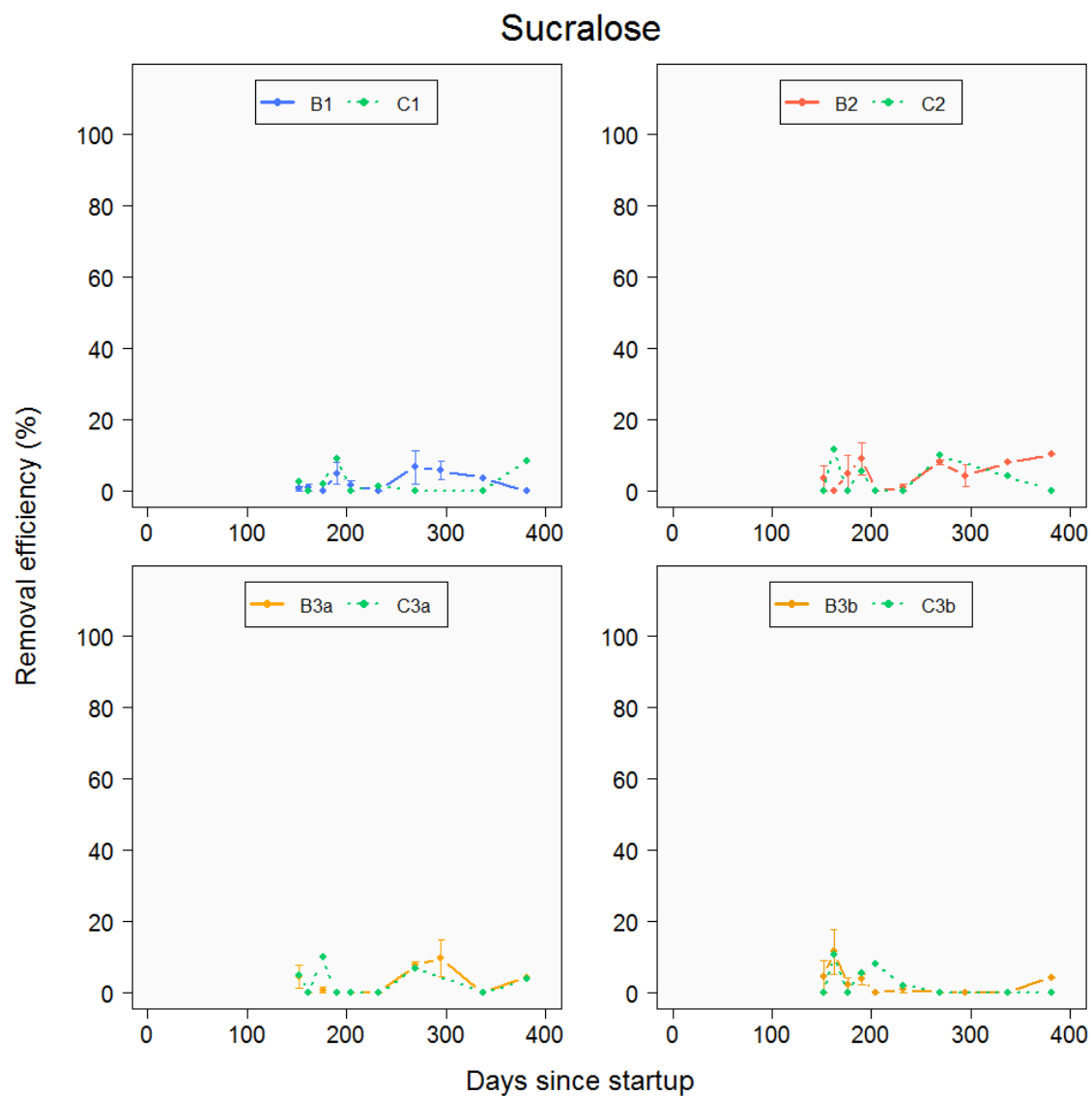


Figure F.22: Removal efficiency of sucralose for the duration of the experiment.

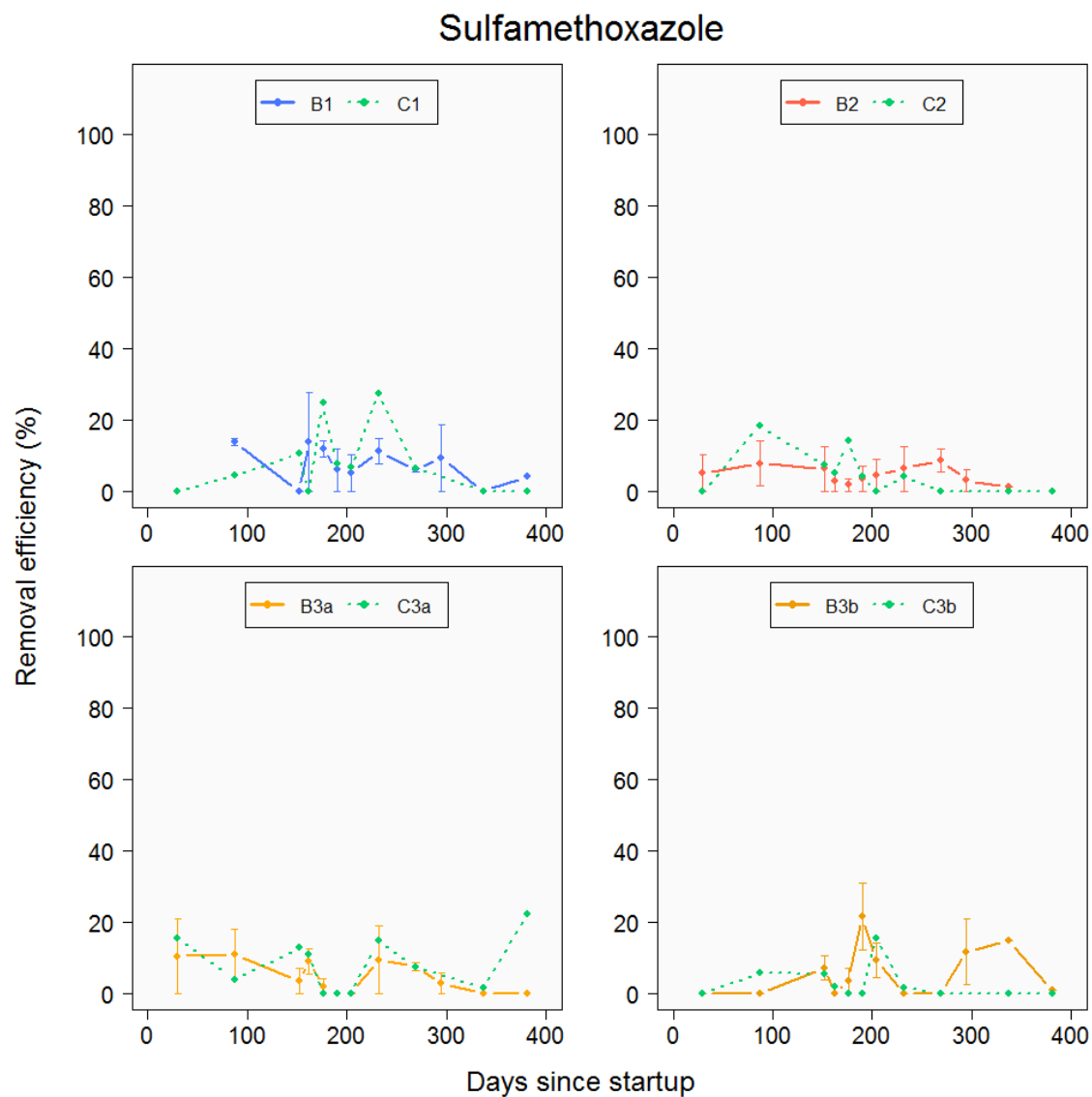


Figure F.23: Removal efficiency of sulfamethoxazole for the duration of the experiment.

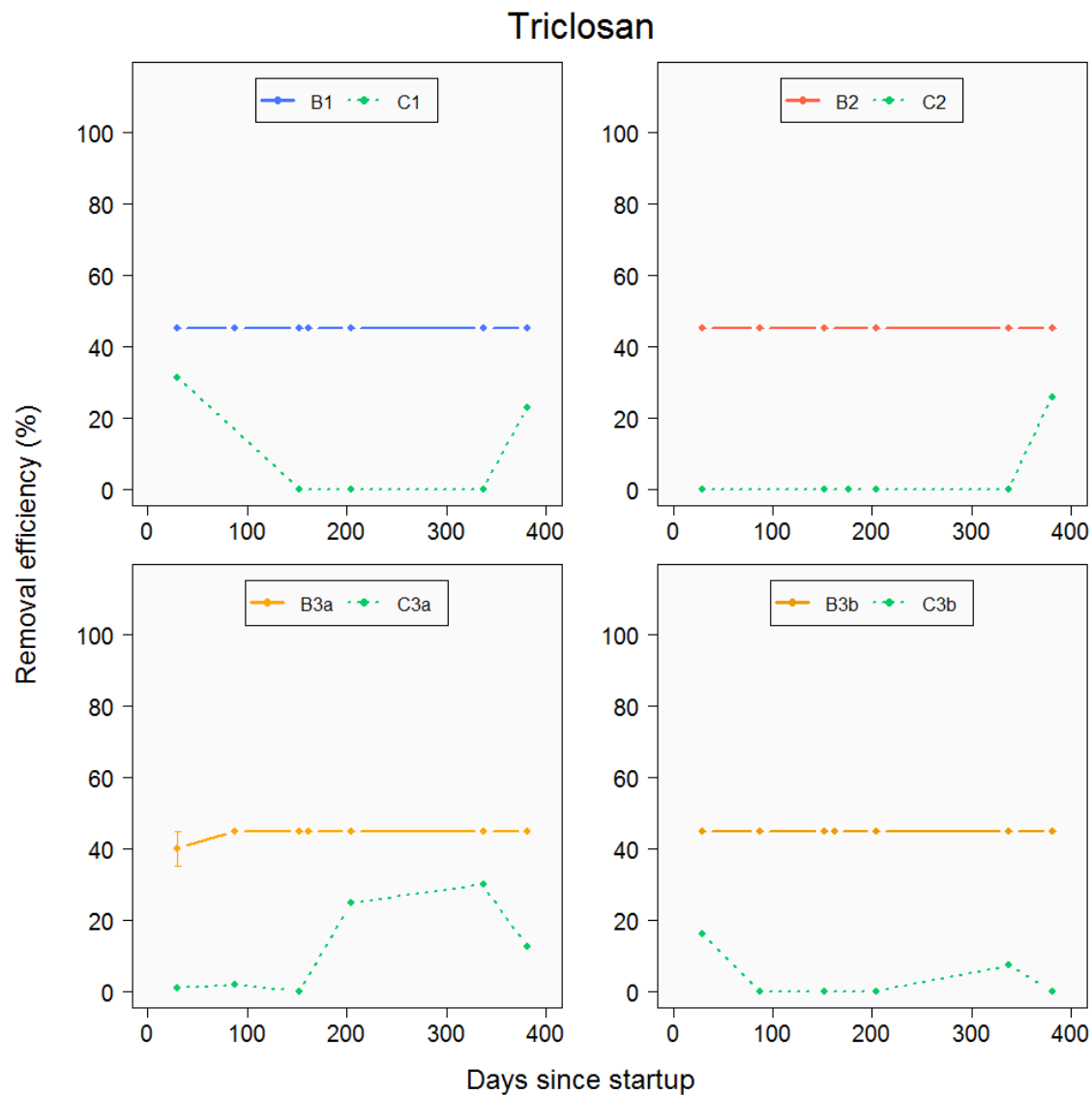


Figure F.24: Removal efficiency of triclosan for the duration of the experiment.

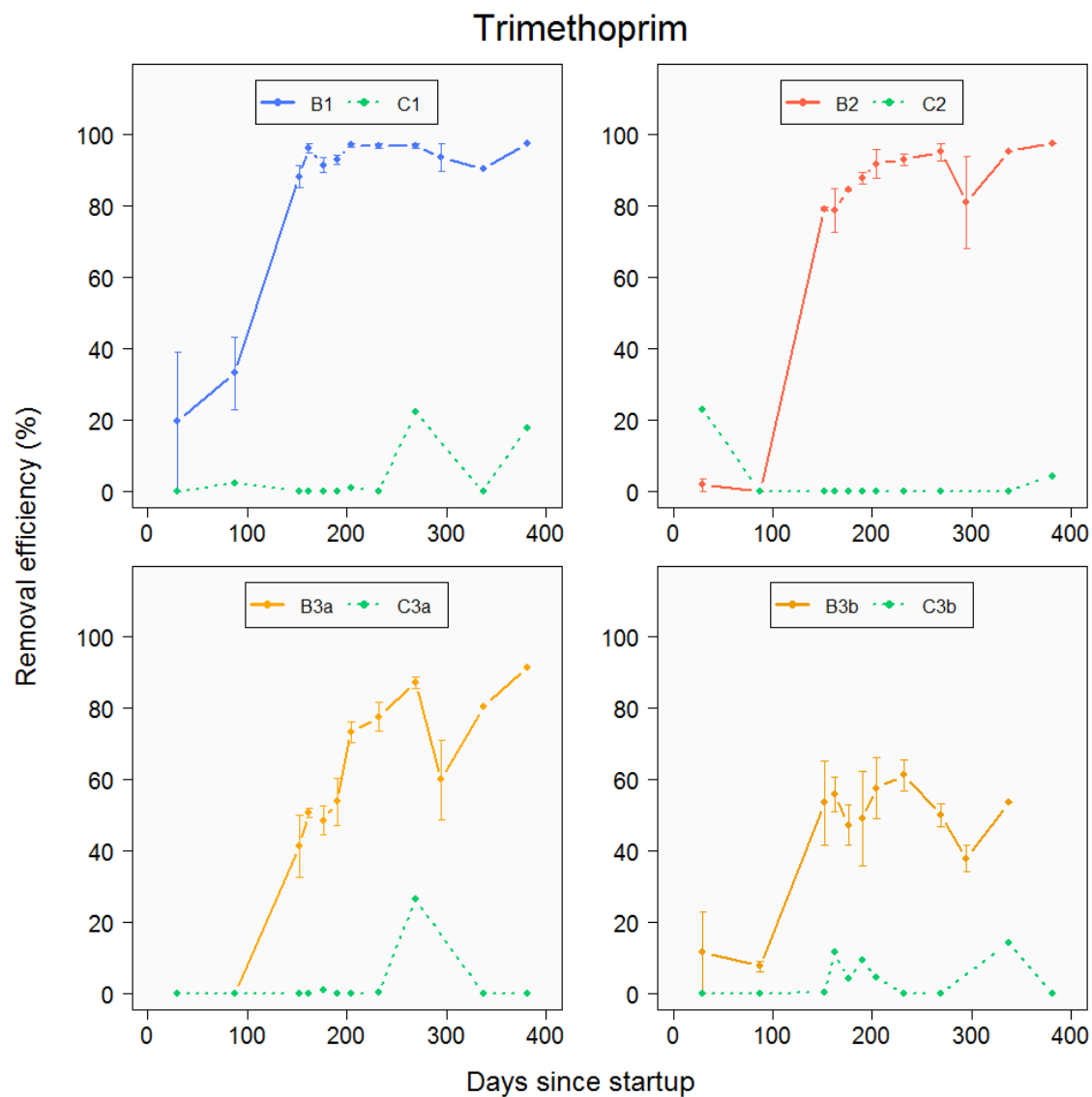


Figure F.25: Removal efficiency of trimethoprim for the duration of the experiment.

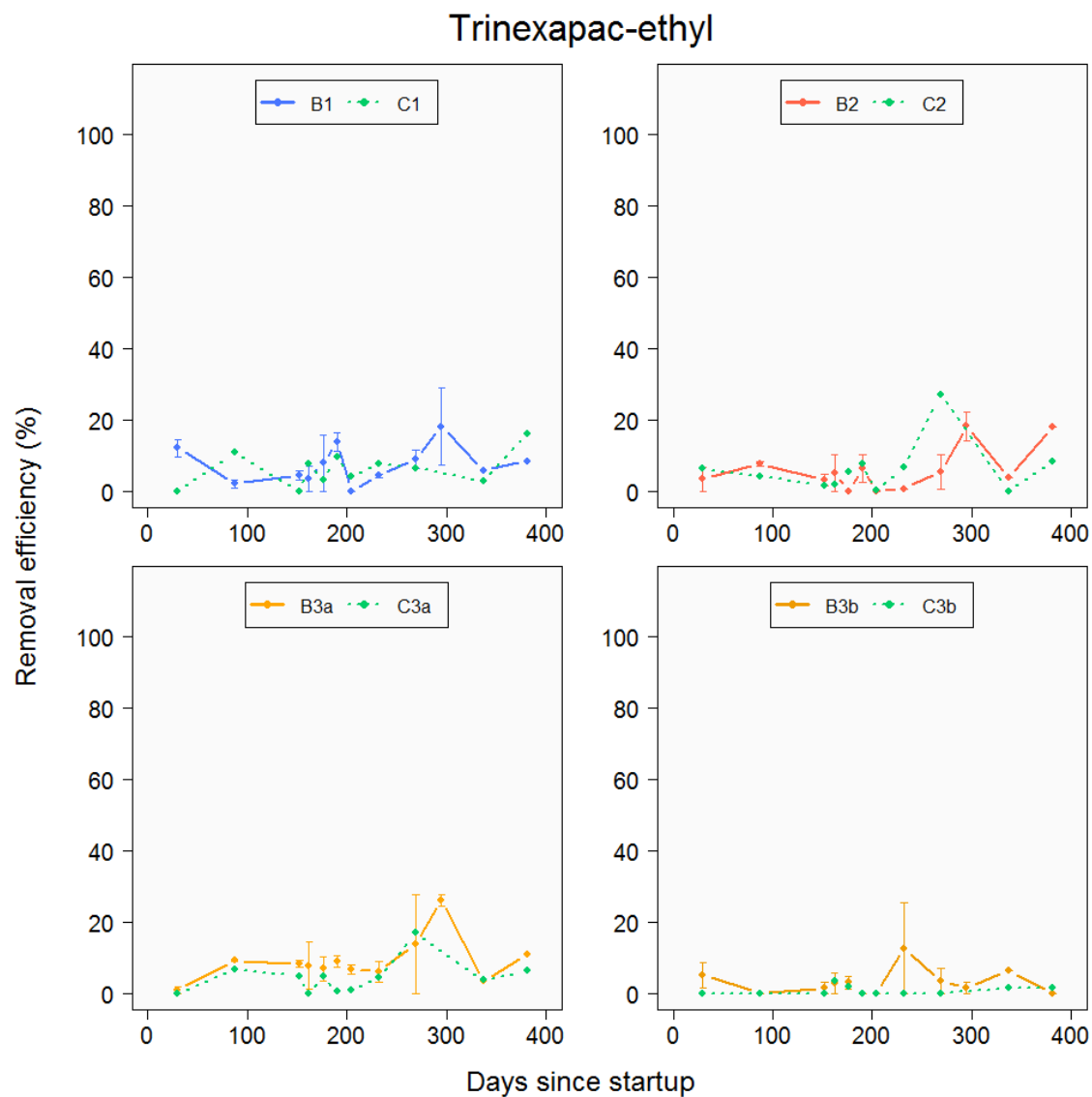


Figure F.26: Removal efficiency of trinexapac-ethyl for the duration of the experiment.



Figure F.27: Removal efficiency of valsartan for the duration of the experiment.

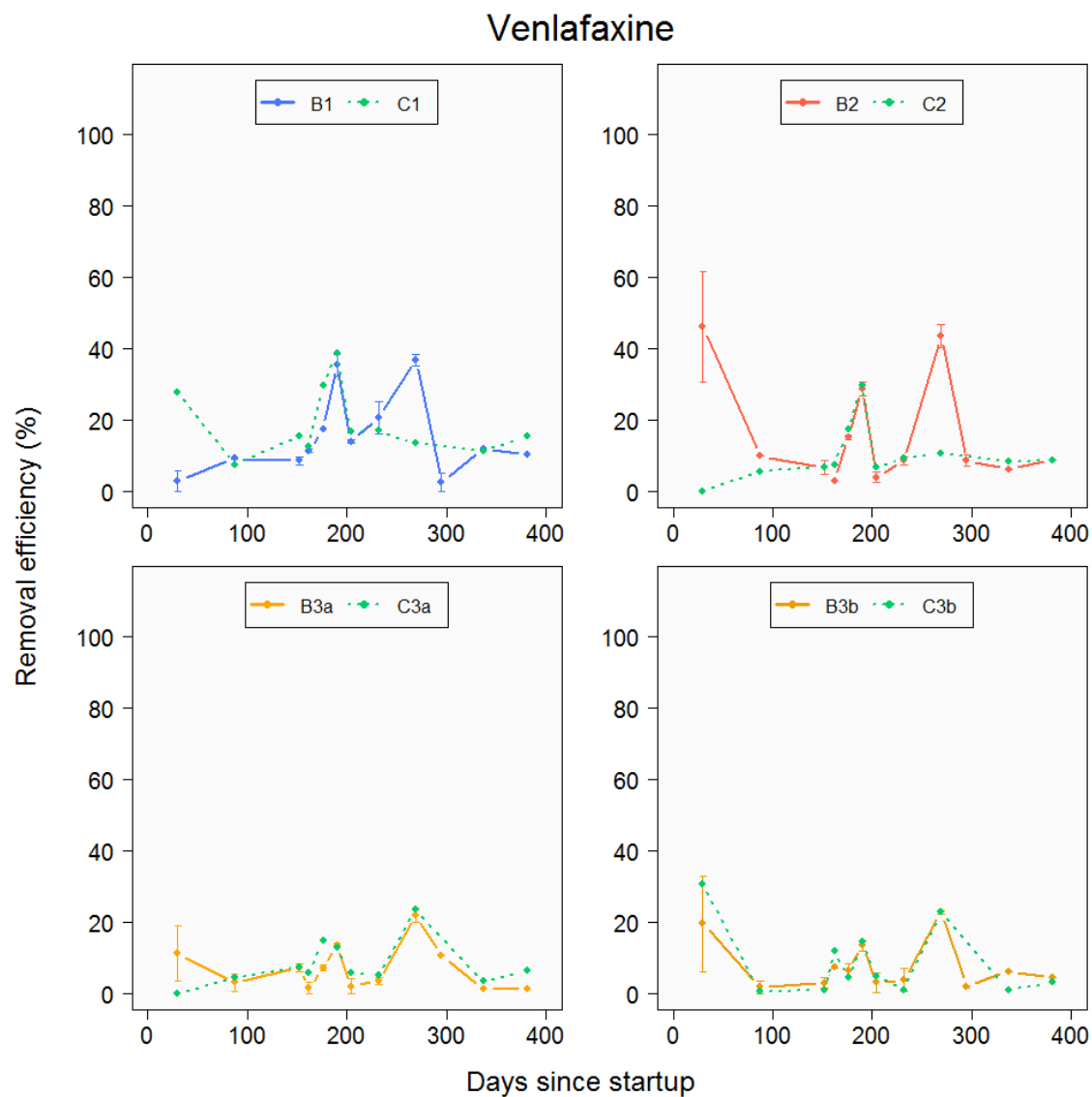


Figure F.28: Removal efficiency of venlafaxine for the duration of the experiment.

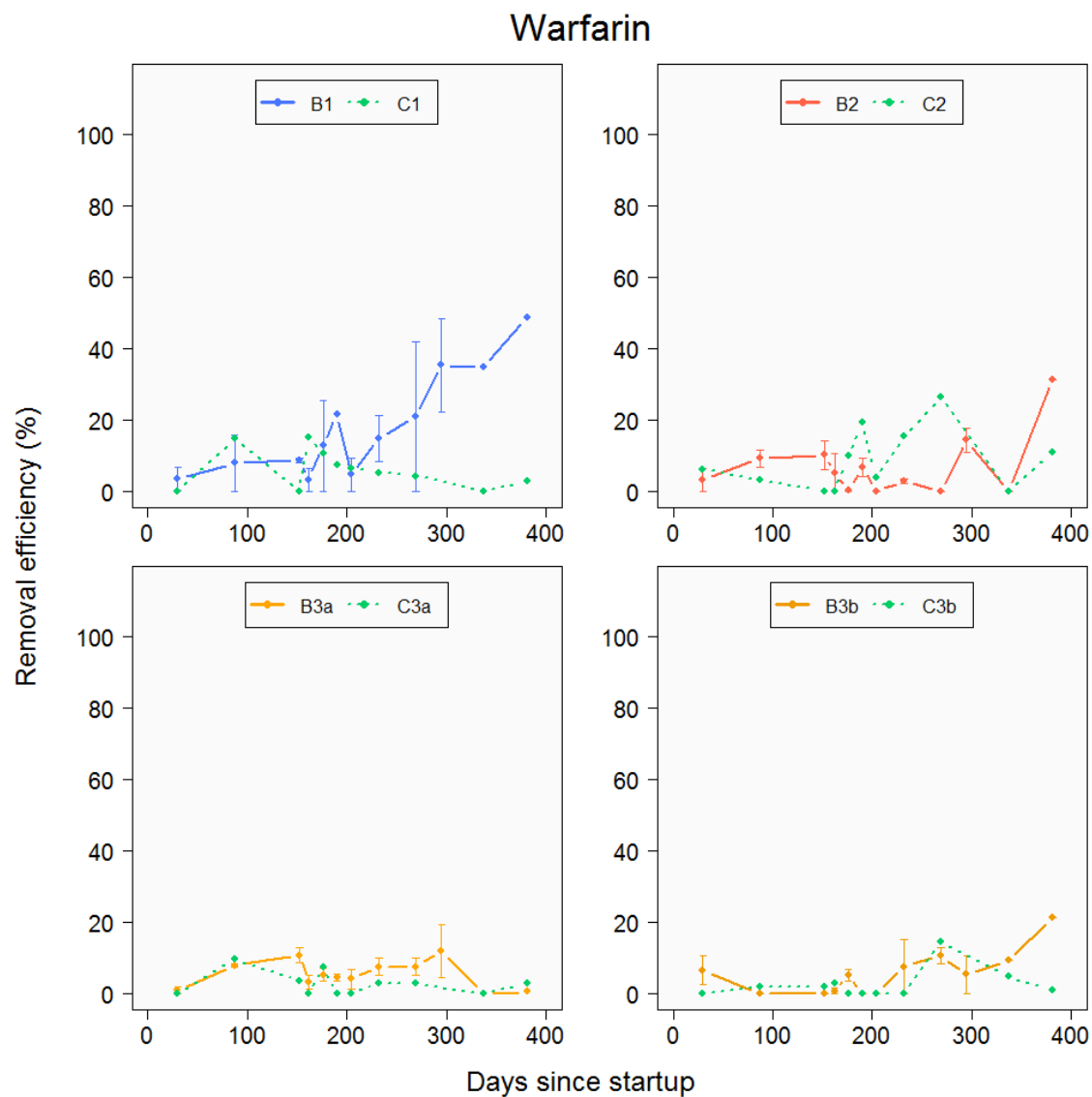


Figure F.29: Removal efficiency of warfarin for the duration of the experiment.

Appendix G: Transformation product identification

To examine the formation of TPs through the biofilters, the influent MP concentrations were briefly increased. Since the influent concentration was low ($1 \mu\text{g L}^{-1}$), most TPs were unable to be detected as they are likely present at concentrations below their limits of detection. On day 339 of filter operation, the influent MP concentrations were briefly increased 100-fold ($100 \mu\text{g L}^{-1}$) and the columns were operated continuously for 16 hours in this condition prior to sampling. Samples were taken from the influent and effluent of each biofilter and control filter, centrifuged to remove particulates, stored at -20°C until analysis, and analyzed for TPs as described in **Appendix C**.

To identify candidate TPs, the following data analysis was adapted from a previous MP biotransformation study (Helbling et al., 2010). Briefly, a list of TPs for the 11 MPs that underwent biotic removal was generated using EnviPath. The output is a list of simplified molecular-input line-entry system (SMILES) strings which were converted into molecular formulas and exact masses using JChem for Office (Excel). In addition to the predicted TPs found using EnviPath, known TPs found in the literature were also examined. Extracted ion chromatograms (EICs) were manually inspected for each suspect TP at $[\text{M}+\text{H}]^{+}$, $[\text{M}+\text{Na}]^{+}$, and $[\text{M}-\text{H}]^{-}$ m/z values. Chromatographic peaks present at higher peak areas in the biofilter effluent than in the influent and control filter effluent were inspected further for matching mass spectra ($\Delta m < 5$ ppm) and corresponding isotopic patterns. Then, MS/MS fragments were verified with fragments generated by the suspect TP structure using Mass Frontier (Thermo Fisher Scientific) and/or with previously published MS data. RT, isotopic patterns, and MS/MS fragments were verified with authentic reference standards when available. Identified TPs are presented in **Figures G.1–G.16**, where chromatographic peaks, mass spectra, and MS/MS fragments are used as identifiers of the

compounds. Atenolol acid and propachlor-OXA are reported with a confidence of Level 1 (confirmed structure with reference standard) and other TPs are reported with a confidence of Level 2 (probable structure by library/diagnostic evidence) as described in Schymanski et al.,2014.

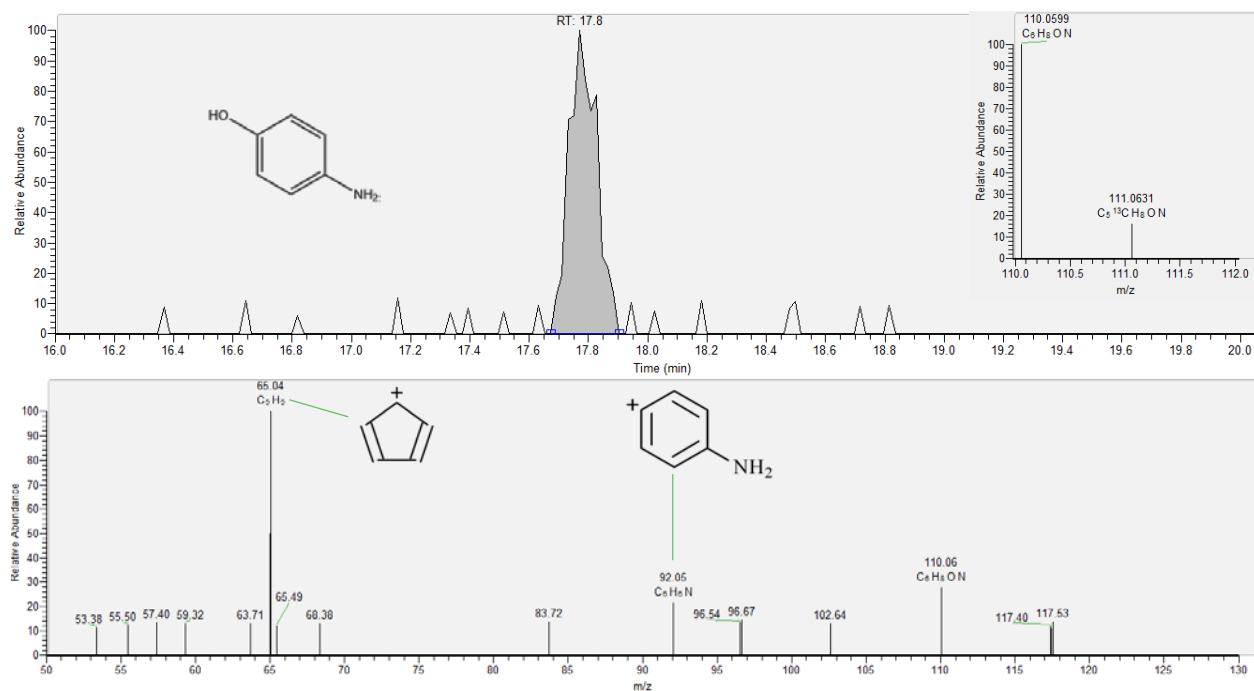


Figure G.1: Identification of 4-aminophenol.

Acetaminophen was predicted to undergo biotransformation reaction *bt0067* to form 4-aminophenol which had a RT of 17.8 min and was present in the biofilter effluent at 1.4x the peak area than the influent and the control filter effluent. The MS spectra matched the exact mass of the proposed compound ($m/z = 110.0599$ for $[M+H]^+$, $\Delta m = -1.817$ ppm) and the theoretical abundance (6%) of the ^{13}C monoisotopic mass. The MS/MS fragments with $m/z = 65.04$ and 92.05 matched with fragments generated by the predicted structure using Mass Frontier.

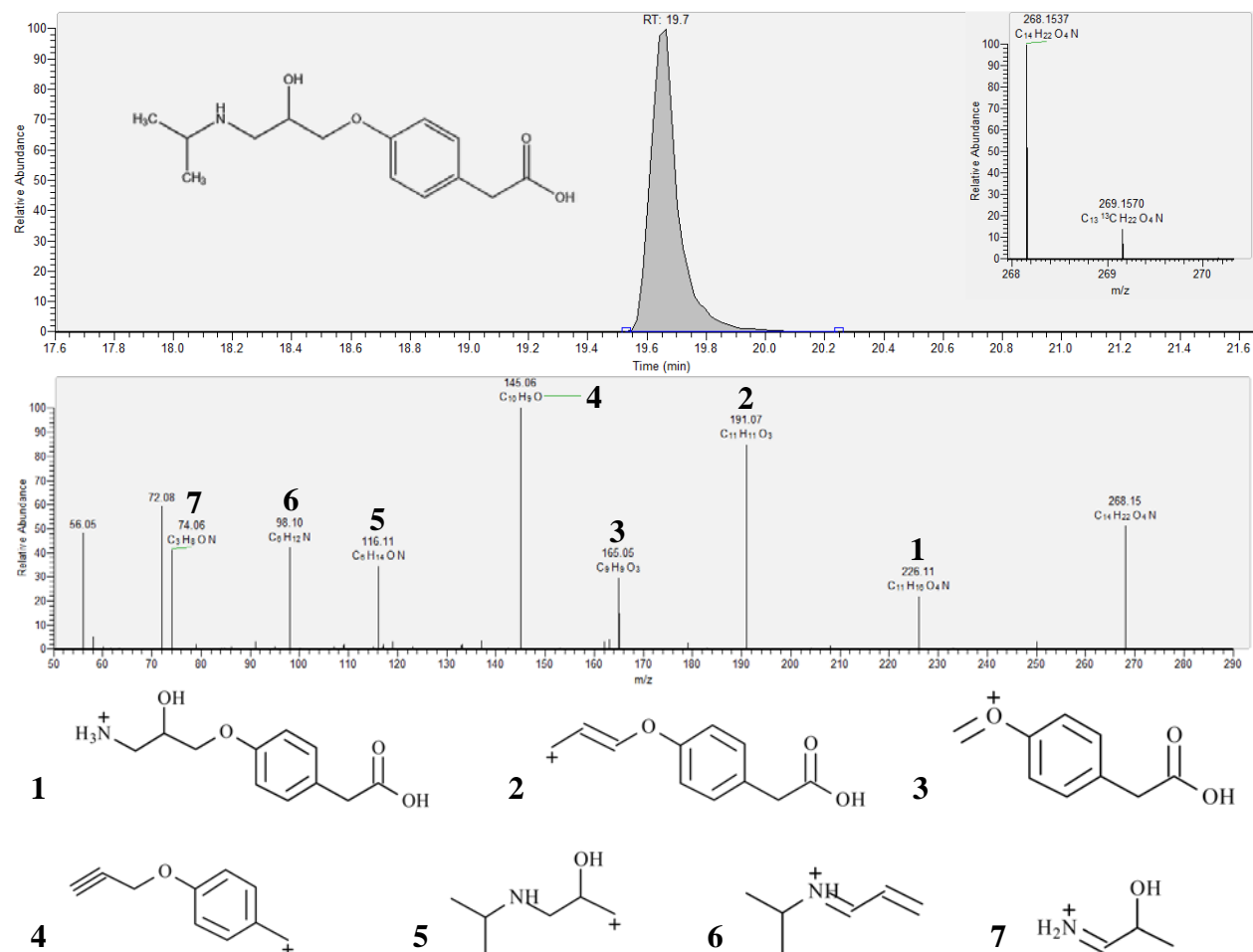


Figure G.2: Identification of atenolol-acid.

Atenolol is known to undergo biotransformation reaction *bt0027* to form atenolol-acid (Helbling et al., 2010) which had a RT of 19.7 min and was present in the biofilter effluent at 4x the peak area than the influent and the control filter effluent. Metoprolol can also be biotransformed into atenolol-acid (Rubirola et al., 2014). The MS spectra matched the exact mass of the proposed compound ($m/z = 268.1535$ for $[M+H]^+$, $\Delta m = -3.356$ ppm) and the theoretical abundance (14%) of the ¹³C monoisotopic mass. The RT and MS/MS fragments with $m/z = 226.11$, 191.07, 165.05, 145.06, 116.11, 98.10, and 74.06 were verified with an authentic reference standard and matched the fragments generated by the predicted structure using Mass Frontier.

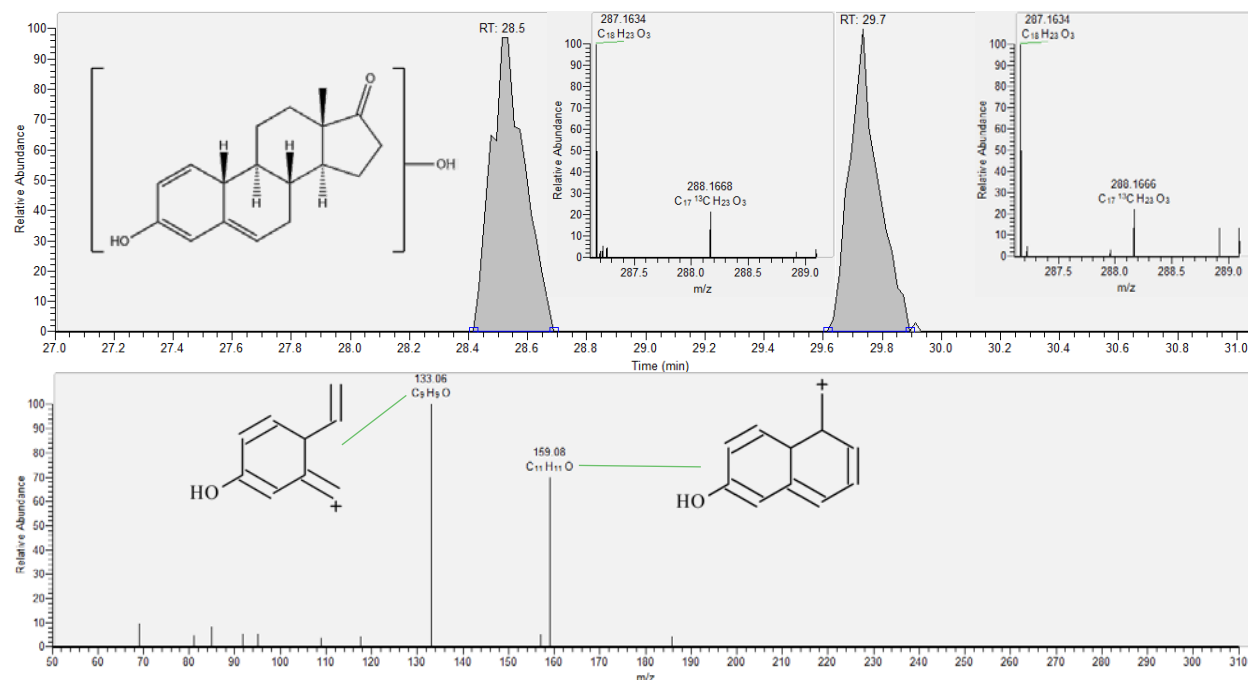


Figure G.3: Identification of hydroxy-estrone.

Estrone was predicted to undergo biotransformation reaction *bt0014* at two locations to form two isomers of hydroxy-estrone which had RTs of 28.5 and 29.7 min and was only present in the biofilter effluent. The MS spectra matched the exact mass of the proposed compound ($m/z = 287.1634$ for $[M+H]^+$, $\Delta m = -2.786$ ppm) and the theoretical abundance (18%) of the ^{13}C monoisotopic mass. The MS/MS fragments with $m/z = 159.08$ and 133.06 matched with fragments generated by the predicted structure using Mass Frontier.

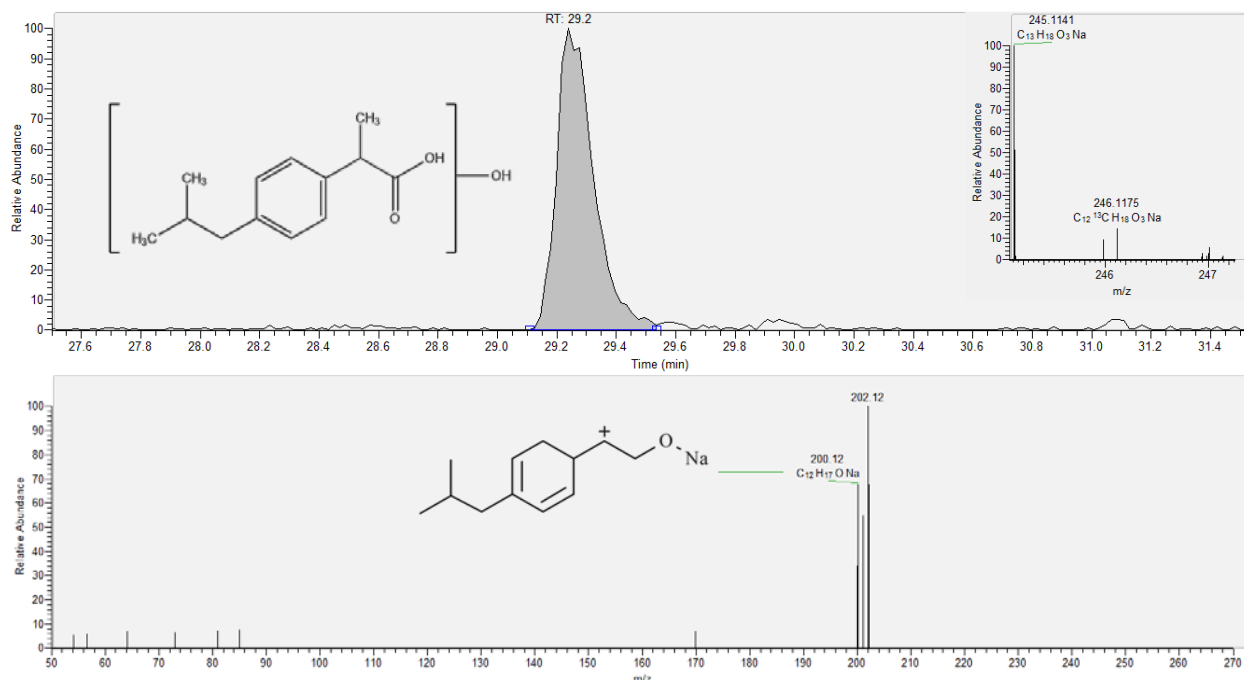


Figure G.4: Identification of hydroxy-ibuprofen.

Ibuprofen was predicted to undergo biotransformation reactions *bt0241*, *bt0242* and *bt0333* at several locations to form hydroxy-ibuprofen which had a RT of 29.2 min and was only present in the biofilter effluent. The MS spectra matched the exact mass of the proposed compound ($m/z = 245.1141$ for $[M+Na]^+$, $\Delta m = -2.856$ ppm) and the theoretical abundance (13%) of the ^{13}C monoisotopic mass. The MS/MS fragment with $m/z = 200.12$ matched with fragments generated by the predicted structure using Mass Frontier.

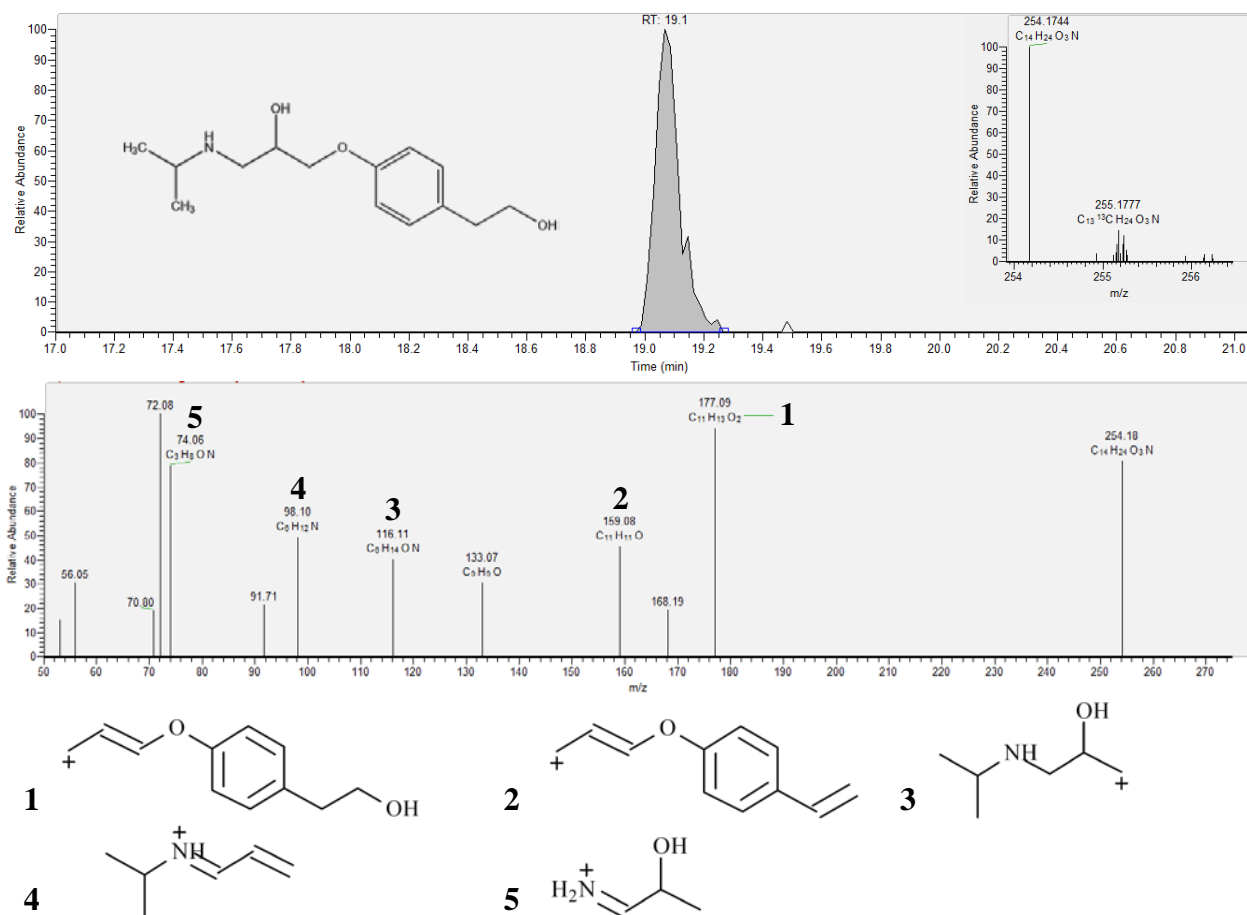


Figure G.5: Identification of O-desmethyl-metoprolol.

Metoprolol was predicted to undergo biotransformation reaction *bt0023* to form O-desmethyl-metoprolol which had a RT of 19.1 min and was present in the biofilter effluent at 4x the peak area than the influent and the control filter effluent. The MS spectra matched the exact mass of the proposed compound ($m/z = 254.1744$ for $[M+H]^+$, $\Delta m = -2.754$ ppm) and the theoretical abundance (14%) of the ^{13}C monoisotopic mass. The MS/MS fragments with $m/z = 177.09$, 159.08, 116.11, 98.01, and 74.06 matched with fragments generated by the predicted structure using Mass Frontier.

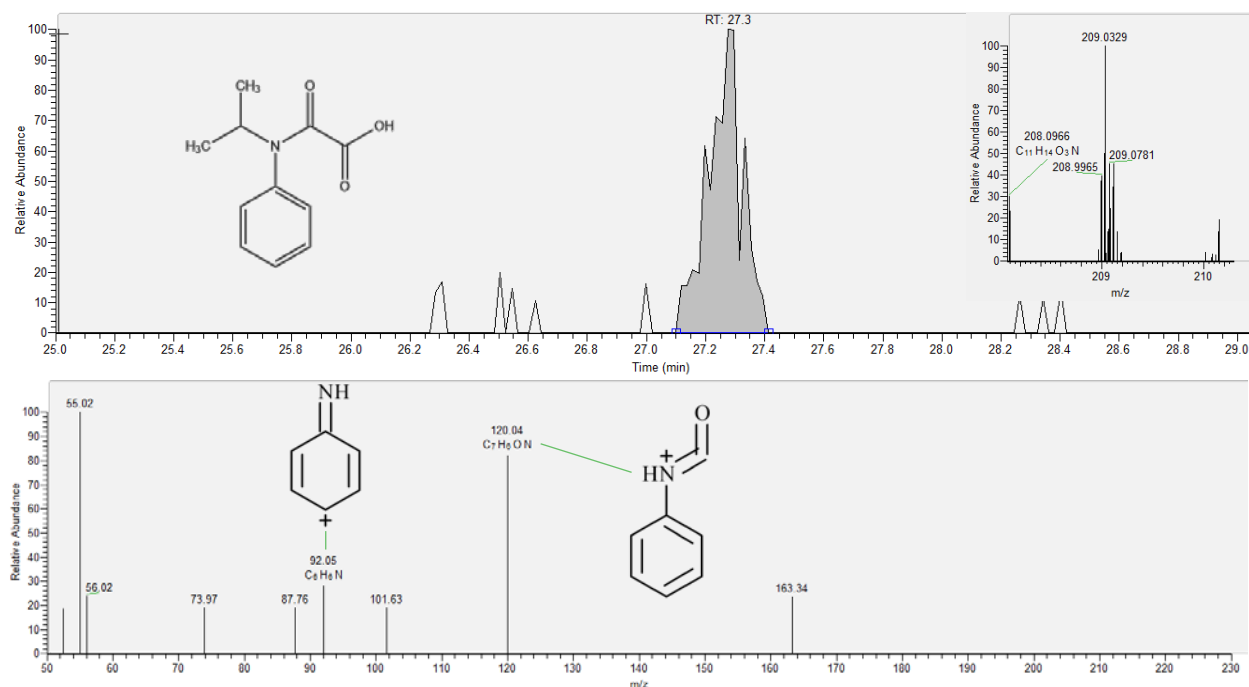


Figure G.6: Identification of propachlor-OXA.

Propachlor has been shown to be biotransformed into propachlor-OXA in biological systems (Helbling et al., 2010) which had a RT of 27.3 min and was only present in the biofilter effluent. The MS spectra matched the exact mass of the proposed compound ($m/z = 208.0968$ for $[M+H]^+$, $\Delta m = -1.922$ ppm). The RT and MS/MS fragments with $m/z = 120.04$ and 92.05 were verified with an authentic reference standard and matched the fragments generated by the predicted structure using Mass Frontier.

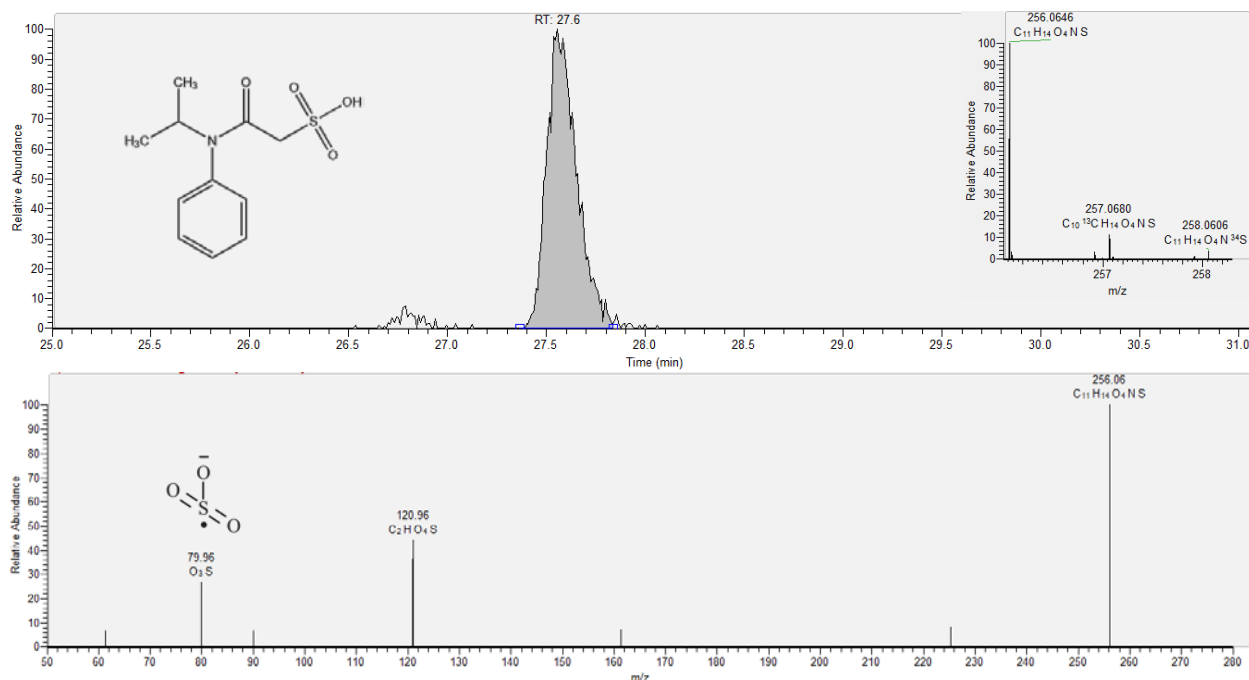


Figure G.7: Identification of propachlor-ESA.

Propachlor has been shown to be biotransformed into propachlor-ESA in biological systems (Helbling et al., 2010) which had a RT of 27.6 min and was present only in the biofilter effluent. The MS spectra matched the exact mass of the proposed compound ($m/z = 256.0646$ for $[M-H]^-$, $\Delta m = -1.172$ ppm) and the theoretical abundance (11%) of the ^{13}C monoisotopic mass and the theoretical abundance (4.5%) of the ^{34}S monoisotopic mass. The MS/MS fragment with $m/z = 79.96$ matched with fragments generated by the predicted structure using Mass Frontier.

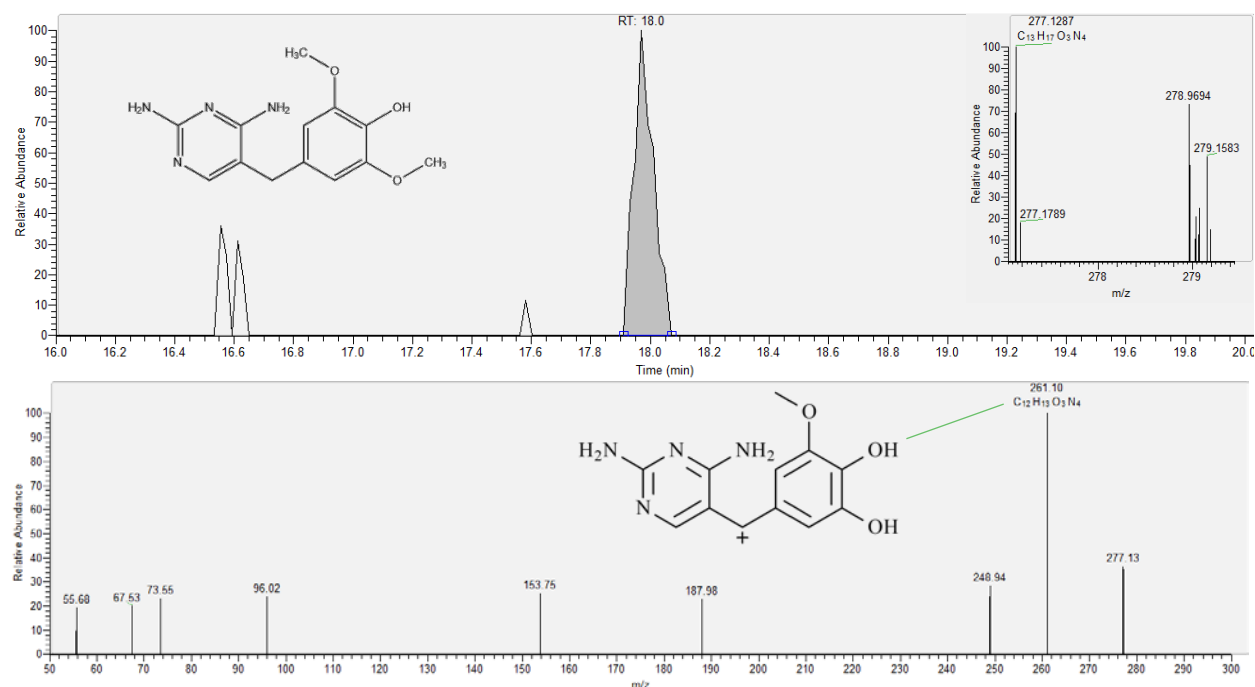


Figure G.8: Identification of 4-desmethyl-trimethoprim.

Trimethoprim was predicted to undergo biotransformation reaction *bt0023* at two locations to form O-desmethyl-trimethoprim which had a RT of 18.0 min and was only present in the biofilter effluent. This reaction is expected to form 4-desmethyl-trimethoprim (Jewell et al., 2016). The MS spectra matched the exact mass of the proposed compound ($m/z = 277.1287$ for $[M+H]^+$, $\Delta m = -2.887$ ppm). The MS/MS fragment with $m/z = 161.10$ matched with fragments generated by the predicted structure using Mass Frontier.

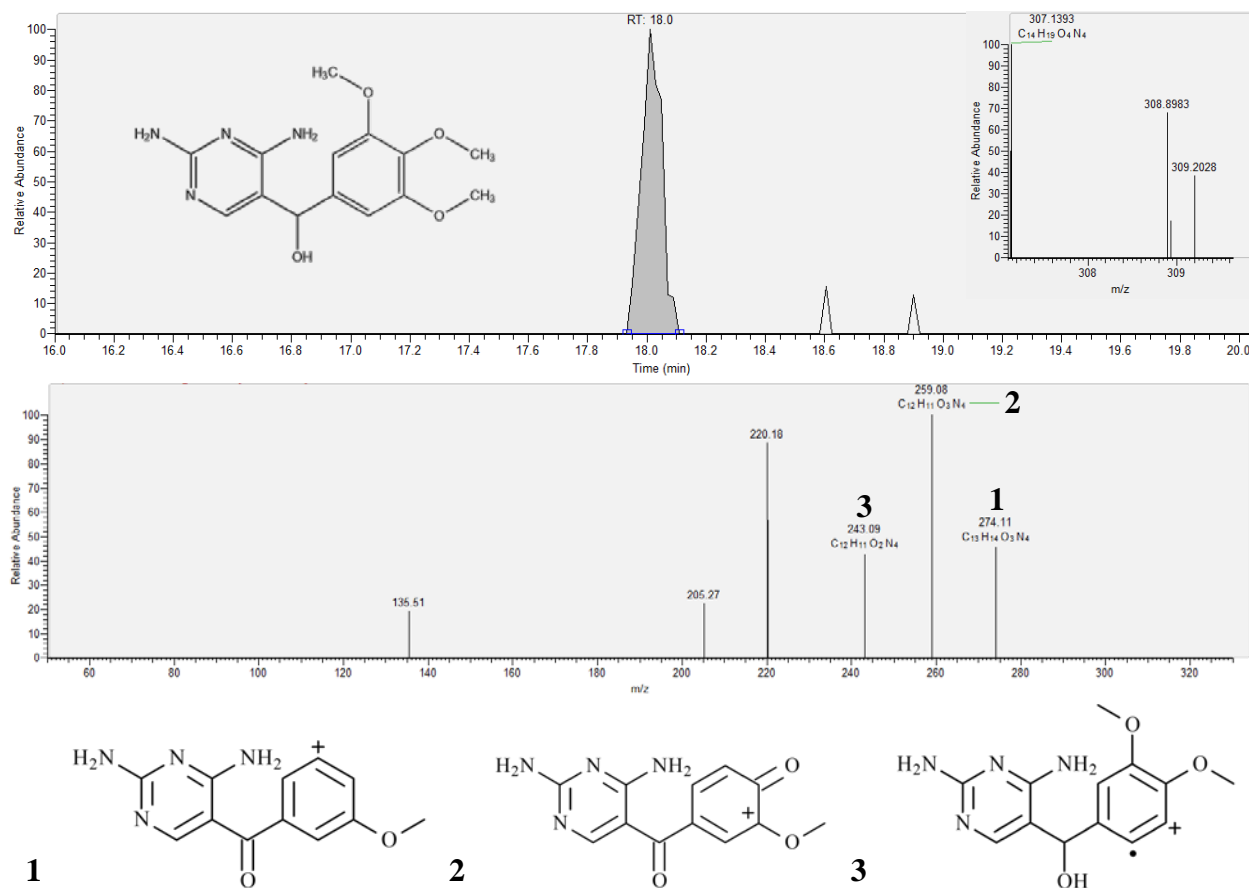


Figure G.9: Identification of hydroxy-trimethoprim.

Trimethoprim was predicted to undergo biotransformation reaction *bt0242* to form hydroxy-trimethoprim which had a RT of 18.0 min and was only present in the biofilter effluent. The MS spectra matched the exact mass of the proposed compound ($m/z = 307.1393$ for $[M+H]^+$, $\Delta m = -2.605$ ppm). The MS/MS fragments with $m/z = 274.11$, 259.08, and 243.09 matched with fragments generated by the predicted structure using Mass Frontier.

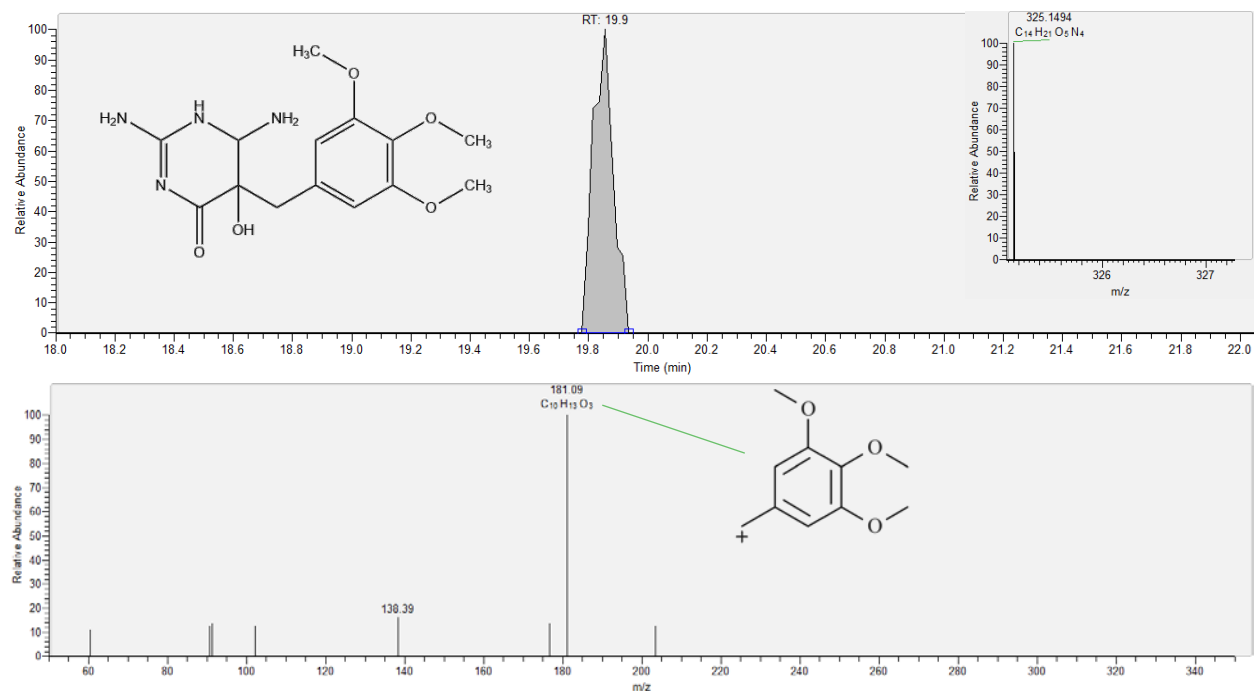


Figure G.10: Identification of TRI-324.

Trimethoprim has been shown to be biotransformed into TRI-324 in biological systems (Jewell et al., 2016) which had a RT of 19.9 min and was only present in the biofilter effluent. The MS spectra matched the exact mass of the proposed compound ($m/z = 325.1494$ for $[M+H]^+$, $\Delta m = -3.691$ ppm). The MS/MS fragment with $m/z = 181.09$ matched with fragments generated by the predicted structure using Mass Frontier.

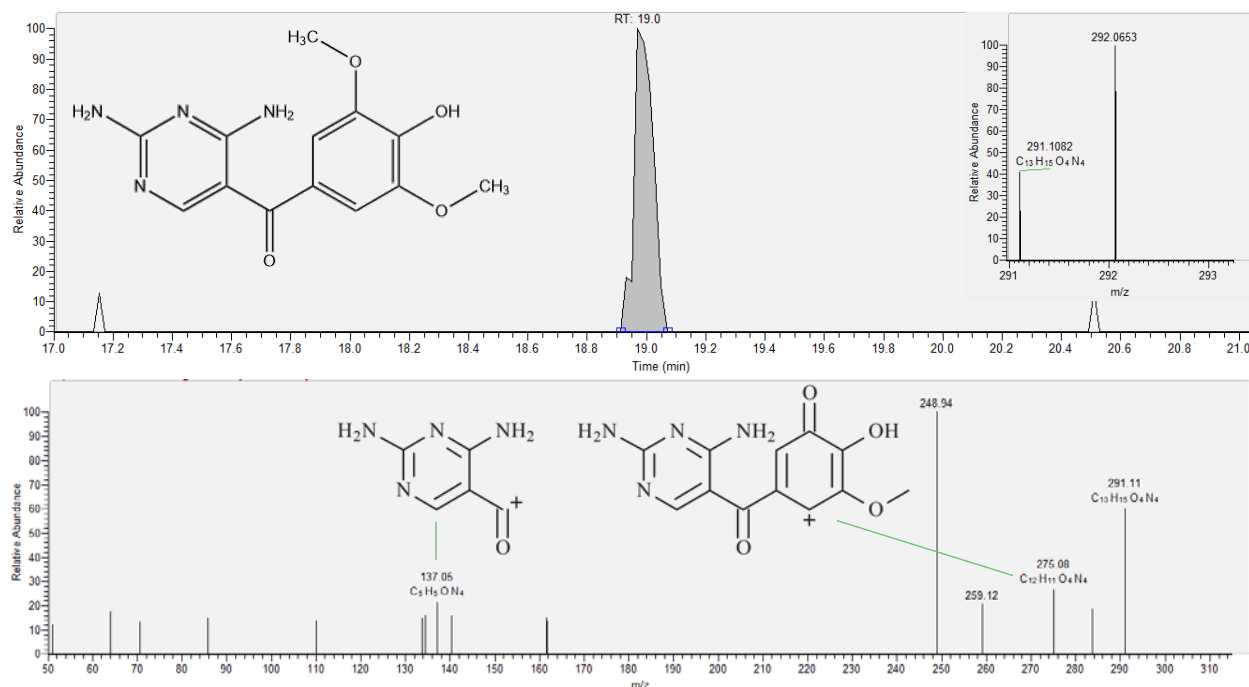


Figure G.11: Identification of TRI-290.

Trimethoprim has been shown to be biotransformed into TRI-290 in biological systems (Jewell et al., 2016) which had a RT of 19.0 min and was only present in the biofilter effluent. The MS spectra matched the exact mass of the proposed compound ($m/z = 291.1082$ for $[M+H]^+$, $\Delta m = -2.061$ ppm). The MS/MS fragments with $m/z = 137.05$ and 275.08 matched with fragments generated by the predicted structure using Mass Frontier.

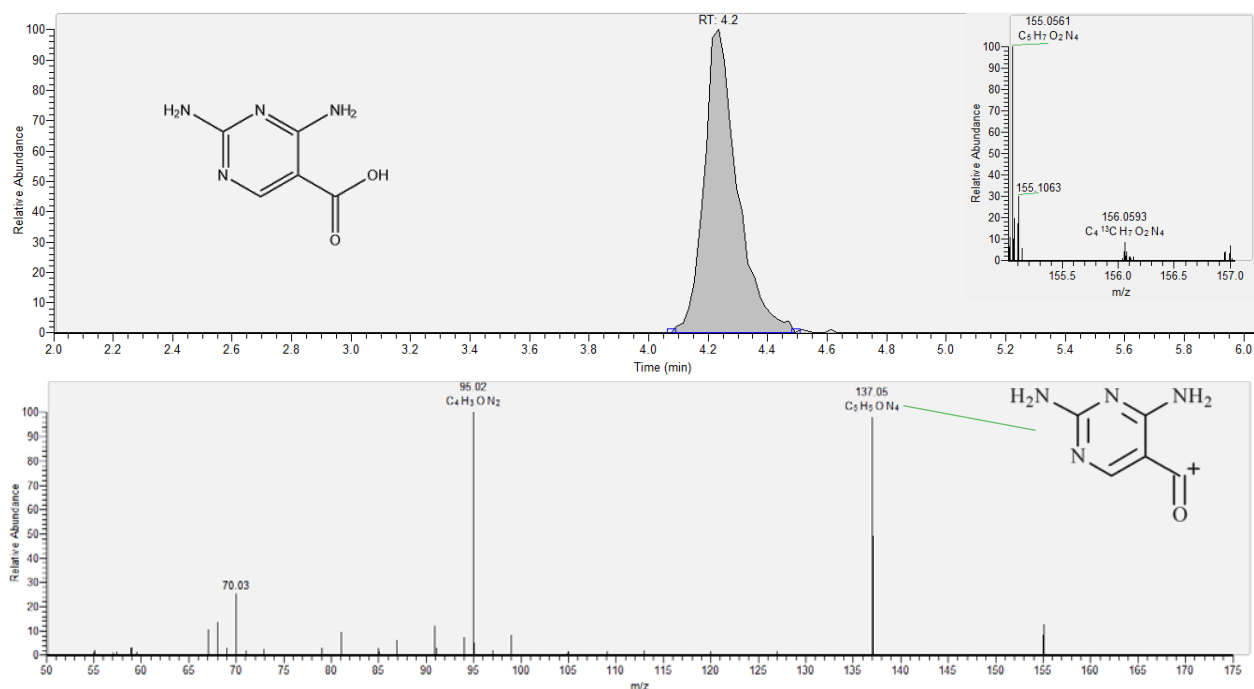


Figure G.12: Identification of DAPC.

Trimethoprim has been shown to be biotransformed into DAPC (2,4-diaminopyrimidine-5-carboxylic acid) in biological systems (Jewell et al., 2016) which had a RT of 4.2 min and was only present in the biofilter effluent. The MS spectra matched the exact mass of the proposed compound ($m/z = 155.0561$ for $[M+H]^+$, $\Delta m = -1.935$ ppm) and the theoretical abundance (5%) of the ^{13}C monoisotopic mass. The MS/MS fragment with $m/z = 137.05$ matched with fragments generated by the predicted structure using Mass Frontier.

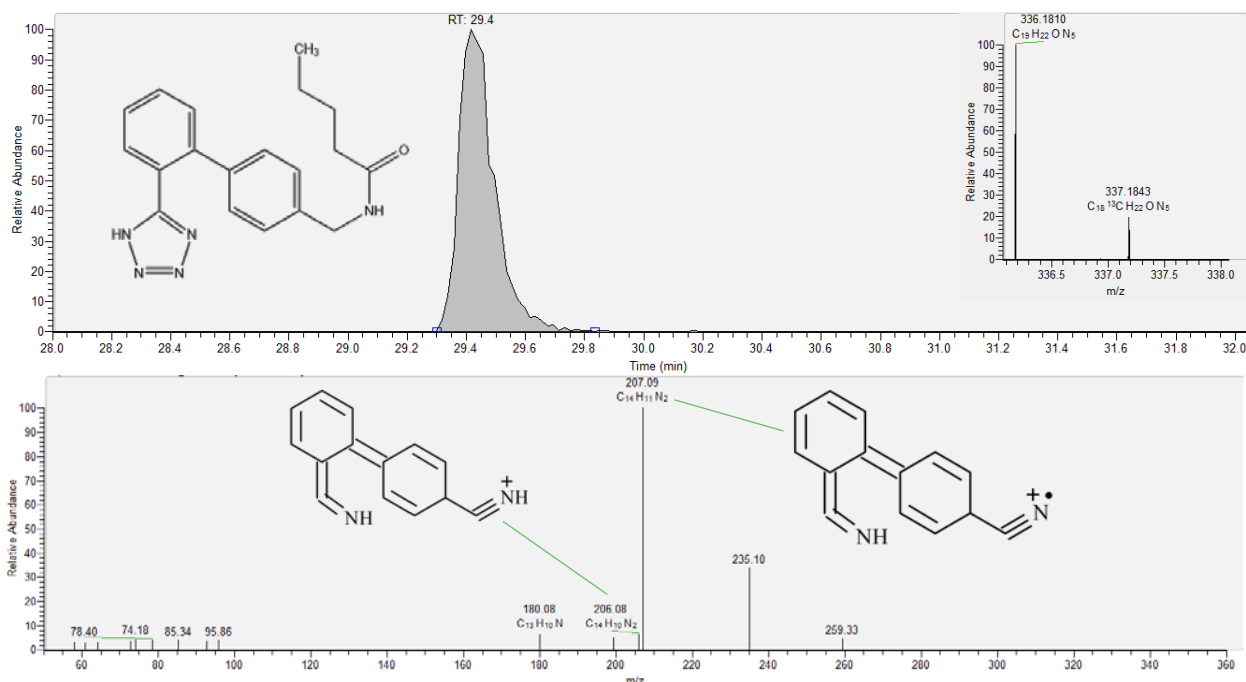


Figure G.13: Identification of VAL-335.

Valsartan was predicted to undergo biotransformation reaction *bt0243* to form VAL-335 which had a RT of 29.4 min and was present in the biofilter effluent at 32x the peak area than the influent and the control filter effluent. The MS spectra matched the exact mass of the proposed compound ($m/z = 336.1810$ for $[M+H]^+$, $\Delta m = -2.677$ ppm) and the theoretical abundance (19%) of the ^{13}C monoisotopic mass. The MS/MS fragments with $m/z = 207.09$ and 206.08 matched with fragments generated by the predicted structure using Mass Frontier.

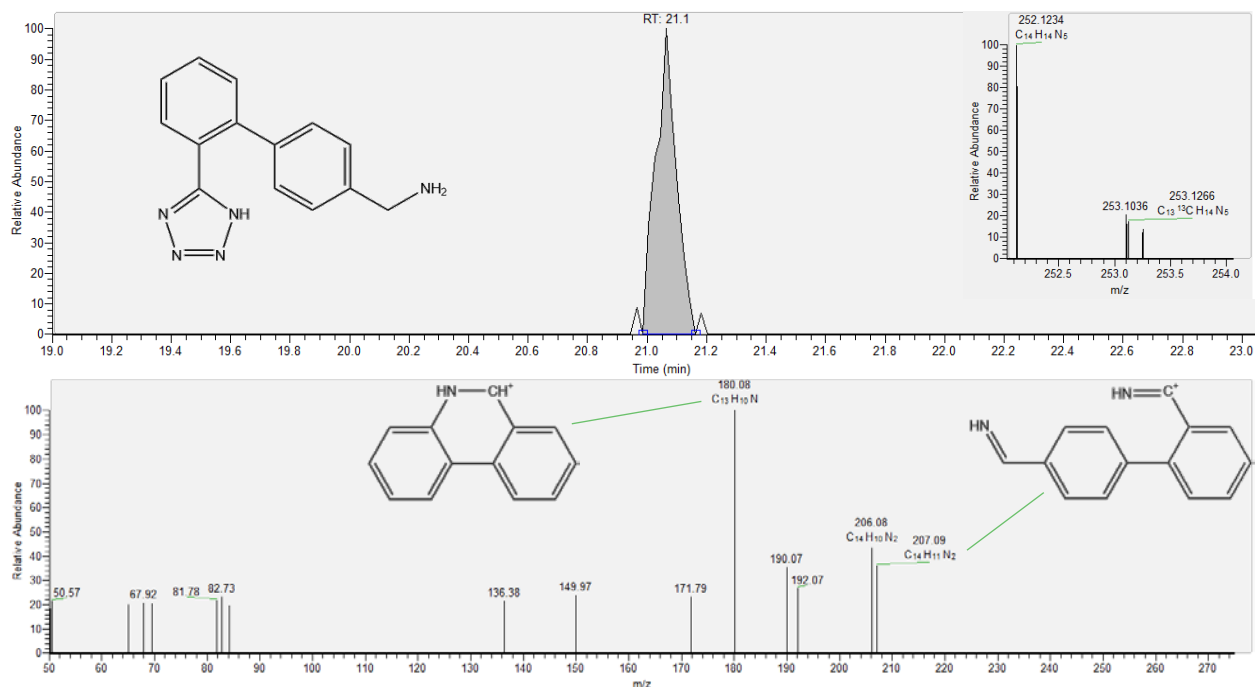


Figure G.14: Identification of VAL-251.

Valsartan has been shown to be biotransformed into VAL-251 in biological systems (Helbling et al., 2010) which had a RT of 21.1 min and was present in the biofilter effluent at 3x the peak area than the influent and the control filter effluent. The MS spectra matched the exact mass of the proposed compound ($m/z = 252.1234$ for $[M+H]^+$, $\Delta m = -3.966$ ppm) and the theoretical abundance (14%) of the ^{13}C monoisotopic mass. The MS/MS fragments with $m/z = 180.08$ and 207.09 matched with previously reported fragments (Helbling et al., 2010).

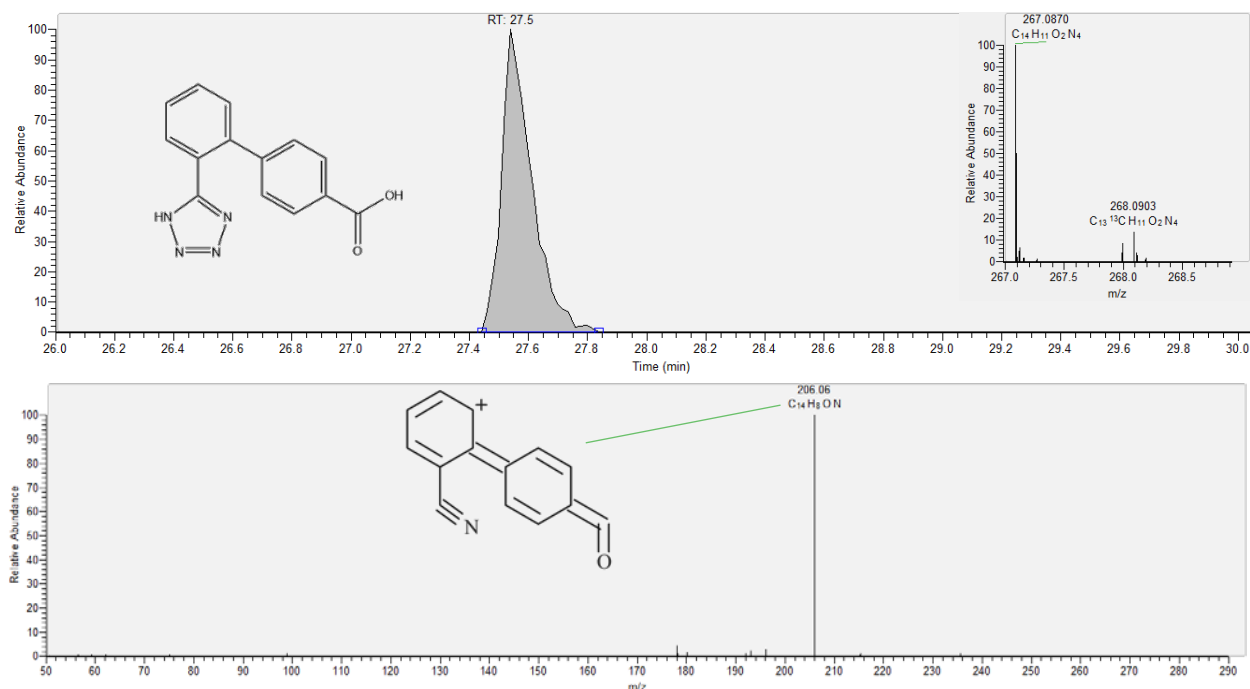


Figure G.15: Identification of valsartan-acid.

Valsartan has been shown to be biotransformed into valsartan-acid in biological systems (Helbling et al., 2010) which had a RT of 27.5 min and was only present in the biofilter effluent. The MS spectra matched the exact mass of the proposed compound ($m/z = 267.0870$ for $[M+H]^+$, $\Delta m = -2.621$ ppm) and the theoretical abundance (14%) of the ^{13}C monoisotopic mass. The MS/MS fragment with $m/z = 206.06$ matched with fragments generated by the predicted structure using Mass Frontier.

REFERENCES

- Alexander, M., 1981. Biodegradation of chemicals of environmental concern. *Science* (80-.). 211, 132–138. doi:10.1126/science.7444456
- Alidina, M., Li, D., Drewes, J.E., 2014. Investigating the role for adaptation of the microbial community to transform trace organic chemicals during managed aquifer recharge. *Water Res.* 56, 172–180. doi:10.1016/j.watres.2014.02.046
- Altenburger, R., Backhaus, T., Boedeker, W., Faust, M., Scholze, M., 2013. Simplifying complexity: Mixture toxicity assessment in the last 20 years. *Environ. Toxicol. Chem.* 32, 1685–1687. doi:10.1002/etc.2294
- Altmann, J., Ruhl, A.S., Zietzschmann, F., Jekel, M., 2014. Direct comparison of ozonation and adsorption onto powdered activated carbon for micropollutant removal in advanced wastewater treatment. *Water Res.* 55, 185–193. doi:10.1016/j.watres.2014.02.025
- Benner, J., Helbling, D.E., Kohler, H.-P.E., Wittebol, J., Kaiser, E., Prasse, C., Ternes, T. a, Albers, C.N., Aamand, J., Horemans, B., Springael, D., Walravens, E., Boon, N., 2013. Is biological treatment a viable alternative for micropollutant removal in drinking water treatment processes? *Water Res.* 47, 5955–76. doi:10.1016/j.watres.2013.07.015
- Bertelkamp, C., Reungoat, J., Cornelissen, E.R., Singhal, N., Reynisson, J., Cabo, a. J., van der Hoek, J.P., Verliefe, a. R.D., 2014. Sorption and biodegradation of organic micropollutants during river bank filtration: A laboratory column study. *Water Res.* 52, 231–241. doi:10.1016/j.watres.2013.10.068
- Bertelkamp, C., Schoutteten, K., Vanhaecke, L., Vanden Bussche, J., Callewaert, C., Boon, N., Singhal, N., van der Hoek, J.P., Verliefe, A.R.D., 2015. A laboratory-scale column study comparing organic micropollutant removal and microbial diversity for two soil types. *Sci. Total Environ.* 536, 632–638. doi:10.1016/j.scitotenv.2015.07.056
- Bertelkamp, C., van der Hoek, J.P., Schoutteten, K., Hulpiau, L., Vanhaecke, L., Vanden Bussche, J., Cabo, A.J., Callewaert, C., Boon, N., Lowenberg, J., Singhal, N., Verliefe, A.R.D., 2016a. The effect of feed water dissolved organic carbon concentration and composition on organic micropollutant removal and microbial diversity in soil columns simulating river bank filtration. *Chemosphere* 144, 932–939. doi:10.1016/j.chemosphere.2015.09.017

- Bertelkamp, C., Verliefde, A.R.D., Reynisson, J., Singhal, N., Cabo, A.J., Jonge, M. De, 2016b. A predictive multi-linear regression model for organic micropollutants , based on a laboratory-scale column study simulating the river bank filtration process. *J. Hazard. Mater.* 304, 502–511.
- Bonvin, F., Jost, L., Randin, L., Bonvin, E., Kohn, T., 2016. Super-fine powdered activated carbon (SPAC) for efficient removal of micropollutants from wastewater treatment plant effluent. *Water Res.* 90, 90–99. doi:10.1016/j.watres.2015.12.001
- Bouwer, E.J., Crowe, P.B., 1988. Biological Processes in Drinking Water Treatment. *Am. Water Work. Assoc.* 80, 82–93.
- Boxall, A.B.A., Kolpin, D.W., Halling-Sørensen, B., Tolls, J., 2003. Are Veterinary Medicines Causing Environmental Risks? *Environ. Sci. Technol.* 37, 286A–294A.
- Carlson, K.H., Amy, G.L., 1998. BOM removal during biofiltration. *J. / Am. Water Work. Assoc.* 90, 42–52.
- Collins, M.R., Eighmy, T.T., Jr, J.M.F., Spanos, S.K., 1992. Removing natural organic matter by conventional slow sand filtration. *Am. Water Work. Assoc.*
- D'Alessio, M., Yoneyama, B., Kirs, M., Kisand, V., Ray, C., 2015. Pharmaceutically active compounds: Their removal during slow sand filtration and their impact on slow sand filtration bacterial removal. *Sci. Total Environ.* 524–525, 124–135. doi:10.1016/j.scitotenv.2015.04.014
- Daughton, C.G., Ternes, T.A., 1999. Pharmaceuticals and Personal Care Products in the Environment: Agents of Subtle Change? *Environ. Health Perspect.* 107, 907–938.
- Deborde, M., von Gunten, U., 2008. Reactions of chlorine with inorganic and organic compounds during water treatment-Kinetics and mechanisms: A critical review. *Water Res.* 42, 13–51. doi:10.1016/j.watres.2007.07.025
- Del Rosario, K.L., Mitra, S., Humphrey, C.P., O'Driscoll, M.A., 2014. Detection of pharmaceuticals and other personal care products in groundwater beneath and adjacent to onsite wastewater treatment systems in a coastal plain shallow aquifer. *Sci. Total Environ.* 487, 216–223. doi:10.1016/j.scitotenv.2014.03.135

Drewes, J.E., Xu, P., Bellona, C., Oedekoven, M., Macalady, D., Amy, G., Kim, T.-U., 2007. WaterReuse Foundation.

Egli, T., 2010. How to live at very low substrate concentration. *Water Res.* 44, 4826–4837. doi:10.1016/j.watres.2010.07.023

Egli, T., 1995. The Ecological and Physiological Significance of the Growth of Heterotrophic Microorganisms with Mixtures of Substrates, in: *Advances in Microbial Ecology*. pp. 305–386.

Erickson, M.L., Langer, S.K., Roth, J.L., Kroening, S.E., 2014. Contaminants of Emerging Concern in Ambient Groundwater in Urbanized Areas of Minnesota, 2009–12. Reston, VA.

Escolà Casas, M., Bester, K., 2015. Can those organic micro-pollutants that are recalcitrant in activated sludge treatment be removed from wastewater by biofilm reactors (slow sand filters)? *Sci. Total Environ.* 506–507, 315–322. doi:10.1016/j.scitotenv.2014.10.113

Evans, P.J., Opitz, E.M., Daniel, P. a., Schulz, C.R., 2010. Biological Drinking Water Treatment Perceptions and Actual Experiences in North America, Web Report #4129.

Evgenidou, E.N., Konstantinou, I.K., Lambropoulou, D.A., 2015. Occurrence and removal of transformation products of PPCPs and illicit drugs in wastewaters: A review. *Sci. Total Environ.* 505, 905–926. doi:10.1016/j.scitotenv.2014.10.021

Fairbairn, D.J., Arnold, W.A., Barber, B.L., Kaufenberg, E.F., Koskinen, W.C., Novak, P.J., Rice, P.J., Swackhamer, D.L., 2015. Contaminants of Emerging Concern: Mass Balance and Comparison of Wastewater Effluent and Upstream Sources in a Mixed-Use Watershed. *Environ. Sci. Technol.* doi:10.1021/acs.est.5b03109

FDA, U.S., 2016. Resources for Information on Approved Drugs [WWW Document]. URL <http://www.fda.gov/Drugs/InformationOnDrugs/ApprovedDrugs/default.htm>

Focazio, M.J., Kolpin, D.W., Barnes, K.K., Furlong, E.T., Meyer, M.T., Zaugg, S.D., Barber, L.B., Thurman, M.E., 2008. A national reconnaissance for pharmaceuticals and other organic wastewater contaminants in the United States - II) Untreated drinking water sources. *Sci. Total Environ.* 402, 201–216. doi:10.1016/j.scitotenv.2008.02.021

Gilliom, R., 2007. Pesticides in U.S. Streams and Groundwater. *Environ. Sci. Technol.* 41, 3407–3413.

- Gimball, R., Graham, N., Collins, M., 2006. Recent Progress in Slow Sand and Alternative Biofiltration Processes. IWA Publishing.
- Gros, M., Rodríguez-Mozaz, S., Barceló, D., 2012. Fast and comprehensive multi-residue analysis of a broad range of human and veterinary pharmaceuticals and some of their metabolites in surface and treated waters by ultra-high-performance liquid chromatography coupled to quadrupole-linear ion trap tandem. *J. Chromatogr. A* 1248, 104–21. doi:10.1016/j.chroma.2012.05.084
- Gulde, R., Meier, U., Schymanski, E.L., Kohler, H.P.E., Helbling, D.E., Derrer, S., Rentsch, D., Fenner, K., 2016. Systematic Exploration of Biotransformation Reactions of Amine-Containing Micropollutants in Activated Sludge. *Environ. Sci. Technol.* 50, 2908–2920. doi:10.1021/acs.est.5b05186
- Harris-Lovett, S.R., Binz, C., Sedlak, D.L., Kiparsky, M., Truffer, B., 2015. Beyond User Acceptance: A Legitimacy Framework for Potable Water Reuse in California. *Environ. Sci. Technol.* 49, 7552–7561. doi:10.1021/acs.est.5b00504
- Helbling, D.E., Hollender, J., Kohler, H.P.E., Singer, H., Fenner, K., 2010. High-throughput identification of microbial transformation products of organic micropollutants. *Environ. Sci. Technol.* 44, 6621–6627. doi:10.1021/es100970m
- Hering, J.G., Waite, T.D., Luthy, R.G., Drewes, J.E., Sedlak, D.L., 2013. A changing framework for urban water systems. *Environ. Sci. Technol.* 47, 10721–10726. doi:10.1021/es4007096
- Hinkle, S.R., Weick, R.J., Johnson, J.M., Cahill, J.D., Smith, S.G., Rich, B.J., 2005. Organic wastewater compounds, pharmaceuticals, and coliphage in ground water receiving discharge from onsite wastewater treatment systems near La Pine, Oregon: Occurrence and implications for transport. USGS SIR 2005-5055 98 p.
- Hollender, J., Zimmermann, S.G., Koepke, S., Krauss, M., McArdell, C.S., Ort, C., Singer, H., von Gunten, U., Siegrist, H., 2009. Elimination of organic micropollutants in a municipal wastewater treatment plant upgraded with a full scale post-ozonation followed by sand filtration. *Environ. Sci. Technol.* 43, 7862–7869.
- Hoppe-Jones, C., Dickenson, E.R. V, Drewes, J.E., 2012. The role of microbial adaptation and biodegradable dissolved organic carbon on the attenuation of trace organic chemicals during groundwater recharge. *Sci. Total Environ.* 437, 137–144. doi:10.1016/j.scitotenv.2012.08.009

- Hozalski, R.M., Bouwer, E.J., 1998. Deposition and retention of bacteria in backwashed filters. *Am. Water Work. Assoc.* 90, 71–85.
- Jewell, K.S., Castronovo, S., Wick, A., Falås, P., Joss, A., Ternes, T.A., 2016. New insights into the transformation of trimethoprim during biological wastewater treatment. *Water Res.* 88, 550–557. doi:10.1016/j.watres.2015.10.026
- Johnson, D.R., Helbling, D.E., Lee, T.K., Park, J., Fenner, K., Kohler, H.-P.E., Ackermann, M., 2015a. Association of Biodiversity with the Rates of Micropollutant Biotransformations among Full-Scale Wastewater Treatment Plant Communities. *Appl. Environ. Microbiol.* 81, 666–675. doi:10.1128/aem.03286-14
- Johnson, D.R., Lee, T.K., Park, J., Fenner, K., Helbling, D.E., 2015b. The functional and taxonomic richness of wastewater treatment plant microbial communities are associated with each other and with ambient nitrogen and carbon availability. *Environ. Microbiol.* 17, 4851–4860. doi:10.1111/1462-2920.12429
- Karpuzcu, M.E., Fairbairn, D., Arnold, W. a, Barber, B.L., Kaufenberg, E., Koskinen, W.C., Novak, P.J., Rice, P.J., Swackhamer, D.L., 2014. Identifying sources of emerging organic contaminants in a mixed use watershed using principal components analysis. *Environ. Sci. Process. Impacts* 16, 2390–9. doi:10.1039/c4em00324a
- Klotz, D., Moser, H., 1974. Hydrodynamic dispersion as aquifer characteristic: model experiments with radioactive tracers. *Isot. Tech. Groundw. Hydrol.* Vol. 2 II, 341–355.
- Kolpin, D., Furlong, E., Zaugg, S., Barber, L., Buxton, H., 2002. Pharmaceuticals, Hormones, and Other Organic Wastewater Contaminants in U. S. Streams, 1999-2000: A National Reconnaissance. *J. Environ. Sci. Technol.* 36, 1202–1211. doi:10.1021/es011055j
- Kovalova, L., Knappe, D.R.U., Lehnberg, K., Kazner, C., Hollender, J., 2013. Removal of highly polar micropollutants from wastewater by powdered activated carbon. *Environ. Sci. Pollut. Res.* 20, 3607–3615. doi:10.1007/s11356-012-1432-9
- Krkošek, W.H., Payne, S.J., Gagnon, G. a., 2014. Removal of acidic pharmaceuticals within a nitrifying recirculating biofilter. *J. Hazard. Mater.* 273, 85–93. doi:10.1016/j.jhazmat.2014.03.031

- Lautenschlager, K., Hwang, C., Ling, F., Liu, W.T., Boon, N., Köster, O., Egli, T., Hammes, F., 2014. Abundance and composition of indigenous bacterial communities in a multi-step biofiltration-based drinking water treatment plant. *Water Res.* 62, 40–52. doi:10.1016/j.watres.2014.05.035
- LeChevallier, M.W., Au, K.-K., 2004. *Water Treatment and Pathogen Control: Process efficiency in achieving safe drinking-water*. WHO Drink. Water Qual. Ser. 107. doi:ISBN:1 84339 069 8
- Lee, C.O., Howe, K.J., Thomson, B.M., 2012. Ozone and biofiltration as an alternative to reverse osmosis for removing PPCPs and micropollutants from treated wastewater. *Water Res.* 46, 1005–1014. doi:10.1016/j.watres.2011.11.069
- Li, D., Alidina, M., Drewes, J.E., 2014. Role of primary substrate composition on microbial community structure and function and trace organic chemical attenuation in managed aquifer recharge systems. *Appl. Microbiol. Biotechnol.* 98, 5747–5756. doi:10.1007/s00253-014-5677-8
- Li, Y., Zhu, G., Ng, W.J., Tan, S.K., 2014. A review on removing pharmaceutical contaminants from wastewater by constructed wetlands: Design, performance and mechanism. *Sci. Total Environ.* 468–469, 908–932. doi:10.1016/j.scitotenv.2013.09.018
- Li, Z., Chang, P.H., Jiang, W.T., Jean, J.S., Hong, H., Liao, L., 2011. Removal of diphenhydramine from water by swelling clay minerals. *J. Colloid Interface Sci.* 360, 227–232. doi:10.1016/j.jcis.2011.04.030
- Luo, Y., Guo, W., Ngo, H.H., Nghiem, L.D., Hai, F.I., Zhang, J., Liang, S., Wang, X.C., 2014. A review on the occurrence of micropollutants in the aquatic environment and their fate and removal during wastewater treatment. *Sci. Total Environ.* 473–474, 619–641. doi:10.1016/j.scitotenv.2013.12.065
- Margot, J., Kienle, C., Magnet, A., Weil, M., Rossi, L., de Alencastro, L.F., Abegglen, C., Thonney, D., Chèvre, N., Schärer, M., Barry, D.A., 2013. Treatment of micropollutants in municipal wastewater: Ozone or powdered activated carbon? *Sci. Total Environ.* 461–462, 480–498. doi:10.1016/j.scitotenv.2013.05.034
- McCarroll, N.E., Protzel, A., Ioannou, Y., Frank Stack, H., Jackson, M.A., Waters, M.D., Dearfield, K.L., 2002. A survey of EPA/OPP and open literature on selected pesticide chemicals - III. Mutagenicity and carcinogenicity of benomyl and carbendazim. *Mutat. Res. - Rev. Mutat. Res.* 512, 1–35. doi:10.1016/S1383-5742(02)00026-1

- Meckenstock, R.U., Elsner, M., Griebler, C., Lueders, T., Stump, C., Aamand, J., Agathos, S.N., Albrechtsen, H.-J., Bastiaens, L., Bjerg, P.L., Boon, N., Dejonghe, W., Huang, W.E., Schmidt, S.I., Smolders, E., Sørensen, S.R., Springael, D., van Breukelen, B.M., 2015. Biodegradation: Updating the Concepts of Control for Microbial Cleanup in Contaminated Aquifers. *Environ. Sci. Technol.* 49, 7073–7081. doi:10.1021/acs.est.5b00715
- Murtagh, F., Legendre, P., 2014. Ward's Hierarchical Agglomerative Clustering Method: Which Algorithms Implement Ward's Criterion? *J. Classif.* 31, 274–295. doi:10.1007/s00357-
- Nam, S.-W., Choi, D.-J., Kim, S.-K., Her, N., Zoh, K.-D., 2014. Adsorption characteristics of selected hydrophilic and hydrophobic micropollutants in water using activated carbon. *J. Hazard. Mater.* 270, 144–52. doi:10.1016/j.jhazmat.2014.01.037
- Ogata, A., Banks, R.B., 1961. A solution of the differential equation of longitudinal dispersion in porous media. *U. S. Geol. Surv. Prof. Pap.* 411-A.
- Onesios, K.M., Bouwer, E.J., 2012. Biological removal of pharmaceuticals and personal care products during laboratory soil aquifer treatment simulation with different primary substrate concentrations. *Water Res.* 46, 2365–2375. doi:10.1016/j.watres.2012.02.001
- Onesios-Barry, K.M., Berry, D., Proescher, J.B., Ashok Sivakumar, I.K., Bouwer, E.J., 2014. Removal of pharmaceuticals and personal care products during water recycling: Microbial community structure and effects of substrate concentration. *Appl. Environ. Microbiol.* 80, 2440–2450. doi:10.1128/AEM.03693-13
- Ormad, M.P., Miguel, N., Claver, A., Matesanz, J.M., Ovelheiro, J.L., 2008. Pesticides removal in the process of drinking water production. *Chemosphere* 71, 97–106. doi:10.1016/j.chemosphere.2007.10.006
- Oturan, N., Van Hullebusch, E.D., Zhang, H., Mazeas, L., Budzinski, H., Le Menach, K., Oturan, M.A., 2015. Occurrence and removal of organic micropollutants in landfill leachates treated by electrochemical advanced oxidation processes. *Environ. Sci. Technol.* 151001145245006. doi:10.1021/acs.est.5b02809
- Phillips, P.J., Schubert, C., Argue, D., Fisher, I., Furlong, E.T., Foreman, W., Gray, J., Chalmers, A., 2015. Concentrations of hormones, pharmaceuticals and other micropollutants in groundwater affected by septic systems in New England and New York. *Sci. Total Environ.* 512–513, 43–54. doi:10.1016/j.scitotenv.2014.12.067

- Prasse, C., Wagner, M., Schulz, R., Ternes, T.A., 2012. Oxidation of the antiviral drug acyclovir and its biodegradation product carboxy-acyclovir with ozone: Kinetics and identification of oxidation products. *Environ. Sci. Technol.* 46, 2169–2178. doi:10.1021/es203712z
- R Core Team, 2016. R: A Language and Environment for Statistical Computing. R Found. Stat. Comput.
- Rattier, M., Reungoat, J., Keller, J., Gernjak, W., 2014. Removal of micropollutants during tertiary wastewater treatment by biofiltration: Role of nitrifiers and removal mechanisms. *Water Res.* 54, 89–99. doi:10.1016/j.watres.2014.01.030
- Rauch-Williams, T., Hoppe-Jones, C., Drewes, J.E., 2010. The role of organic matter in the removal of emerging trace organic chemicals during managed aquifer recharge. *Water Res.* 44, 449–460. doi:10.1016/j.watres.2009.08.027
- Reungoat, J., Escher, B.I., Macova, M., Argaud, F.X., Gernjak, W., Keller, J., 2012. Ozonation and biological activated carbon filtration of wastewater treatment plant effluents. *Water Res.* 46, 863–872. doi:10.1016/j.watres.2011.11.064
- Reungoat, J., Escher, B.I., Macova, M., Keller, J., 2011. Biofiltration of wastewater treatment plant effluent: Effective removal of pharmaceuticals and personal care products and reduction of toxicity. *Water Res.* 45, 2751–2762. doi:10.1016/j.watres.2011.02.013
- Richardson, S.D., Kimura, S.Y., 2016. Water Analysis: Emerging Contaminants and Current Issues. *Anal. Chem.* 88, 546–582. doi:10.1021/acs.analchem.5b04493
- Richardson, S.D., Ternes, T.A., 2014. Water Analysis: Emerging Contaminants and Current Issues. *Anal. Chem.* 2813–2848. doi:10.1021/ac500508t
- Rittmann, B.E., Huck, P.M., Bouwer, E.J., 1989. Biological treatment of public water supplies. *Crit. Rev. Environ. Control* 19, 119–184. doi:10.1080/10643388909388362
- Rubirola, A., Llorca, M., Rodriguez-Mozaz, S., Casas, N., Rodriguez-Roda, I., Barceló, D., Buttiglieri, G., 2014. Characterization of metoprolol biodegradation and its transformation products generated in activated sludge batch experiments and in full scale WWTPs. *Water Res.* 63, 21–32. doi:10.1016/j.watres.2014.05.031

- Ruff, M., Mueller, M.S., Loos, M., Singer, H.P., 2015. Quantitative target and systematic non-target analysis of polar organic micro-pollutants along the river Rhine using high-resolution mass-spectrometry - Identification of unknown sources and compounds. *Water Res.* 87, 145–154. doi:10.1016/j.watres.2015.09.017
- Sangster, J.L., Oke, H., Zhang, Y., Bartelt-Hunt, S.L., 2015. The effect of particle size on sorption of estrogens, androgens and progestagens in aquatic sediment. *J. Hazard. Mater.* 299, 112–121. doi:10.1016/j.jhazmat.2015.05.046
- Schenck, K., Rosenblum, L., Ramakrishnan, B., Carson, J., 2015. Correlation of trace contaminants to wastewater management practices in small watersheds. *Environ. Sci. Process. Impacts* 17, 956–964. doi:10.1039/C4EM00583J
- Schmidt, C.K., Lange, F.T., Brauch, H.J., Kühn, W., 2003. Experiences with riverbank filtration and infiltration in Germany. *Proc. Int. Symp. Artif. Recharg. Groundw.* 115–141.
- Schwarzenbach, R.P., Escher, B.I., Fenner, K., Hofstetter, T.B., Johnson, C.A., Gunten, U. Von, Wehrli, B., 2006. The Challenge of Micropollutants in Aquatic Systems. *Science* (80-.). 313, 1072–1077.
- Schymanski, E.L., Jeon, J., Gulde, R., Fenner, K., Ru, M., Singer, H.P., Hollender, J., 2014. Identifying Small Molecules via High Resolution Mass Spectrometry: Communicating Confidence. *Environ. Sci. Technol.* 48, 2097–2098. doi:10.1021/es5002105 |
- Schymanski, E.L., Singer, H.P., Slobodnik, J., Ipolyi, I.M., Oswald, P., Krauss, M., Schulze, T., Haglund, P., Letzel, T., Grosse, S., Thomaidis, N.S., Bletsou, A., Zwiener, C., Ibáñez, M., Portolés, T., De Boer, R., Reid, M.J., Onghena, M., Kunkel, U., Schulz, W., Guillon, A., Noyon, N., Leroy, G., Bados, P., Bogialli, S., Stipaničev, D., Rostkowski, P., Hollender, J., 2015. Non-target screening with high-resolution mass spectrometry: Critical review using a collaborative trial on water analysis. *Anal. Bioanal. Chem.* 407, 6237–6255. doi:10.1007/s00216-015-8681-7
- Seifert, D., Engesgaard, P., 2007. Use of tracer tests to investigate changes in flow and transport properties due to bioclogging of porous media. *J. Contam. Hydrol.* 93, 58–71. doi:10.1016/j.jconhyd.2007.01.014
- Sharif, F., Westerhoff, P., Herckes, P., 2014. Impact of hydraulic and carbon loading rates of constructed wetlands on contaminants of emerging concern (CECs) removal. *Environ. Pollut.* 185, 107–115. doi:10.1016/j.envpol.2013.10.001

- Singer, H.P., Wössner, A.E., McArdell, C.S., Fenner, K., 2016. Rapid Screening for Exposure to “Non-Target” Pharmaceuticals from Wastewater Effluents by Combining HRMS-Based Suspect Screening and Exposure Modeling. *Environ. Sci. Technol.* acs.est.5b03332. doi:10.1021/acs.est.5b03332
- Snyder, S., Wert, E., Lei, H., Westerhoff, P., Yoon, Y., 2007. Removal of EDCs and Pharmaceuticals in Drinking and Reuse Treatment Processes [WWW Document]. *Am. Water Work. Assoc.*
- Stackelberg, P.E., Gibs, J., Furlong, E.T., Meyer, M.T., Zaugg, S.D., Lippincott, R.L., 2007. Efficiency of conventional drinking-water-treatment processes in removal of pharmaceuticals and other organic compounds. *Sci. Total Environ.* 377, 255–272. doi:10.1016/j.scitotenv.2007.01.095
- Suliman, F., French, H.K., Haugen, L.E., Sovik, A.K., 2006. Change in flow and transport patterns in horizontal subsurface flow constructed wetlands as a result of biological growth. *Ecol. Eng.* 27, 124–133. doi:10.1016/j.ecoleng.2005.12.007
- Summers, R.S., Shimabuku, K., Zearley, T.L., 2015. A review of biologically-based drinking water treatment processes for organic micropollutant removal, in: *Progress in Slow Sand and Alternative Biofiltration Processes*. IWA Publishing, London.
- Tatari, K., Smets, B.F., Albrechtsen, H.J., 2013. A novel bench-scale column assay to investigate site-specific nitrification biokinetics in biological rapid sand filters. *Water Res.* 47, 6380–6387. doi:10.1016/j.watres.2013.08.005
- Teerlink, J., Martínez-Hernández, V., Higgins, C.P., Drewes, J.E., 2012. Removal of trace organic chemicals in onsite wastewater soil treatment units: A laboratory experiment. *Water Res.* 46, 5174–5184. doi:10.1016/j.watres.2012.06.024
- Topp, E., Sumarah, M.W., Sabourin, L., 2012. The antihistamine diphenhydramine is extremely persistent in agricultural soil. *Sci. Total Environ.* 439, 136–140. doi:10.1016/j.scitotenv.2012.09.033
- U.S. EPA, 2016a. Toxic Substances Control Act [WWW Document]. United States Environmental Prot. Agency. URL <https://www.epa.gov/laws-regulations/summary-toxic-substances-control-act>
- U.S. EPA, 2016b. Index of chemical names & pesticide chemical codes report.

U.S. EPA, 2015. Fact Sheet : Drinking Water Contaminant Candidate List 4 – Draft.

U.S. EPA, 2014. Drinking Water Contaminants [WWW Document]. United States Environmental Prot. Agency. URL <https://www.epa.gov/ground-water-and-drinking-water/table-regulated-drinking-water-contaminants>

Urfer, D., Huck, P.M., 2001. Measurement of biomass activity in drinking water biofilters using a respirometric method. *Water Res.* 35, 1469–1477. doi:10.1016/S0043-1354(00)00405-X

Urfer, D., Huck, P.M., Booth, S.D.J., Coffey, B.M., 1997. Biological filtration for BOM and particle removal: a critical review. *J. - AWWA* 89, 83–98.

Veach, A.M., Bernot, M.J., 2011. Temporal variation of pharmaceuticals in an urban and agriculturally influenced stream. *Sci. Total Environ.* 409, 4553–4563. doi:10.1016/j.scitotenv.2011.07.022

Vedachalam, S., Joo, T., Riha, S., 2015. Septic Systems in New York: A Statewide Enumeration using Census Tract-Level Parcel Data. Ithaca, NY: New York State Water Resources Institute.

Wang, J.Z., Summers, R.S., Miltner, R.J., Wang, J.Z., Summers, R.S., Miltner, R.J., 1995. Biofiltration performance: part 1, relationship to biomass. *Am. Water Work. Assoc.* 87, 55–63.

Wicker, J., Lorsbach, T., Gu tlein, M., Schmid, E., Latino, D., Kramer, S., Fenner, K., 2015. enviPath - The environmental contaminant biotransformation pathway resource. *Nucleic Acids Res.* 44, 502–508. doi:10.1093/nar/gkv1229

Zearley, T.L., Summers, R.S., 2012. Removal of trace organic micropollutants by drinking water biological filters. *Environ. Sci. Technol.* 46, 9412–9419. doi:10.1021/es301428e

Zhu, I.X., Getting, T., Bruce, D., 2010. Review of biologically active filters in drinking water applications. *Am. Water Work. Assoc.* 102, 67–77.

Zimmermann, S.G., Wittenwiler, M., Hollender, J., Krauss, M., Ort, C., Siegrist, H., von Gunten, U., 2011. Kinetic assessment and modeling of an ozonation step for full-scale municipal wastewater treatment: Micropollutant oxidation, by-product formation and disinfection. *Water Res.* 45, 605–617. doi:10.1016/j.watres.2010.07.080